DISSERTATION

Titel der Dissertation

Heads decide: Structural and functional characterization of selected plectin isoform-specific sequences

Verfasser

Július Košťan

angestrebter akademischer Grad

Doctor of Philosophy (PhD)

Wien, 2014

At this place I would like to thank to all who supported me during my PhD studies and contributed to this work.

Many thanks go to all my former and present colleagues, members of Prof. Gerhard Wiche's group and Prof. Kristina Djinovic-Carugo's group, foremost to Martin, Radovan, Branislav, Björn, and Claudia.

I would like to thank Prof. Gerhard Wiche for giving me the opportunity to carry out my PhD work in his group, for his supervision and support.

Special thanks go to Prof. Kristina Djinovic-Carugo for her support in all things concerning the finishing and writing of my PhD thesis.

It is also time to express my thanks to my wife, who accompanied me through this time, incessantly believing in me and supported me at all times as much as possible. A huge part of this work belongs to her.

Finally, I would like thanks to my "three girls", for…everything.

Table of contents

List of abbreviations

ABD	actin binding domain
ABS	actin binding sequences/sites
BPAG	bullous pemphigoid antigen
BSA	bovine serum albumin
CaM	calmodulin
CBB	coomassie brilliant blue
CH	calponin homology domain
DTT	dithiothreitol
EBS-MD	epidermolysis bullosa simplex associated with muscular dystrophy
ECM	extracellular matrix
EGF	epidermal growth factor
F-actin	filamentous actin
FnIII	fibronectin type III domain
HD	hemidesmosome
IDP	intrinsically disordered protein
IF	intermediate filament
IFBS	intermediate filament binding site
MACF	microtubule actin crosslinking factor
MBP	maltose-binding protein
MFs	actin microfilaments
MTs	microtubules
P	plectin
PBS	phosphate buffered saline
PIP_2	phosphatidylinositol 4,5-bisphosphate
PKCα	protein kinase C alpha
PRD	plectin repeat domain
SAXS	small angle X-ray scattering
SDS	sodium dodecyl sulfate
SDS-PAGE	SDS-polyacrylamide gel electrophoresis
SH3	Src homology 3 domain
SR	spectrin repeat domain

Abstract

Plectin is a large and highly versatile cytolinker protein, which cross-links actin, tubulin, and various intermediate filament proteins, having a great impact on their spatial-temporal arrangements and dynamics. Due to alternative splicing, plectin is expressed as various isoforms with differing N-terminal heads, which dictate subcellular targeting of the protein. However, detailed mechanism(s) how plectin's heads direct the giant protein to different location and/or binding partners and thus modulate its function is not well understood yet, and needs to be, elucidated.

To investigate structural properties of plectin 1a and plectin 1c isoform specific sequences and relate them to their function, we established method(s) for purification of tagged and un-tagged plectin fragments comprising these sequences fused to plectin's ABD or to longer N-terminal parts of plectin including its plakin domain as well. Crystallization of these fragments was not successful, and indicated that plectin 1a and plectin 1c isoform specific sequences might be highly flexible or disordered, at least in their unbound state.

In the second part biochemical and cell biological approaches were used to identify novel binding partners of plectin interacting preferentially with its N-terminal part. Of the two novel binding partners identified, vimentin, an intermediate filament protein, was found to interact with the N-terminal part of plectin's ABD in its soluble "tetrameric" form.

In addition, isoform specific interaction of plectin with calmodulin, a Ca^{2+}-sensing protein, has been characterized. Calmodulin was showed to bind to the CH1 domain of plectin 1a in a Ca^{2+}- and isoform-dependent fashion. Furthermore, binding of Ca^{2+}/calmodulin to plectin 1a was found to prevent its binding to F-actin, and integrin β4. Interestingly, the interaction of integrin α6β4 with plectin 1a plays a major role in the formation of hemidesmosomes, multiprotein adhesion complexes, connecting epithelial cells to the basal matrix. Moreover, the detachment of epithelial cells from the basal matrix during wound healing and differentiation of keratinocytes requires the disassembly of the hemidesmosomal complexes, which formerly was believed to be mediated only by phosphorylation of integrin β4 by protein kinases.

Thus our results allowed us to propose a novel model for the disassembly of hemidesmosomes during keratinocyte differentiation, where both, binding of calmodulin to plectin 1a and phosphorylation of integrin β4, are required for disruption of the integrin α6β4-plectin complex.

Introduction

Cytoskeleton

The cytoskeleton, as its name implies, helps to maintain cell shape. But the primary importance of the cytoskeleton is in cell motility and mechanical properties of a cell. The internal movement of cell organelles, as well as cell locomotion and muscle fiber contraction could not take place without the cytoskeleton. The cytoskeleton of eukaryotic cells consists of three clearly defined filamentous systems: the microtubules (MTs), the intermediate filaments (IFs) and the actin microfilaments (MFs, F-actin), which constantly change their organization during cellular activities. These systems, distinguished by their size with microtubules being the thickest and microfilaments being the thinnest, share a critical feature. They are all composed of proteins that have the unique property of being able to self-assemble into a filamentous network. The elementary 'building blocks' of both MFs and MTs are represented by globular proteins, a monomeric actin and an αβ-tubulin heterodimer, respectively, while the elementary unit of IFs is a very elongated and thin rod-like dimer. The actin cytoskeleton is directly involved in cell locomotion, cytokinesis, cell-cell and cell-substratum interactions, the localization of cellular components, vesicular and organelle transport. Furthermore, it functions in the generation and maintenance of cell morphology and polarity, in endocytosis and intracellular trafficking, in contractility, motility and cell division. MTs, another principal component of the cytoskeleton, function both to determine cell shape and in a variety of cell movements, including some forms of cell locomotion, the intracellular transport of organelles, and the separation of chromosomes during mitosis. IFs are of prime importance for the functional organization of structural elements. Besides their primary role in cell plasticity and their established function as cellular stress absorbers, IFs are also involved both in signaling and in controlling gene regulatory networks (Herrmann *et al.*, 2009). Although unique functions have been ascribed to each of these filamentous systems, certain biological processes, such as the generation of cell polarity and cell migration, require the coordinated action of more than one filament type. The molecular basis of such cytoskeletal crosstalk are proteins such as these of the plakin family that mediate interactions between different cytoskeletal networks and specific cellular compartments (Jefferson *et al.*, 2004; Leung *et al.*, 2002; Ruhrberg and Watt, 1997).

Plakins

Plakins were first identified in the late 1970s and early 1980s in epithelial cells where they were found to connect the IFs to desmosomes and hemidesmosomes (Ruhrberg and Watt, 1997). They are a group of large (>200kDa) multi-domain proteins that have also been referred to as 'cytolinkers', thus highlighting their roles in crosslinking of cytoskeletal networks (Ruhrberg and Watt, 1997; Steinböck and Wiche, 1999). In mammals, this family includes desmoplakin, bullous pemphigoid antigen 1 (BPAG1), microtubule actin crosslinking factor (MACF1/ACF7), envoplakin, periplakin, epiplakin, and plectin (**Figure 1**). Interestingly, many of them have alternatively spliced forms leading to a very complex group of proteins potentially with tissue-specific functions (Jefferson *et al.*, 2004). In general, cytolinkers are multi-modular proteins, containing, in variable combinations, a plakin domain, plectin repeat domains (Janda *et al.*, 2001), an actin binding domain consisting of two calponin homology domains, a coiled-coil or spectrin repeat-containing rod (**Figure 1**) and microtubule-binding domains. In addition, recently solved crystal structures of the plakin domain, which is present in all plakins, except of epiplakin, suggested that plakins are members of the spectrin superfamily as well (Choi and Weis, 2011; Jefferson *et al.*, 2007; Ortega *et al.*, 2011). The proteins that function as molecular adaptors in epithelial IF-based junctions constitute the prototypical members of the plakins; that is, the epithelial form of BPAG1 (BPAG1e), desmoplakin and plectin. BPAG1e is a component of hemidesmosomes where it binds to IFs. In addition to BPAG1e, the *BPAG1* gene also encodes several structurally distinct proteins (Leung *et al.*, 2001). These alternatively spliced products exhibit a distinctive tissue distribution and are important in maintaining the cell architecture of neuron, muscle and epithelial cells. Desmoplakin is an important component of desmosomes, structures that mediate intercellular adhesion in tissues subjected to mechanical stress and that serve as anchoring sites for IFs. There are two isoforms of desmoplakin: DPI and DPII, which are the result of alternative splicing in the region of the central rod domain (Virata *et al.*, 1992). Two additional epithelial plakins, periplakin and envoplakin, have been identified as constituents of the cornified envelope and desmosomes (Ruhrberg *et al.*, 1996; Ruhrberg *et al.*, 1997). They associate with IFs and were proposed to function as a scaffold on which the cornified envelope is assembled. Epiplakin, too was found to be expressed in epithelial tissues. In comparison to other plakins, epiplakin has a unique structure consisting entirely of plectin repeat domains. For a long time, the biological functions of epiplakin have not been elucidated.
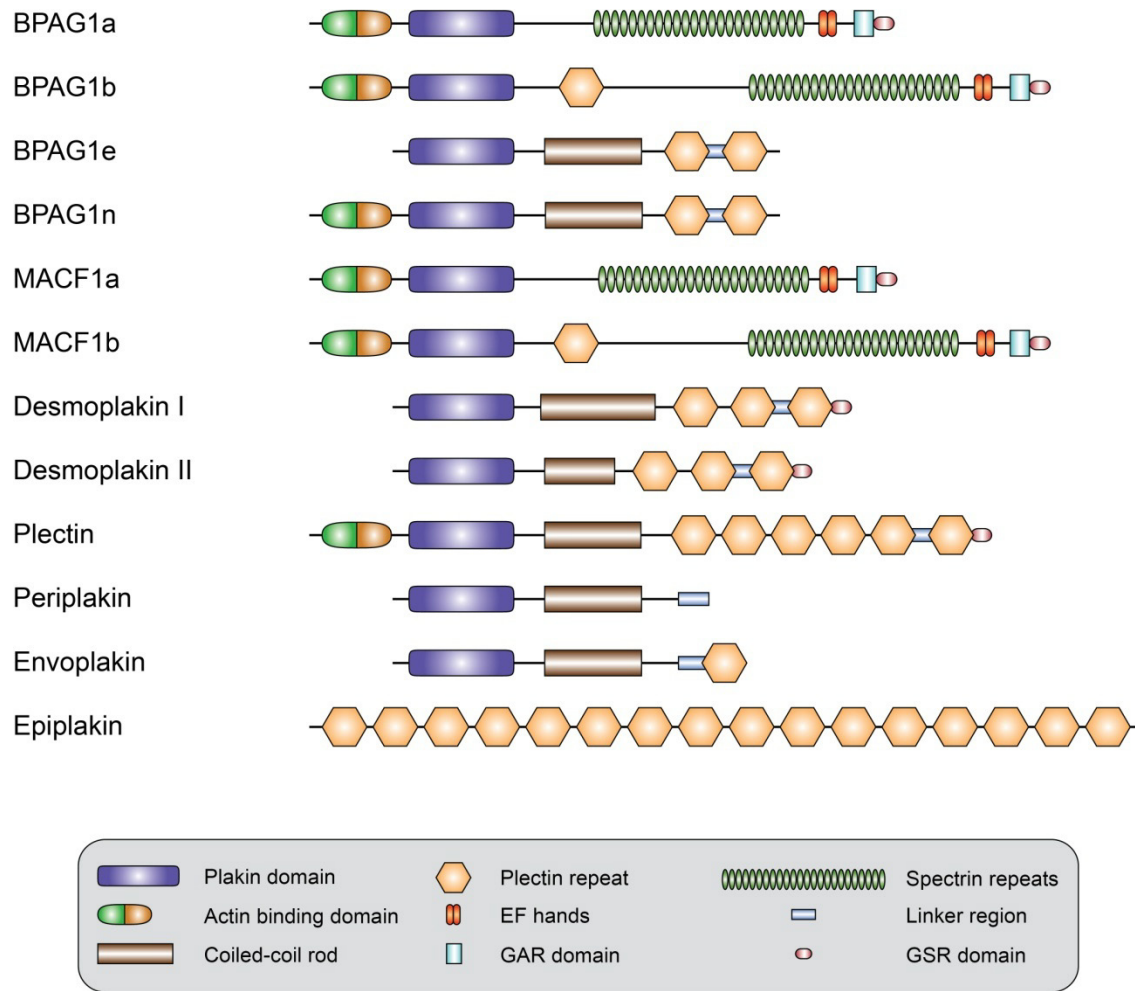
Figure 1. Schematic domain architecture of mammalian plakins. All plakin family members are large proteins possessing a globular plakin domain at the amino terminus, a central coiled-coil rod domain and a variable number of plectin repeat domains at the carboxyl terminus. This domain organization is a characteristic feature of plakins, however it is not fully conserved in all members of the family. Exceptions are made by periplakin and epiplakin. In addition, in some plakins, numerous spectrin repeats replace the central coiled-coil rod domain. Various isoforms of desmoplakin, plectin, BPAG1 and MACF have been identified; however only some (major) isoforms of are shown. Details on isoforms of plectin are given in later chapters. Functional domains are indicated. GAR, GAS2 related; GSR repeats, glycine-serine-arginine repeats. The figure was modified from (Jefferson *et. al*, 2004).

However, recent data suggest that epiplakin plays a role in keratin filament reorganization in response to stress factors (Spazierer *et al.*, 2008) and during wound healing (Ishikawa *et al.*, 2010). MACF, also known as ACF7 is expressed in the nervous system and function as a cytoskeletal linker protein connecting and coordinating actin filaments and microtubules (Karakesisoglou *et al.*, 2000; Leung *et al.*, 1999). Alternative splicing of the 5` end of MACF generates isoforms with different numbers of calponin homology (CH) domais (Bernier *et*

al., 1996). However, so far, the most versatile and best characterized cytolinker identified is plectin.

Plectin

Plectin`s versatility, is based on its wide distribution among tissues, varied subcellular localization, complex gene organization, isoform diversity, variable protein structure, and its ability to interact with a variety of proteins involved in formation and maintenance of the cytoskeleton, as well as in cell signaling. Plectin was first identified as a major component of intermediate filament preparations obtained from rat glioma C6 cells (Pytela and Wiche, 1980). Subsequently, using antiserum (Wiche and Baker, 1982) and a panel of mAbs (Foisner *et al.*, 1994), the protein was shown to be abundantly expressed in a wide variety of mammalian tissues and cells types. In fact, plectin was found to be prominent in various types of muscle, stratified and simple epithelia, cells forming the blood-brain barrier, and tissue layers at the interface between tissue and fluid-filled cavities of kidney glomeruli, liver bile canaliculi, bladder urothelium, gut villi, ependymal layers lining the cavities of brain and spinal cord, and endothelial cells of blood vessels (Errante *et al.*, 1994; Wiche, 1989; Wiche *et al.*, 1984; Wiche *et al.*, 1983; Yaoita *et al.*, 1996). At the cellular level, plectin co-distributes with different types of IFs and is located at plasma membrane attachment sites of IFs and MFs, such as hemidesmosomes (HDs) (Rezniczek *et al.*, 1998; Wiche *et al.*, 1984), desmosomes (Eger *et al.*, 1997), Z-line structures and dense plaques of striated and smooth muscle, intercalated discs of cardiac muscle, and focal contacts (Burgstaller *et al.*, 2010; Seifert *et al.*, 1992; Wiche *et al.*, 1983).

Based on plectin's prominence at plasma membrane junctional sites of IFs, particularly in HDs of basal keratinocytes, an involvement of plectin in bullous skin diseases has been suggested almost 30 years ago (Wiche *et al.*, 1984). A decade later, abnormalities in plectin expression in humans were found to cause epidermolysis bullosa simplex associated with muscular dystrophy (EBS-MD), manifesting as severe skin blistering and muscle disorders (for review see Pfendner *et al.*, 2005; Rezniczek *et al.*, 2010; Winter and Wiche, 2013); an autosomal dominant form of the disease (EBS-Ogna) manifests just in skin (Koss-Harnes *et al.*, 2002). In addition to EBS-MD and EBS-Ogna, plectin mutations have been shown to cause EBS-MD with a myasthenic syndrome, limb-girdle muscular dystrophy type 2Q, and EBS with pyloric atresia (for review see:

Introduction   9

Winter and Wiche, 2013). Conventional, as well as conditional (K5-Cre-driven) plectin knockouts in prenatal mice led to the death of animals, 2 to 3 days after birth (Ackerl *et al.*, 2007; Andrä *et al.*, 1997), whereas after induced disruption of the plectin gene in the skin of adult mice, keratinocyte fragility and lesional epidermal barrier defects were reported (Ackerl *et al.*, 2007).

Initially, plectin has been cloned and sequenced from rat (Elliott *et al.*, 1997; Wiche *et al.*, 1991), from human (Liu *et al.*, 1996) and partially from mouse (Andrä *et al.*, 1997). Analyses of the human gene locus revealed a complex organization of 32 exons spanning over ~32kb of DNA located in telomeric region (q24) of chromosome 8 (Liu *et al.*, 1996; McLean *et al.*, 1996). Later, analysis of the plectin gene locus in mouse identified a genomic exon-intron organization with more than 40 exons spanning 62 kb on chromosome 15 and an unusual 5′ transcript complexity of plectin isoforms. In total, 16 alternatively spliced exons were identified, 11 of which are directly spliced into exon 2, the first of 7 exons (exons 2-8) encoding plectin's ABD (**Figure 2**) (Fuchs *et al.*, 1999). Three of the exons are non-coding and splice into exon 1c, and two additional exons (2α and 3α) are optionally spliced within the exons encoding the ABD (Fuchs *et al.*, 1999). In a more recent study, 11 and 8 alternative first exons identified in mouse were found in the rat and human genes, respectively (Zhang *et al.*, 2004).
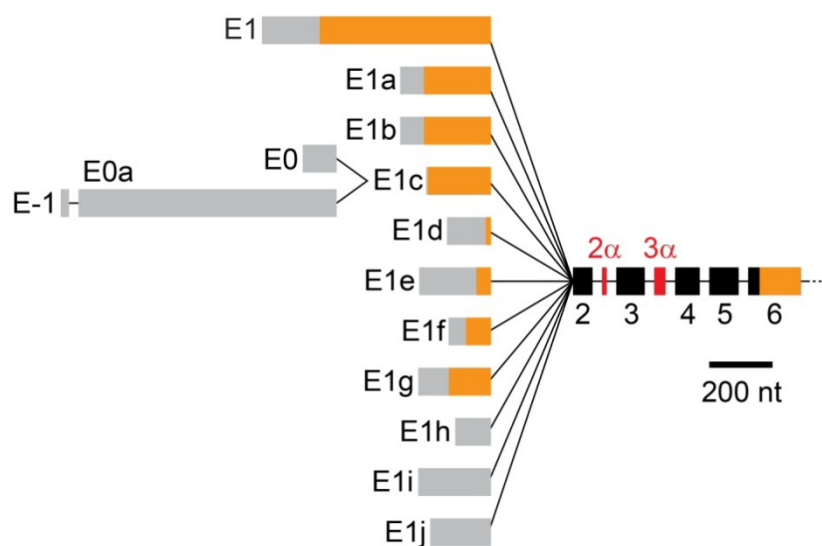
Figure 2. Transcripts generated by alternative splicing of the 5' end of the plectin gene. Exons are indicated by boxes, orange areas within the boxes denote regions coding in all cases, while light grey areas, denote non-coding regions. Black boxes indicate coding sequences if preceded by one of the first coding exons (E1-E1g, E1k), or noncoding sequences if preceded by one of the three noncoding exons (E1h-E1j). Three additional noncoding exons (E0, E0a, E-1) are also shown. Two optionally spliced exons (2α and 3α) inserted between exons 2 and 4 are shown in red. The figure was modified from (Fuchs *et al.*, 1999).

Plectin isoforms are differentially distributed among tissues. For instance, expression of plectin 1d transcripts is restricted to muscles, while plectin 1a represents the most prominent isoform of skin, lung, and small intestine (Fuchs *et al.*, 1999). The second isoform of plectin expressed in epithelial cells at high levels is plectin 1c (Andrä *et al.*, 2003; Walko *et al.*, 2011), which is also a major isoform of neural cells (Fuchs *et al.*, 1999) that share with epidermal cells a common developmental origin, the ectoderm. Tissue-specific expression is characteristic also of the two optionally spliced exons, 2α and 3α, with isoforms containing exon 2α being expressed in brain, heart, and skeletal muscle, and exon 3α, in combination with 2α, being brain-specific (Fuchs *et al.*, 1999). Moreover, using isoform-specific antibodies and cell lines transiently transfected with cDNAs encoding different plectin isoforms, some of the isoform-specific sequences have been shown to direct the protein to distinct cellular locations, such as HDs, microtubules, mitochondria, costameres, Z-disks, and focal adhesions (Andrä *et al.*, 2003; Burgstaller *et al.*, 2010; Konieczny *et al.*, 2008; Rezniczek *et al.*, 2003; Rezniczek *et al.*, 2007; Winter *et al.*, 2008). Concordantly, individual isoforms were found to carry out distinct and specific functions, some of which will be discuss later.

Similarly to other plakins, plectin possesses a multidomain architecture. Rotary shadowing electron microscopy of purified plectin revealed a dumbbell-like structure comprising a central 200 nm-long α-helical coiled-coil rod domain flanked by large N- and C-terminal globular domains (Foisner and Wiche, 1987). Depending on the particular isoform, plectin has a predicted molecular mass ranging from 499 to 533 kDa. However, based on its microscopic dimensions and gel permeation HPLC data, plectin exist in solution as a dimer. Dimerization of plectin is mediated by its central rod domain most likely in a parallel fashion (Wiche *et al.*, 1991). In addition, higher oligomeric states of plectin are formed and might involve interactions of its globular end domains (Foisner and Wiche, 1987; Weitzer and Wiche, 1987; Walko *et al.*, 2011).

The C terminus of plectin (~1900 amino acids) features six highly homologous plectin repeat domains (PRD) (**Figure 3**) separated from each other by linker sequences of variable lengths. The 214-kDa C-terminal globular domain has an estimated diameter of 9 nm (Foisner and Wiche, 1987), suggesting tight packing and circular arrangement of antiparallel oriented plectin PRD1-PRD5 domains with the PRD6 domain in their center (Janda *et al.*, 2001). In its C-terminal domain, plectin contains a multifunctional IF-binding site (IFBS) that was mapped to an

approximately 50 amino acid-long sequence located between the highly conserved core regions of its C-terminal repeats 5 and 6 (Nikolic *et al.*, 1996) (**Figure 3**). This site mediates binding to several types of IF subunit proteins, including vimentin (Nikolic *et al.*, 1996), desmin (Reipert *et al.*, 1999), glial fibrillary acidic protein (Foisner *et al.*, 1988), the nuclear IF protein lamin B (Foisner *et al.*, 1991), and type I and type II cytokeratins (Steinböck *et al.*, 2000). In addition to the IFBS, extreme C-terminus of plectin was found to play important regulatory role in the interaction of plectin with IFs (Bouameur *et al.*, 2013).
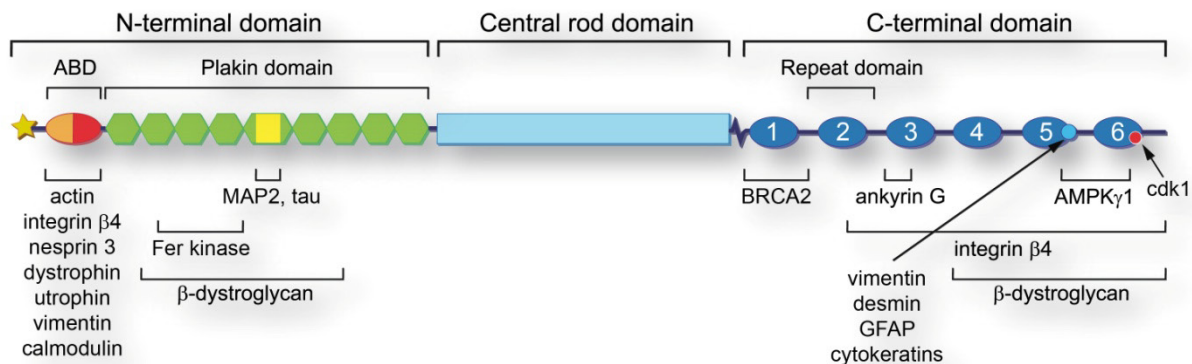
Figure 3. Schematic domain structure of plectin. The N-terminal domain contains an actin-binding domain (ABD) consisting of two calponin homology domains (orange and light red), and a plakin domain comprising nine spectrin repeats (green) and one SH3 domain (yellow). The central rod domain comprises an approximately 200 nm long coiled-coil. The C-terminal domain contains six plectin repeat domains (blue). The region of plectin involved in interaction with different IF-proteins is shown in light blue. Regions responsible for binding to various proteins are indicated below the scheme. Star indicates different N termini of the plectin isoforms generated by alternative splicing of plectin transcripts as shown on Figure 2. The figure was modified from (Castañón *et al.*, 2013).

The N-terminal domain of plectin comprises an actin-binding domain (ABD) (**Figure 3**) shared by a large superfamily of actin-binding proteins (Gimona *et al.*, 2002; Stradal *et al.*, 1998). Several different proteins were shown to directly interact with plectin's ABD, pointing out the multifunctional character of this domain (**Figure 3**). Details about the structure and function of plectin's ABD are described in following sections. Adjacent to the ABD there extends an approximately 1000 residue long region, the so called plakin domain that is conserved among all plakins, except for epiplakin (for detail see previous section). Plectin's plakin domain consists of nine spectrin repeats interrupted by an SH3 domain (Jefferson *et al.*, 2007; Sonnenberg *et al.*, 2007). This domain harbors binding sites for integrin β4 (Koster *et al.*, 2004; Rezniczek *et al.*, 1998), the cytoplasmic domain of BPAG2 (Koster *et al.*, 2003), β-dystroglycan (Rezniczek *et al.*,

2007), β-synemin (Hijikata *et al.*, 2008), and the nonreceptor tyrosine kinase Fer (Lunter and Wiche, 2002).

Several other interaction partners of plectin have been identified, but so far their binding sites on the plectin molecule are not known. In this respect, direct interactions of plectin with the membrane skeleton proteins fodrin and α-spectrin (Herrmann and Wiche, 1987), the desmosomal protein desmoplakin (Eger *et al.*, 1997), and microtubule-associated proteins (MAP2 and tau) from brain (Herrmann and Wiche, 1987), keratinocytes (Valencia *et al.*, 2013), and myocytes (Raith *et al.*, 2013) have been reported. Furthermore, whole-mount electron microscopy was used to demonstrate that plectin is capable of physically linking IFs to microtubules (Svitkina *et al.*, 1996). Except of Fer kinase, plectin was found to interact with other proteins involved in signaling, for instance the receptor for activated C kinase 1 (Osmanagic-Myers and Wiche, 2004), and the γ1 subunit of the energy-controlling AMP-activated protein kinase (Gregor *et al.*, 2006), anchoring them at specific cellular locations.

Actin-binding domain

The ABD is a relatively small (~ 30kDa) domain found in many actin-binding proteins like α-actinin, filamin, fimbrin, but also cytolinkers like BPAG1 and plectin, or proteins connecting membrane-associated proteins with actin network like dystrophin and utrophin. The ABD consists of two related domains, which have been termed 'calponin homology' or CH domains (Castresana and Saraste, 1995), due to their homology to the N-terminal domain in calponins, actin-binding proteins that regulate smooth muscle contraction. So far, several types of CH domains have been identified in the family of CH domain proteins (Gimona *et al.*, 2002). Two CH domains, the type 1 (CH1) and type 2 (CH2), in tandem constitute the ABD. As a single copy, the type 3 CH domain (CH3) is found in proteins that regulate muscle contraction, such as calponin and smooth muscle protein 22-alpha, and signal transduction proteins such as Vav and IQGAPs (GTPase-activating proteins that contain calmodulin-binding IQ motifs). Fimbrin is unique among this family in that it contains two tandem repeats of the actin-binding domain (ABD1, ABD2), and its four CH domains are representative of a fourth type of CH domains.

The first structure of a single CH domain was resolved for CH2 of β-spectrin and CH2 of utrophin (Djinovic Carugo *et al.*, 1997; Keep *et al.*, 1999a). The structure of a canonical ABD consisting of CH1 and CH2 domains was first reported for the N-terminal ABD1 of human

fimbrin (Goldsmith *et al.*, 1997). In the following decade the structures of the ABDs of utrophin (Keep *et al.*, 1999b), dystrophin (Norwood *et al.*, 2000), plectin (Garcia-Alvarez *et al.*, 2003; Ševčík *et al.*, 2004), α-actinin (Borrego-Diaz *et al.*, 2006; Franzot *et al.*, 2005; Lee *et al.*, 2008), and filamin A and B (Clark *et al.*, 2009; Sawyer *et al.*, 2009), were determined. The comparison of these structures revealed that the single CH domain is structurally conserved among the family members and has a novel fold, which is stabilized by almost invariant residues. On the structural level the ABD was found to be dumbbell-shaped, and composed of two α-helical subdomains (CH1/CH2, CH1/CH1' in the case of fimbrin) connected by a variable linker. Interestingly, in contrast to utrophin's and dystrophin's ABD, which crystallized as antiparallel dimers with the two CH domains in relatively extend or open conformation (Keep *et al.*, 1999b; Norwood *et al.*, 2000), all other ABDs crystallised as a compact monomer with the two CH domains closely associated. The orientation of the CH domains in the utrophin and dystrophin crystal structures, however, was such that the CH1 and CH2 domains from each of the separate chains in the crystal dimer closely resembled the orientation of the two CH domains in the crystal structures of other, monomeric ABDs. The major differences between ABDs are found in the linker connecting the CH1 and CH2 domains. In some ABDs, *e.g.* those of utrophin and dystrophin, the linker is a helix, in other ABDs (*e.g.* in that of plectin) it is a loop, or a loop-helix combination (*e.g.* fimbrin) (Goldsmith *et al.*, 1997; Keep *et al.*, 1999b; Norwood *et al.*, 2000; Ševčík *et al.*, 2004). Thus, different flexibility of the linkers between CH domains, was suggested to be responsible for different conformations of the ABDs. In addition, although CH1 and CH2 possess identical topologies, CH1 domains are more closely related to each other across the range of actin-binding domains than to the CH2 domain present in the same protein (Franzot *et al.*, 2005; Stradal *et al.*, 1998). Similar, CH2 domains are more similar to other CH2 domains than to the CH1 of the same protein.

In all cases, the canonical ABD is an efficient F-actin-binding domain with an affinity for F-actin in the low μM range, and no other significant effect on the actin dynamics. Binding assays using mutants and truncated fragments of ABDs (Bresnick *et al.*, 1990; Corrado *et al.*, 1994; Fabbrizio *et al.*, 1993; Hemmings *et al.*, 1992; Kuhlman *et al.*, 1992; Lebart *et al.*, 1990; Levine *et al.*, 1990; Levine *et al.*, 1992), as well as antibody protection studies (Morris *et al.*, 1999) have identified three consensus sequences within the ABDs of filamin, α-actinin, dystrophin and utrophin important for actin-binding and, by homology, it is assumed that these

regions are important for the activity of all ABDs, including plectin. Actin-binding sequences/sites (ABS) 1 and 2 are located near the N- and C termini of the CH1 domain, while ABS3 maps to the N-terminal region of CH2, suggesting these sequences are not sufficient for actin-binding in isolation (Lorenzi and Gimona, 2008). Indeed, whilst the ABDs as a whole are functionally equivalent, in as much as they interact with F-actin, the CH domains they comprise are functionally distinct (Gimona and Winder, 1998). In vitro actin-binding assays have indicated that CH1 alone binds actin, but less strongly than the complete ABD, while CH2 has little affinity in isolation either in vitro (Way *et al.*, 1992a) or ex vivo (Lorenzi and Gimona, 2008).

In recent years, structural approaches have begun to shed light on the mechanism of association of protein possessing ABDs with the F-actin, but precise details of this mechanism are still not clear. Crystal structures of fimbrin's, plectin's, α-actinin's and filamin's ABDs revealed that regions implicated in F-actin-binding are largely inaccessible to solvent (Goldsmith *et al.*, 1997). In fact, in all of these crystal structures, the ABD adopts a closed conformation, which is achieved by an extensive interdomain interaction interface, causing ABS1 to be largely buried between the two CH domains of the ABDs. However, in dimeric, open ABD structures of utrophin (Keep *et al.*, 1999b) and dystrophin (Norwood *et al.*, 2000) the closed conformation is brought about by the domain swapping between two molecules, suggesting that the exposure of ABSs in the ABD, necessary for interaction with F-actin, requires some domain rearrangements. In a search for an answer how CH domains interact with F-actin, several electron microscopy studies of ABD-decorated actin filaments (Galkin *et al.*, 2002; Hanein *et al.*, 1998; McGough *et al.*, 1994; Moores *et al.*, 2000) and of two-dimensional protein crystals (Hampton *et al.*, 2007; Liu *et al.*, 2004) have been performed in recent years. Some electron microscopy studies found that the compact conformation is preserved upon binding to F-actin, whereas other studies suggested that the CHs separate and the ABD becomes extended, leading to controversy between reported results, caused mainly by their ambiguous interpretation (Egelman, 2004; Galkin *et al.*, 2010). Some light into this topic was brought recently by studies on α-actinin's (Galkin *et al.*, 2010) and utophin's ABDs (Lin *et al.*, 2011), indicating that ABDs bind to F-actin in an open conformation (using an induced-fit mechanism), thus regulating their affinity for F-actin. Moreover, different affinities of ABDs for F-actin were suggested to be responsible for directing ABD-containing proteins to various cytoskeletal locations (Washington and Knecht, 2008).

CH domains display an unusually high structural conservation. However, as revealed by

many recent studies, they appear to be highly diverse in their biological functions. α-Actinin in the muscle Z-line was shown to contain bound phosphatidylinositol-4,5-bisphosphate (PIP_2) (Fukami *et al.*, 1992). Later, PIP_2 as well as phosphatidylinositol-3,4,5-triphosphate (PIP_3) were found to interact with the CH2 domain of α-actinin, thus regulating its interactions with actin filaments and integrin β1 receptors (Fraley *et al.*, 2003; Fraley *et al.*, 2005; Greenwood *et al.*, 2000; Kelly and Taylor, 2005). Furthermore, the mechanism of phosphoinositide regulation of α-actinin-F-actin binding, involving structural changes within the CH2 domain of α-actinin upon binding of PIP_2, was recently described (Full *et al.*, 2007). Similarly to α-actinin, PIP_2-binding to both, filamin and dystrophin inhibits their interactions with F-actin (Furuhashi *et al.*, 1992; Mejean *et al.*, 1995), although the precise binding sites in neither of these molecules are known and the physiological significance is uncertain. Calmodulin (CaM) has also been shown to regulate the interaction of dystrophin, utrophin, and filamin A with F-actin through direct binding to the CH1 domains, although again the physiological relevance of this is not clear (Bonet-Kerrache *et al.*, 1994; Jarrett and Foster, 1995; Nakamura *et al.*, 2005; Winder *et al.*, 1995; Winder and Kendrick-Jones, 1995). In the case of filamin A, neither the full-length filamin A nor its ABD were found to bind to CaM in the absence of F-actin, suggesting that the CaM-binding site in the CH1 domain of filamin A is hidden and becomes exposed only upon binding to F-actin (Nakamura *et al.*, 2005).

Tandem CH domains have long been known to make up the ABD of many F-actin-binding proteins. In recent years, it has become clear that single CH domains or ABDs with tandemly arranged CHs can bind to IFs, while pairs of CH domains, coming either from two identical or distinct polypeptide chains can bind MTs. In this context, calponin has been reported to interact with desmin, the major IF protein of smooth and striated muscle (Fujii *et al.*, 2000; Mabuchi *et al.*, 1997; Wang and Gusev, 1996), and for fimbrin a colocalization with vimentin was observed in cultured macrophages (Correia *et al.*, 1999). In both cases it was suggested that interactions were mediated by CH domains. Moreover, specific interaction of dystrophin's ABD with intermediate filaments containing keratin 19 was confirmed both *in vitro* as well *in vivo* (Stone *et al.*, 2005). Examples of microtubule-interacting CH domains coming from two separate polypeptides were found in the Ncd80 complex, a core component of the kinetochore, linking the chromosomal spindle to microtubules of the mitotic spindle, and in CH domain-containing proteins of the EB1 family binding to plus ends of microtubules (Sjöblom *et al.*, 2008a).

Actin-binding domain of plectin

cDNA sequencing revealed a highly conserved ABD in proximity of plectin's amino-terminal end, which is of the type found in a large family of actin-binding proteins (see above) (Elliott *et al.*, 1997). Later, the structure of plectin's ABD was determined, revealing the ABD to be an α-helical protein consisting of 11 helices possessing the same structural fold as it was observed for other ABDs (**Figure 4**) (Garcia-Alvarez *et al.*, 2003; Ševčík *et al.*, 2004). Concerning its binding to F-actin, plectin's ABD was shown to be functional, both *in vitro*, upon expression in recombinant form, and *in vivo*, when ectopically expressed in cells (Andrä *et al.*, 1998; Rezniczek *et al.*, 2003). A yeast two hybrid assay using plectin's ABD showed that plectin is able to bind to various actin isoforms: α-skeletal muscle, β-cytoplasmic and γ-cytoplasmic actin (Fontao *et al.*, 2001). In the same study, the ABS2 of plectin's ABD was found to be important not only for binding to actin, but also for dimerization of plectin's ABD. However, although ABS2 seems to be involved in both interaction types, dimerization of plectin's ABD does not prevent interaction with actin (Fontao *et al.*, 2001). Similar to the CH2 domain of other CH-family members (see above), plectin's CH2 domain does not seem to be implicated in the binding to actin. Rather it appears to have a regulatory function on actin-binding, since its partial or complete removal increases plectin-actin binding (Fontao *et al.*, 2001). Binding of plectin's ABD to F-actin was shown to induce a conformational change in plectin that was inhibited by an engineered interdomain disulfide bridge (Garcia-Alvarez *et al.*, 2003). Based on this observation, a two-step induced-fit mechanism, involving binding of plectin to F-actin with subsequent domain rearrangement of plectin's ABD, was proposed. In a recent study, the crystal structure of the closed plectin ABD was superimposed on the high resolution model of α-actinin's CH1 domain bound to F-actin, revealing that in this conformation, the CH2 domain of plectin makes a steric clash with the actin subunit (Galkin *et al.*, 2010). This implied that opening of the two CH domains, important for elimination of resulting steric clash, is required for binding of plectin to actin (Galkin *et al.*, 2010).

Except for its primary function, i.e. binding to actin, plectin's ABD was shown to interact with the cytosolic tail of integrin β4 (Geerts *et al.*, 1999; de Pereda *et al.*, 2009; Rezniczek *et al.*, 1998). Residues crucial for this binding are clustered on the surface of the first N-terminal CH domain (CH1) of plectin's ABD. The binding of integrin β4 to the ABD is mutually exclusive with that of F-actin, which may explain why plectin mediates the linkage of HDs to the cytok-

eratin system and not to actin filaments (Geerts *et al.*, 1999). In addition, the formation of the integrin β4-plectin complex induces conformational changes in β4 and plectin, suggesting that their interaction is subject to allosteric regulation (de Pereda *et al.*, 2009). The ABD of plectin also binds to the first spectrin repeat of nesprin 3α, which is an outer nuclear membrane protein (Ketema *et al.*, 2007; Postel *et al.*, 2011; Wilhelmsen *et al.*, 2005). Several residues in the ABD of plectin that are crucial for binding to the integrin β4 subunit are also important for the binding to nesprin-3α, indicating partial overlapping binding sequences for nesprin 3α and integrin β4 (Postel *et al.*, 2011). Binding to nesprin 3α also competes with the interaction between the ABD and F-actin (Ketema *et al.*, 2007), suggesting competitive behavior between F-actin, nesprin 3α and the integrin β4 subunit for binding to plectin's ABD. In skeletal muscle, plectin was found to directly interact with the WW-ZZ domain of dystrophin/utrophin via its ABD (Rezniczek *et al.*, 2007). Moreover, the WW-ZZ domain of dystrophin competed with that of utrophin for plectin ABD-binding, as did actin, indicating that simultaneous binding of actin and WW-ZZ domains to the plectin's ABD is unlikely to occur (Rezniczek *et al.*, 2007). Furthermore, interaction of plectin's ABD with the ABD of BPAG1-b was observed in *vitro* (Litjens *et al.*, 2003), and later on also *in vivo* (Steiner-Champliaud *et al.*, 2010). Finally, interaction of plectin's ABD with calmodulin and the non-filamentous vimentin was identified and characterized within this thesis (for details see Results section) (Kostan *et al.*, 2009; Ševčík *et al.*, 2004).

In essence, plectin's ABD is capable to interact with a plethora of different proteins, thus being multifunctional. In order to mediate different tasks, the activity of plectin's ABD needs to be regulated and/or fine tuned. Similarly to α-actinin, filamin and dystrophin, PIP_2 was found to inhibit binding of plectin's ABD to F-actin (Andrä *et al.*, 1998). Although the direct binding of PIP_2 to plectin's ABD was not shown, based on structural similarities between plectin's ABD and the ABDs of other members of the CH family (Ševčík *et al.*, 2004), it is assumed that PIP_2 interacts with the CH2 domain of plectin. On the other hand, a recent correlation of the predicted amino acid residues that bind to PIP_2 with the structural information on the ABD of the human α-actinin isoform 3 (Franzot *et al.*, 2005), suggested a new set of residues involved in PIP_2-binding, which are, however, present only in the CH2 domains of α-actinin isoforms (Sjöblom *et al.*, 2008b). The ABD of plectin is unique among the ABDs of other CH family member due to its isoform diversity. Until now, depending on the presence of the alternative exons 2α and 3α (**Figure 2**), three isoforms of plectin's ABD have been identified (Fuchs *et al.*, 1999). One is the

isoform without any additional exons, the others are isoforms containing exon 2α or both, exon 2α and 3α (Fuchs *et al.*, 1999). No ABD containing exon 3α alone has been identified so far. The role of these additional sequences is still not clear, but it was already shown, that they could influence binding to actin, as the isoform ABD/2α binds actin better than other isoforms (Fuchs *et al.*, 1999). The variability of plectin's ABD is further increased by an unusually high number of 14 alternatively spliced exons, 11 of which are directly spliced into exon 2, a first of 7 exons (exons 2-8) encoding plectin's ABD (Fuchs *et al.*, 1999). Interestingly, using of 5'-RACE analysis, exon 2α was found in combination only with exons 1, 1b, and 1d, whereas 2α and 3α together were found in cDNAs starting with exon 1c or 1j. Thus being localized in the vicinity of the ABD, first exon-encoded sequences are assumed to influence the structure and/or function of the ABD, by providing a new binding site for regulatory molecules or binding partners, or to introduce conformational changes within the ABD, thus modulating the affinities of plectin towards known interaction partners. So far, the precise function(s) of the various N-terminal sequences of plectin have not been fully elucidated. However, some of the isoform-specific sequences have been shown to direct the protein to distinct cellular locations, such as HDs, microtubules, mitochondria, costameres, and Z-disks (Andrä *et al.*, 2003; Konieczny *et al.*, 2008; Rezniczek *et al.*, 2003; Rezniczek *et al.*, 2007; Winter *et al.*, 2008). Recently, plectin isoform 1f has been reported to be recruited to focal adhesion of mouse fibroblasts via direct binding to actin with the preceding 1f isoform-specific sequence regulating/fine tuning its binding affinity (Burgstaller *et al.*, 2010). Uncovering the role of first exon-encoded sequences in regulating different activities of plectin's ABD was part of this thesis, and the results obtanied are presented in the following sections.

3D structure of plectin

During the last decade, the crystallographic 3D structures of several fragments of plectin have been elucidated (**Figure 4**). These include the structure of the ABD of human and mouse plectin (Garcia-Alvarez *et al.*, 2003; Ševčík *et al.*, 2004), the structure of a tandem pair of plectin`s spectrin repeats SR1-SR2 (Sonnenberg *et al.*, 2007), the structure of the first half of the plakin domain of plectin (Ortega *et al.*, 2011), and the crystal structure of the primary integrin α6β4-plectin complex, formed by the first pair of fibronectin type III domains and the N-terminal region of the connecting segment of integrin β4 and the actin-binding domain of plectin (de

Pereda *et al.*, 2009). In addition, secondary structure analysis revealed that the plectin repeat domain (PRD), possess a globular fold similar to the fold of the ankyrin repeat (Janda *et al.*, 2001). This was later supported by the structures of two PRDs of desmoplakin, which are homologous to the repeats found in the C-terminal region of plectin and BPAG1e (Choi *et al.*, 2002). Structure model of both, the human and mouse plectin ABDs revealed that plectin's ABD is an α-helical protein formed by two calponin homology domains, CH1 and CH2, each of which is built around a conserved core of four α-helices **(Figure 4A)**. The plectin ABD structure (human as well as mouse) was found to be in the "closed" monomeric conformation similar to that previously observed for α-actinin-3 (Franzot *et al.*, 2005), fimbrin (Goldsmith *et al.*, 1997) and filamin B (Sawyer *et al.*, 2009), which contrasts with the domain-swapped dimer observed in utrophin (Keep *et al.*, 1999b) and dystrophin (Norwood *et al.*, 2000). The latter conserves the same CH1-CH2 interface but between two "open" monomers. In both cases, where the crystal structure of plectin's ABD were reported, the ABDs analyzed, corresponded to the isoform containing the extra five amino acids (HWRAE) encoded by exon 2α, a differentially spliced exon inserted between the common exons 2 and 3 (Urbániková *et al.*, 2002; Garcia-Alvarez *et al.*, 2003; Ševčík *et al.*, 2004).

This insertion was found to make the connecting loop of helices α1 and α2 (located closely to ABS1) longer, thus outlining the mechanism for increased actin-binding activity of the ABD/2α isoform, as reported by Fuchs *et al.* (1999). As observed in other tandem pairs of CH domains, the CH domain of plectin is structurally more similar to the equivalent CH domains of other proteins than to the companion CH domain (Franzot *et al.*, 2005; Ševčík *et al.*, 2004). The major difference in the tertiary structures of human and mouse plectin was found at their N termini, where the first α-helix of human plectin exceeded that from mouse by nine amino acid residues. However, in this case, six of these additional residues were encoded by isoform-specific exon 1c preceding the actual ABD-encoding exons 2-8. Recently, the crystal structure of plectin's ABD preceded with full-length exon 1c in complex with the first pair of FnIII domain and part of the connecting segment (linker region) of integrin β4 has been determined (de Pereda *et al.*, 2009), allowing to compare the structure of plectin exon 1c-encoded sequences in bound and free form **(Figure 4A)**. Interestingly, while in the free structure, residues encoded by exon 1c, were part of the N-terminal α-helix of the CH1 domain (Garcia-Alvarez *et al.*, 2003), in the β4-bound structure, this segment adopted an extended conformation, forming the N-terminal arm that binds
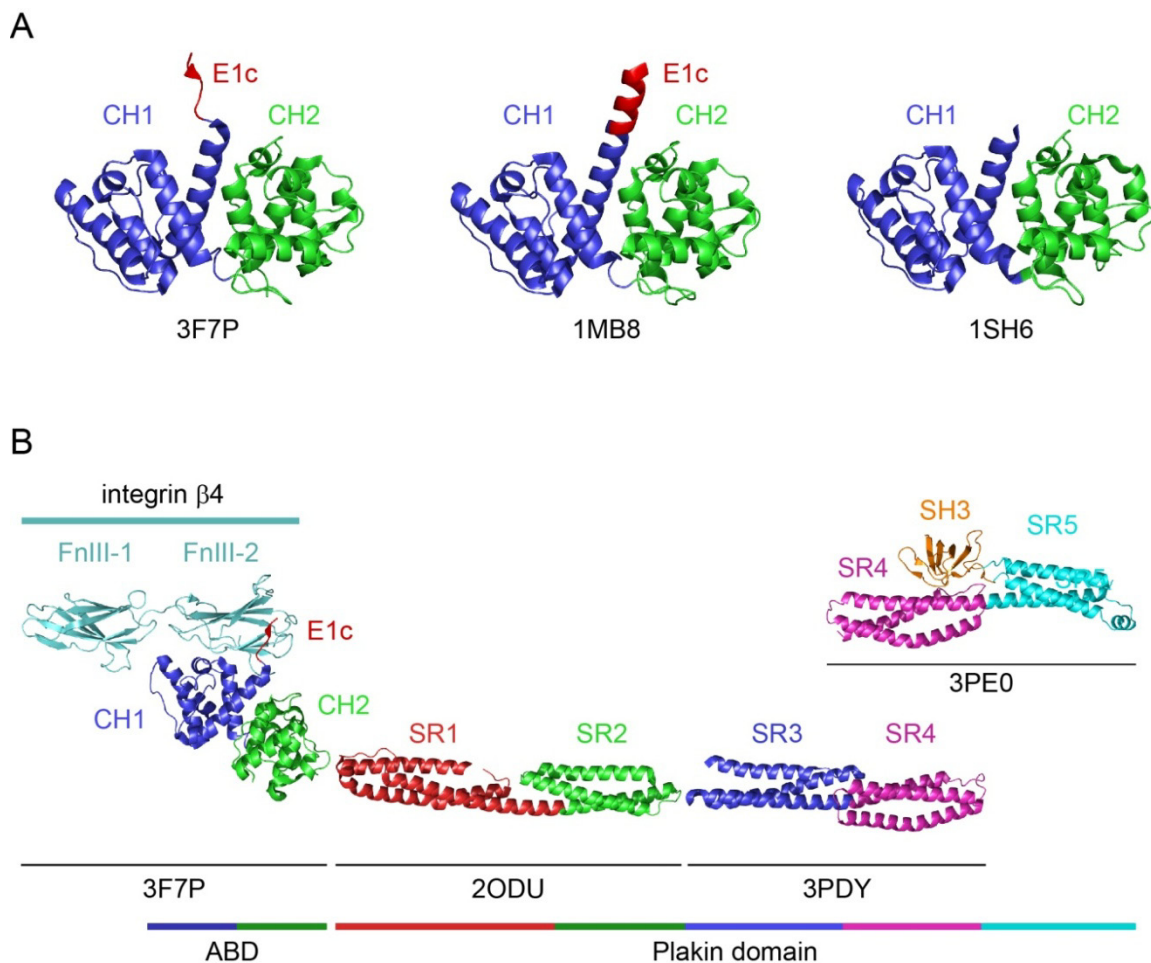
Figure 4. Crystal structures of plectin subdomains. (*A*) Structure of the human plectin ABD crystalized in the complex with integrin β4 (PBD code: 3F7P). Structure of plectin's ABD without integrin β4 is shown. Structure of the human (PBD code: 1MB8) and the mouse (PBD code: 1SH6) plectin ABD crystalized alone. Ribbon presentations of the ABD structures in equvivalent orientations is shown. In all structures, the ABD was found to be in the 'closed' conformation with the CH1 domain (blue) forming extensive contacts with the second CH2 domain (green). Sequences belonging to the N terminus of plectin encoded by exon 1c, adopting different conformation in the integrin β4 bound (PBD code: 3F7P) and free from (PBD code: 1MB8) are shown in red. (*B*) All known crystal stuctures of plectin subdomains map to the N-terminal part of the protein. Structure of plectin's ABD as found in the complex with integrin β4 (PBD code: 3F7P), structures of tandem pair of plectin`s spectrin repeats SR1-SR2 (PBD code: 2ODU), SR3-SR4 (PBD code: 3PDY) and SR4-SR5 with SH3 domain insetred between them (PBD code: 3PE0) resembling the N-terminal part of plectin plakin domain are shown.

in antiparallel fashion to the β-strand E of the second FnIII of integrin β4 (de Pereda *et al.*, 2009). Folding into different structures on binding to different targets is a feature of many intrinsically unfolded proteins and disordered recognition elements (Wright and Dyson, 2009). In this respect, plectin's first exon-encoded sequences might function as recognition and/or binding elements of

several distinct proteins, which modulate the activity of plectin's ABD upon binding.

Adjacent to the ABD extends an approximately 1000 residue-long region named the plakin domain that is conserved in all plakins, except of epiplakin (see above). In plectin this region consists of nine spectrin repeats (SR) and the SH3 domain inserted in the central SR5 repeat making extensive interactions with SR4 (**Figure 4B**). Very recently a combination of X-ray crystallography and small angle X-ray scattering helped to elucidate the structure of the central region of the plakin domain of plectin, comprising the SR3, SR4, SR5, and SH3 domains (Ortega *et al.*, 2011). The crystal structures of the individual SR3-SR4 and SR4-SR5-SH3 fragments were determined (**Figure 4B**) and used to create a model for the SR3-SR4-SR5-SH3 region, which was confirmed with SAXS data in solution. When compared with canonical proline-rich binding SH3 domains, the SH3 of plectin presented major alterations suggesting that plectin does not recognize proline-rich motifs. In addition, the overall structural organization of the plakin domain was found to be highly similar to that of α- and β-spectrins and other members of the spectrin superfamily, suggesting that the region of the plakin domain forms an array of concatenated SRs adopting an elongated rod-like structure (Ortega *et al.*, 2011). This was confirmed by the crystal structure of a rigid four-spectrin-repeat fragment of the human desmoplakin plakin domain (Choi and Weis, 2011).

Plectin´s function in hemidesmosomes

Hemidesmosomes (HDs) are evolutionarily conserved attachment complexes linked to the intracellular intermediate filament (IF) network system that connect epithelial cells, such as keratinocytes, to the extracellular matrix (ECM). HDs are found in epithelial tissues, in particular those exposed to mechanical stress such as the skin, oesophagus, and intestine. They provide tissue integrity and resistance to mechanical forces, but are also involved in cell migration processes, such as wound healing and carcinoma invasion (Lipscomb and Mercurio, 2005; Mercurio *et al.*, 2001). Therefore, alterations in HD structures are responsible for skin blistering, carcinoma invasion, and wound-healing defects. Mammalian HDs include type I HDs in the skin, mouth, and oesophagus, and type II HDs mainly found in intestinal epithelial cells (Margadant *et al.*, 2008). Type I HDs consist of the integrin α6β4, the type XVII collagen/BPAG2, the integrin-associated tetraspanin CD151, plectin and BPAG1e (**Figure 5**). Integrin α6β4, BPAG2 and CD151 are transmembrane proteins, while plectin and BPAG1e are located in the cytoplasm. The

membrane receptor integrin α6β4 connects to the basement membrane through laminin 332. The integrin α6 subunit also interacts with the tetraspanin CD151, and BPAG2 weakly associates with laminin-332. The intermediate filaments, keratin 5 and keratin 14, are associated with integrin α6β4 indirectly through plectin and BPAG1e. In contrast to type I, type II HDs consist of only integrin α6β4 and plectin, and are linked to keratins 8 and 18 (**Figure 5**).

The crucial event in HD assembly is the interaction between β4 and plectin, as indicated by both, the existence of type II HDs, which can apparently form in the absence of BPAG2 and BPAG1e, and by in vitro evidence indicating that by preventing the plectin-integrin β4 interaction, the formation of HDs is severely compromised (Geerts *et al.*, 1999; Koster *et al.*, 2004). Furthermore, plectin`s importance in epithelia is convincingly supported by the severe skin blistering observed in plectin-deficient humans and mice (see above). Similarly, the absence of integrin α6β4 leads to severe skin blistering and near absence of HDs in mice (Georges-Labouesse *et al.*, 1996; van der Neut *et al.*, 1996), while the hypoplastic nature of HDs have been observed in patients with mutations in β4 that prevent this interaction (Koster *et al.*, 2001; Nakano *et al.*, 2001). Various regions of plectin have been shown to be involved in its interaction with integrin α6β4. One of them is a canonical ABD, which binds to the first pair of fibronectin type III (FnIII) domains of the β4 subunit, and the N-terminal region of the segment connecting the second and third FnIII domains of integrin β4 (C-segment). Without this β4 region, plectin is not targeted to HDs (Niessen *et al.*, 1997). The ABD of plectin binds to integrin β4 through its CH1 domain. There is no direct contact between the CH2 domain and integrin β4 (de Pereda *et al.*, 2009), yet the CH2 is required for binding to β4 (Geerts *et al.*, 1999). A second integrin β4-binding site, located in plectin's plakin domain (Rezniczek *et al.*, 1998), interacts with sequences downstream of the second FnIII domain of integrin β4 (Koster *et al.*, 2004). In addition, interactions of plectin's C-terminal repeat domain PRD6 with the C-segment of integrin β4, and with integrin β4's tail domain, have been reported (Rezniczek *et al.*, 1998).

Plectin's versatile crosslinking and scaffolding abilities are augmented by the unusual 5' complexity of its transcripts generated by differential splicing of at least 11 alternative first exons (see above; Fuchs *et al.*, 1999). Of all plectin isoforms expressed in mouse, isoform P1a was found to be dominantly expressed in epithelial tissues (Fuchs *et al.*, 1999). Similarly, using quantitative RNase protection assays, P1a was shown to be most prominently expressed in primary human keratinocytes (71% of all transcripts detected), followed by isoforms containing

exon 1c- (22%), exon 1- (4%), and exon 1b- (1%) encoded sequences (Andrä *et al.*, 2003) In addition, keratinocyte cell lines derived from human basal keratinocytes of patient suffering from pyloric atresia associated with junctional epidermolysis bullosa (PA-JEB), or epidermolysis bullosa simplex associated with muscular dystrophy (EBS-MD), were, found to express P1c at lower levels when compared to P1a (Litjens *et al.*, 2003).
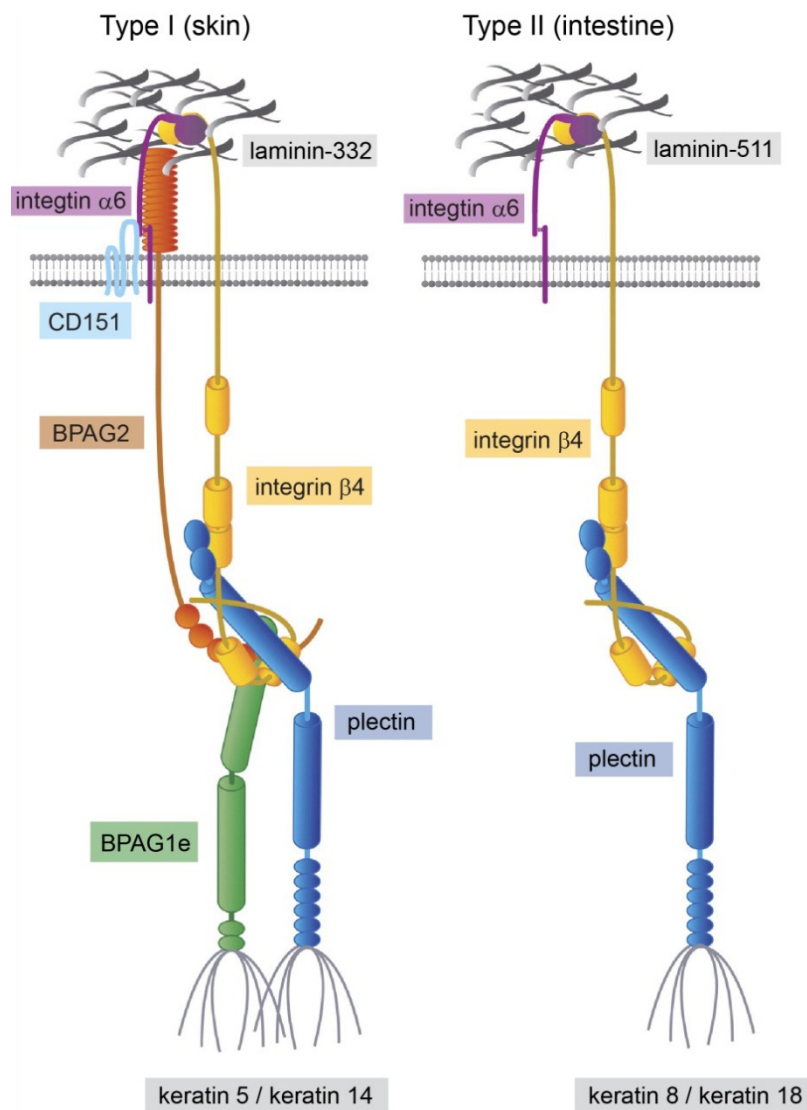
Figure 5. Schematic illustration of the structure and components of hemidesmodomes. Whereas simple epithelia such as that of the intestine express type II hemidesmodomes consisting solely of integrin α6β4 and plectin, the epidermis contains type I hemidesmosomes that consist of integrin α6β4, plectin, tetraspanin CD151, and the bullous pemphigoid antigens BPAG2 and BPAG1e. Binding of α6β4 and BPAG2 to laminin-332 is stabilized intra-cellularly *via* their association with keratins 5 and 14, through plectin and BPAG1e. In contrast to type I, type II hemidesmosomes are linked via plectin to keratins 8 and 18. The figure was modified from (Margadant *et al.*, 2008).

Although, there is no sequence similarity between exon 1a- and 1c-encoded sequences, both P1a and P1c were shown to interact with integrin β4 (Litjens *et al.*, 2003). Recently, the crystal structure of the first pair of FnIII domains in complex with plectin's ABD preceded by

exon 1c-encoded sequences has been published, supporting this observation (de Pereda *et al.*, 2009). Moreover, the plectin fragment comprising plectin's ABD preceded by exon 1a-encoded sequences was shown to have the same affinity for integrin β4, as the analogous fragment preceded with exon 1c-encoded sequences, suggesting that the N-terminal region encoded by exon 1a does not enhance the interaction with integrin β4. On the other hand, upon deletion of both 1a and 1c exon encoded sequences, plectin was found to localize into HDs more efficiently, indicating that binding of plectin to integrin β4 can be regulated via the N-terminal sequences (Litjens *et al.*, 2003), which might bind to other HD components or regulators. Although, P1c can interact with integrin β4, from all plectin isoforms expressed in primary human keratinocytes, only P1a was shown to anchors keratin IFs to HDs (Andrä *et al.*, 2003). In contrast, P1c was found to colocalize with microtubules in these cells, and its localization in HD structures was never observed (Andrä *et al.*, 2003).

The assembly and disassembly of HDs play an important role in keratinocyte migration during wound healing, differentiation, and carcinoma invasion, yet the mechanisms that control HD dynamics are not fully understood. So far, mechanisms found in different organisms revealed that HD formation and maintenance in vivo are carefully controlled by ECM protein folding, ECM-receptor expression and trafficking, and by post-translational modification of HD components. Several growth stimuli, including epidermal growth factor (EGF) and macrophage stimulating protein, have been implicated in the regulation of HD disassembly, and phosphorylation of integrin β4 by its effector molecule protein kinase C (PKC) leads to partial disassembly of HDs (Margadant *et al.*, 2008). In addition, it has been shown that phosphorylation of integrin β4 involving tyrosine protein kinase Fyn plays a role in HD disassembly (Mariotti *et al.*, 2001). However, controversy remains in explaining their roles in HD formation due to unphysiological experimental conditions (Margadant *et al.*, 2008). In addition, a recent study revealed that PMA- and EGF-stimulated phosphorylation of integrin β4 might not be mediated by PKC, but by ERK1/2 and its downstream effector kinase p90RSK1/2 (Frijns *et al.*, 2010). However, the diversity of plectin-integrin binding sites points towards a more complex regulation, especially as the predicted phosphorylation sites on integrin β4 map to the C-segment (Litjens *et al.*, 2006; Wilhelmsen *et al.*, 2007), presumably leaving other major binding interfaces, such as that between plectin's ABD and the first pair of FnIII domains, unaffected. In accordance with this, several models for regulation of integrin β4-plectin disassembly involving phosporylation of

integrin β4 and/or binding of additional, third partner have been proposed (Litjens $et\ al.$, 2006). In addition, Ca^{2+} has been reported to induce the cellular redistribution of the HD protein, BPAG2 (Kitajima $et\ al.$, 1992), and integrin α6β4 has been found to be down-regulated during Ca^{2+}-induced differentiation of cultured keratinocytes (Tennenbaum $et\ al.$, 1996). Thus, Ca^{2+}, which has an established role in the normal homeostasis of mammalian skin and serves as a modulator in keratinocytes proliferation and differentiation, might be an additional regulator of HD formation and/or disassembly.

Aim of Thesis

Plectin is a large protein with a tripartite domain structure containing features allowing it to act as an extremely versatile cytolinker. This versatility is provided through plectin's ability to bind to a variety of other cytoskeletal and signal transduction molecules, allowing it to integrate their functions. Although, plectin's functions are regulated by postranslation modifications as well, main regulatory functions reside in its first exon-encoded sequences which target plectin to different cell compartments and thus predetermine its binding partners. As the activity of the C-terminal IF-binding site of plectin seems to be isofom-independent, first exon-encoded sequences in addition to their proposed targeting function were proposed to regulate the activity of the N-terminal ABD of plectin and thus modulate functions of the whole protein.

The main goal of this thesis was to find mechanisms how isoform-specific first exon-encoded sequences regulate the functions of plectin and its ABD using structural, biochemical and ex vivo approach. The following three subjects were addressed: (1), determination of the 3D structure of first exon-encoded sequences connected to the adjacent ABD. Here I focused on two major plectin isoforms expressed in basal keratinocytes, P1a and P1c, as these were already characterized by in vivo studies showing their differential subcellular localization and function. A major effort was made to establish strategies for the production of proteins in high purity and quality suitable for crystallization studies (2), the identification and the characterization of new binding partner(s) of plectin`s ABD, potentially involved in the structural stabilization of plectin's first exon-encoded sequences. Here the new binding partner(s) were selected based on the structural and functional relationship of plectin's ABD with other CH protein family members. These studies were to be carried out using in vitro binding assays, (3), the identification and characterization of isoform-specific binding partners of P1a, focusing on the biological significance of the interaction rather than its structural implications.

Results

This result section is organized into three parts. The first part deals with the structural characterization of plectin 1a- and 1c- isoform specific sequences. Part two is focused on the interaction of plectin with vimentin via its N-terminal actin binding domain. Finally, part three addresses the role of plectin in HD disassembly, focusing on isoform-specific interaction of plectin 1a with the calcium regulated protein calmodulin. Note that most of the data presented in part two and three have already been published (Ševčík *et al.*, 2004; Kostan *et al.*, 2009)

For simplification, all proteins or expressed fragments are specified by the names or abbreviations followed by their exon/domain composition. When the domain name is used, instead of the exon composition, exons encoding the domain are usually specified when the domain is first introduced. Thus for example, a recombinant plectin protein encoded by exons 1a-8 is termed P1a-8, or P1aABD. In the case of the full-lenght protein, it is simply P1a. When the protein was expressed with a fused tag, which was not proteolytically removed, the name of the fusion tag is written in front (N-terminal fusion) or after (C-terminal fusion) the protein's name separated by a dash. Accordingly, His-P1a-8, or His-P1aABD denotes a protein encoded by plectin exons 1a-8 preceded by His-tag. In the case of plectin's ABD (encoded by exons 2-8), the first exons-encoded sequences preceding it are specified by an exon name in front of ABD, while alternatively spliced exons within the ABD are specified by the exon name separated by a slash (e.g P1aABD/2α). The exon nomenclature follows the one of the mouse plectin gene (Fuchs *et al.*, 1999). The plasmid name corresponding to a particular recombinant protein is usually given when the protein is first introduced. A complete list of all plasmids used can be found in the Material and Methods section.

PART 1 - Purification, crystallization and structure determination of plectin's ABD preceded by exon 1a- or exon 1c-encoded sequences

Secondary structure prediction using Psipred server (Bryson *et al.*, 2005) revealed that plectin's first exon-encoded sequences are mostly disordered (**Figure 6**). This was partially confirmed by using of IUPred server (Dosztányi, at al., 2005), predicting intrinsically unstructured regions of the proteins. However, in almost all of these sequences, distal regions

adjacent to plectin's ABD were predicted to form a helix making the first helix of plectin's ABD (encoded by plectin exon 2) significantly longer (**Figure 6**).

Such a helix would most likely extend from the protein's compact ABD, as it was shown for the ABD preceded with the last six amino acids of exon 1c (Garcia-Alvarez *et al.*, 2003, and **Figure 4A**). In addition, this helix formation might be promoted or inhibited upon binding of plectin to specific binding partner (*e.g.* integrin β4, for details see Introduction)

Figure 6. Secondary structure prediction of selected plectin first exon-encoded sequences connected to plectin's ABD. Secondary structure of P1a -, P1b-, P1c- , and P1f-isoform specific sequences preceding plectin's ABD was predicted by Psipred, Protein Structure Prediction Server at University College London. First exon encoded sequences are highlighted in red, while sequence belonging to plectin's ABD is shown in black. Confidence of prediction to form secondary structural elements for each amino acid is displayed by the size and the intensity of the blue box. Prediction result is shown graphically, as well as, by letter code, where C stands for coil, H for helix, and S for strand.

Purification and crystallization of His-tagged versions of plectin's ABD preceded by P1a- and P1c-specific sequences

Here we tried to gather structural information about plectin ABD preceded either with exon 1a- or 1c- specific sequences, as P1a and P1c are the major isoforms of plectin expressed in primary keratinocytes, being differentially distributed within these cells (Andrä *et al.*, 2003). We decided to focus on full-length versions of these peptides taking advantage of existing constructs encoding N-terminally His-tagged versions of P1aABD and P1cABD/2α. The advantage of using

these constructs was the optional removal of N-terminal His-tags by the protease thrombin. In the case of P1cABD we selected the version of the ABD with a sequence (of 5 amino acids) encoded by the alternatively spliced exon 2α. The reason for this was that the tryptophan residue encoded within this sequence was found to be import for the successful crystallization of the mouse plectin ABD (Ševčík *et al.*, 2004). In addition, exon 1c was found to be expressed in combination with exon 2α, in contrast to exon 1a (Fuchs *et al.*, 1999). A single nickel affinity chromatography step combined with thrombin cleavage and subsequent extensive dialysis to remove cleaved His-tag has previously been found to be efficient for the purification of plectin's ABD alone (Urbániková *et al.*, 2002). Therefore, we used the same methodology for purifying both protein variants. Results of a typical affinity purification step used for the isolation of P1aABD and P1cABD/2α, i.e. an elution profile of P1aABD from a 10 ml His-Bind column is show on **Figure 7**.
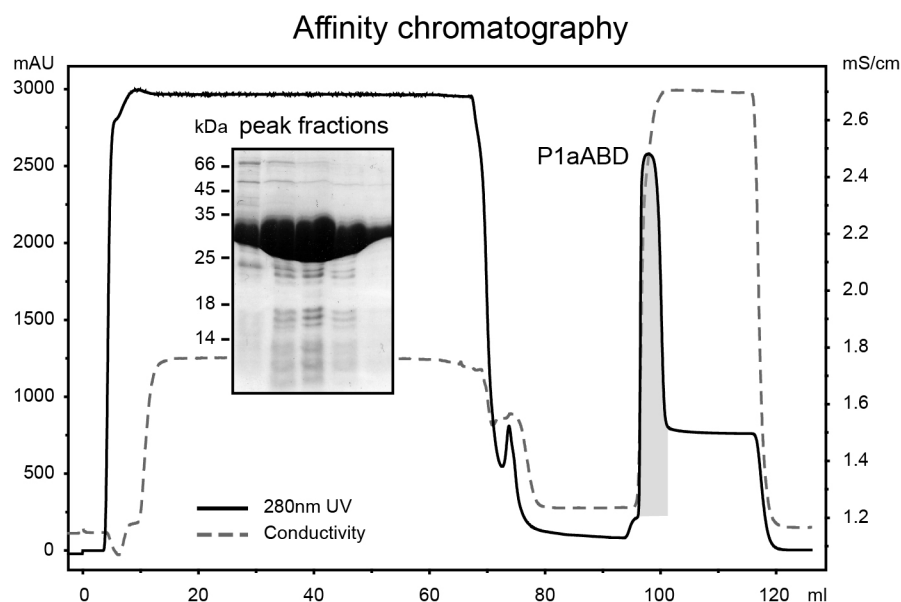
Figure 7. Purification of P1aABD using affinity chromatography. The solid line corresponds to the absorbance ($A_{280\,nm}$) trace of the proteins eluting from the HisTrap HP 5ml column. To follow step gradient elution, conductivity was monitored (dashed line). Panel shows SDS-PAGE of peak fractions, indicated in grey, containing mainly P1aABD. Positions of molecular weight markers are indicated on the left side of the panel.

Protein purity and homogeneity was followed by SDS-PAGE, which yielded a single protein band with an apparent relative molecular mass of 34000 Da, and 37000 Da for P1aABD and P1cABD/2α, respectively. The yields of purified proteins were typically 20-50 miligrams of

lyophilized protein from 1 liter of *E.coli* culture. Prior to crystallization, both proteins (P1aABD and P1cABD/2α) were treated with thrombin to remove the His-tag. Since the cleavage efficiency was close to 100% under the conditions used (see Materials and Methods section), a second purification step for removing uncleaved protein was not carried out. Thus, proteins (P1aABD and P1cABD/2α) were purified using a single purification step resulting in protein samples of sufficient purity and quantity for crystallization trials.
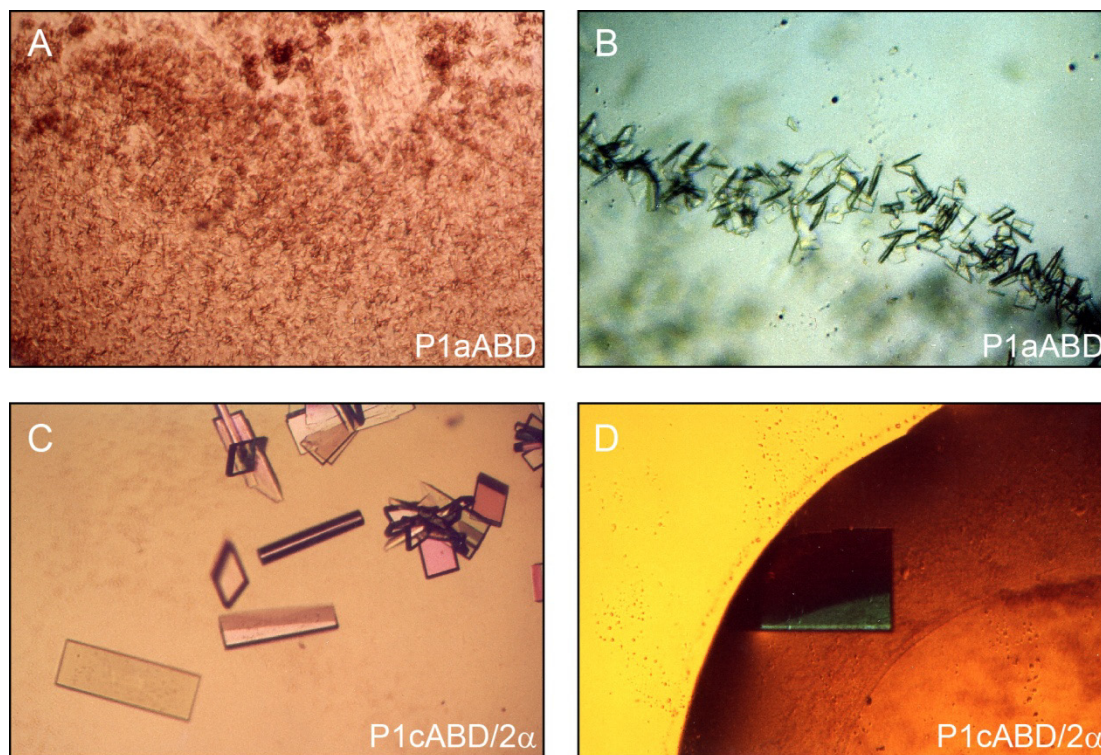
Figure 8. Crystallization of P1aABD and P1cABD/2α. (*A*) Initial microcrystals of P1aABD grew from 0.1 M Tris pH 8.5, 0.2 M magnesium chloride, 3.4 M 1,6-hexanediol at very high density. (*B*) Single crystals were obtained using micro-seeding into a drop equilibrated for 24 h, at 22°C under original conditions. Prior to seeding, precipitated protein and nuclei were removed by centrifugation. (*C*) Plate-like crystals of P1cABD/2α appeared after a few days. (*D*) After several optimization rounds single crystals with dimension of 0.5 x 0.3 x 0.3 mm, suitable for data collection formed in 0.1 M sodium cacodylate, pH 6.5, 0.2 M magnesium acetate, 10 % (w/v) PEG 8000.

Crystallization of purified plectin fragments was done in collaboration with the group of Josef Ševčík (Institute of Molecular Biology, Slovak Academy of Sciences, Bratislava, Slovakia) using the hanging-drop diffusion methodology, and Hampton Screen 1 and 2 (for details see Materials and Methods section). P1aABD initially crystallized in the form of over-nucleated micro-crystals with very high density (**Figure 8A**). Screening for optimal condition with focus on

suppression of over-nucleation did not lead to the desired increase of crystal quality. The biggest improvement was finally achieved by using the micro-seeding technique, which led to the formation of plate-like crystals at sites where streak-seeding had been performed (**Figure 8B**). At this stage, further optimization of P1aABD crystals was discontinued due to the problems with protein sample homogeneity (for details see below). In the case of P1cABD/2α, already under crystallization conditions initially applied, plate shaped crystals (**Figure 8C**) appeared after a few days. Further optimization of these conditions led to the formation of relatively large, single crystals which could be used for data collection (**Figure 8D**).

Structure of P1cABD/2α

Data collection and structure solution were done by Ľubica Urbániková (group Dr. J. Ševčík). The final structure shown was not completely refined (it went through only a few cycles of refinement). However, better refinement of the structure would not improve the quality of the model to an extent which would affect or change our conclusions (see refinement statistics in **Table 1**). P1cABD/2α crystallized in the orthorhombic space group $P2_12_12_1$ with one molecule in the asymmetric unit. Data were collected to 2.0 Å resolution at 100 K on the EMBL X-11 beamline at the DORIS storage ring, DESY, Hamburg. The structure was solved by molecular replacement using the structure of plectin's ABD (PDB code: 1SH6) as a search model. Data collection and refinement statistics are summarized in **Table 1**. Similar to the structure of mouse or human plectin ABD/2α (Ševčík *et al.*, 2004, Garcia-Alvarez *et al.*, 2003), P1cABD/2α was found to be a monomer structurally adopting a closed conformation, in which the CH1 and CH2 domains were in extensive contact. Indeed, superposition of human plectin's ABD/2α (PDB code: 1MB8, Garcia-Alvarez *et al.*, 2003), comprising 6 amino acids residues of P1c specific sequence, with the P1cABD/2α structure gave a root means square deviation of 0.82 Å for 235 (out of 243) Cα atoms, indicating that the two structures were almost identical. However, as P1cABD/2α comprises the entire 66 amino acid long P1c isoform-specific sequence, whereas only the last six C-terminal amino acids of this peptide were present in human plectin ABD/2α (1MB8), the results of this superposition became questionable. In fact, already after several rounds of refinement no interpretable electron density was found for most of the residues encoded by exon 1c sequences (**Figure 9A**). Consequently, only Arg64, Ile65 and Ala66, but not

---

Table 1. Data-collection and refinement statistics for P1cABD/2α.

Data Collection	
Beamline	X11 (EMBL Hamburg)
Wavelength (Å)	1.278
Resolution (Å)[1]	20 - 2.01 (2.03 - 2.01)[1]
Space group	P 21 21 21
Unit cell (Å)	32.74 51.38 155.90 90.00 90.00 90.00
Molecules / a.u.	2
Unique reflections	17286 (3612)
Completeness (%)	93.11 (84.30)
R_{meas}[2]	0.081 (0.769)
R_{merge}[3]	0.043 (0.007)
Multiplicity	37.8 (36.6)
I/σ(I)	39.38 (7.43)

Refinement	
R_{cryst}[4]/ R_{free}[5]	0.191/0.239
R.m.s.d. bonds (Å)	0.012
R.m.s.d. angles (º)	1.314
Wilson B factor	34.69

[1] Values in parentheses are for the highest resolution shell.

$$^2 \; R_{meas} = \sum_{hkl}\left[1-(N-1)\right]^{1/2} \sum_i \left| I_i(hkl) - \overline{I(hkl)} \right| \Big/ \sum_{hkl}\sum_i I_i(hkl)$$

$$^3 \; R_{merge} = \sum_{hkl}\sum_i \left| I_i(hkl) - \overline{I(hkl)} \right| \Big/ \sum_{hkl}\sum_i I_i(hkl)$$

where $I_i(hkl)$ and $\overline{I(hkl)}$ are the ith and the mean measurements of the intensity of reflection hkl and N is the redundancy.

$$^4 \; R_{cryst} = \sum \left| F_o - F_c \right| \Big/ F_o$$

[5] R_{free} is the cross-validation R_{factor} computed for the test set of reflections (5%) which are omitted in the refinement process.

the rest of the P1c isoform-specific sequence could be modelled into existing density (**Figure 9A**). On one hand this was expected, as the major part of the exon 1c-encoded protein was predicted to be unstructured and thus flexible. On the other hand, given that no density was observed for the part of exon 1c-encoded sequence which has previously been shown to form a

helix (Garcia-Alvarez *et al.*, 2003), it was possible that no first exon-encoded sequences were present in the protein molecule analyzed. In support of this notion, residues Arg64 and Ile65 were found to be part of a loop, suggesting that the preceding sequences important for helix formation and stability of this region as found for 1MB8 (**Figure 9B**), were missing. Therefore, we verified
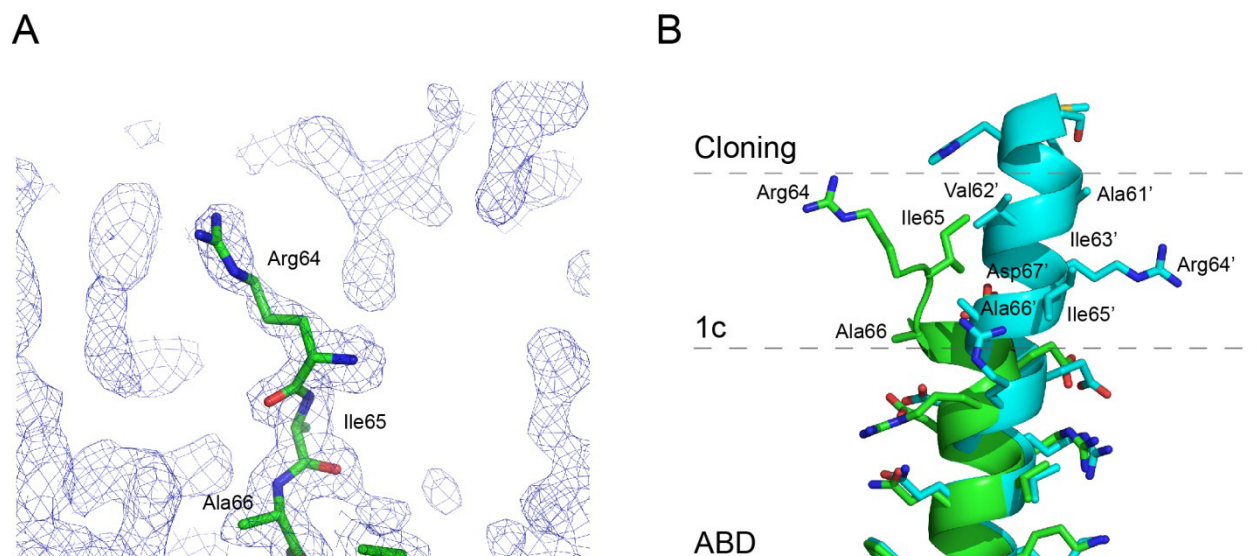
Figure 9. Structure of P1c isoform-specific sequence as found in the crystal of mouse P1cABD/2α purified via its His-tag. (*A*) After several rounds of structure refinement no additional electron density was observed at the N-terminal part of P1cABD/2α, which would allow to model residues of P1c specific peptide preceding Arg65. Thus, only residues Arg65, Ile66, and Ala67 of the P1c specific peptide were found in the crystal structure. The $|2F_o - F_c|$ electron density map was contoured at 1.5σ level. Carbon, oxygen, and nitrogen atoms are shown in green, red, and blue, respectively. Note that most of the additional density visible in the figure belongs to symmetry related molecules. (*B*) Detail view of P1c-specific sequence as found in the structure of mouse P1cABD/2α (green) and human ABD/2α (PBD code: 1MB8) (cyan) superimposed over each other. P1c isoform-specific residues are labeled. Prime mark is used to distinguish residues belonging to P1c-specific residues found in the structure of human plectin ABD/2α (1MB8). Numbering of the residues follows amino acid sequence as described in Fuchs *et al.*, (1999). Main chains are show as cartoon, while side chains are represented as sticks labeled as in A, except of carbon, which follows the coloring of the main chain. Amino acids added to the protein during cloning (cloning), as well as P1c-specific residues (1c) and residues belonging to ABD (ABD) are separated from each other by dashed lines. Note, Arg64 and Ile65 form a loop in the mouse P1cABD/2α (green), whereas in the human ABD/2α (1MB8; cyan) they are part of the first helix. All graphic representations were generated using PyMol (DeLano, 2000).

the quality of both protein samples (P1aABD, P1cABD/2α) used for crystallization by SDS-PAGE (**Figure 10A**). Using plectin ABD/2α (molecular mass: 30151 Da) and P1dABD/2α (30857 Da) as controls, we found that indeed the first exon-encoded sequences were missing and both proteins (P1aABD without His-tag, 32253 Da; and P1cABD/2α, 35401 Da) migrated at

positions similar to ABD/2α (**Figure 10A**). Furthermore, isoform-specific antibodies to exon 1a- and 1c-encoded peptides did not recognize the protein fragments when subjected to immuno-blotting (data not shown). Plausible explanations for these phenomena would be the existence of
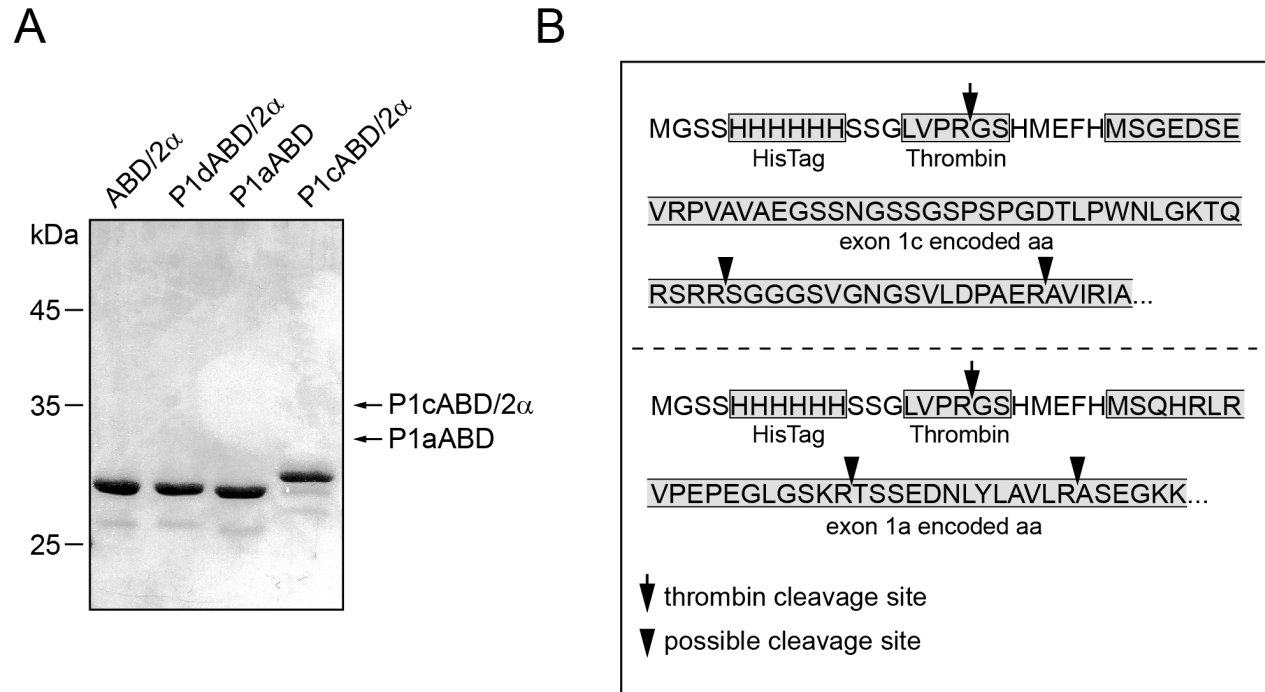
Figure 10. Thrombin removes plectin exon 1a and 1c encoded sequences. (*A*) Protein samples used to prepare crystals of P1aABD and P1cABD/2α were analyzed together with ABD/2α and P1dABD/2α (used as internal controls) on SDS-PAGE. Proteins were visualized by staining with CBB. Arrows shows expected molecular mass of P1aABD and P1cABD/2α. Sizes of molecular mass markers are indicated. (*B*) Mapping of thrombin cleavage sites on P1aABD and P1cABD/2α. Figure shows N-terminal parts of P1cABD/2α (upper panel) and P1aABD (bottom panel) sequences present in both proteins after heterologous expression before treatment with thrombin. Sequence of the His-tag, thrombin recognition site, and P1a- and P1c-specific sequences (grey boxes) are shown.

an additional, less effective thrombin cleavage site in the vicinity of plectin's ABD, and/or self-degradation of the proteins. This prompted us to examine the amino acid sequences of the constructs used for the existence of additional thrombin cleavage sites. A more detailed analysis showed that in both sequences two possible thrombin cleavage sites exist (**Figure 10B**). However, these sites do not follow exactly the rules for thrombin's cleavage specificity, suggesting that there might have been a secondary activity arising from other proteases present in the thrombin sample purchased.

Purification and crystallization of untagged versions of plectin's ABD preceded by P1a- and P1c-specific sequences

Assuming that thrombin cleavage was the main reason for losing plectin's first exon-encoded peptides during the purification process, for the next attempt we decided to isolate plectin fragments without fusion tags. For this, we prepared two constructs encoding P1aABD (pJK1) and P1cABD/2α3α (pJK2) using a modified pET15b vector (pGR66), allowing us to express and purify untagged protein version. Furthermore, we established a new purification protocol consisting of four purification steps: i) ammonium sulphate precipitation, ii) hydrophobic interaction chromatography (Phenyl Sepharose), iii) anion-exchange chromatography (Sepharose Q), iv) size exclusion chromatography (Superdex 75) (for details see Materials and Methods section and **Figure 11**). This new, rather elaborate purification scheme was possible due to the relatively high expression levels of soluble untagged plectin fragments, which were similar (in regard to total amounts of protein) to those observed for His-tagged fusion proteins. Binding of plectin fragments to phenyl Sepharose was usually so strong that the elution of the protein from the column became possible only by using ethylene glycol gradients of 0-50% (v/v) (**Figure 11A**). Furthermore, the proteins eluted from anion-exchange columns usually in one sharp peak indicating sufficient conformational homogeneity of the protein samples (**Figure 11B**). Finally, both plectin fragments (P1aABD and P1cABD/2α3α) eluted from gel filtration column as one single peak at a volume corresponding to the protein monomer, as calculated upon calibration of the column with LMW gel filtration calibration kit (**Figure 11C**). In comparison to our previous purification strategy (affinity chromatography of His-tagged protein versions), the purity and homogeneity of protein samples were significantly increased. In addition, no degradation of first exon-encoded sequences was observed, with both plectin fragments displaying high stability (even after several months), when stored at concentration of 30 mg/ml at -80°C. Finally, as this procedure turned out to be highly efficient, it became the routine purification strategy for all untagged plectin fragments presented in this thesis.

As an alternative to crystallization of plectin fragments prepared by His-tag-based affinity chromatography, we took advantage of a Cartesian liquid dispensing robot, 96 well plates, temperature controlled rooms, and several commercial screens provided by Tim Clausen (Research Institute of Molecular Pathology, Vienna, Austria) and Kristina Djinovic-Carugo

(Max F. Perutz Laboratories, Vienna, Austria) to set up initial crystallization trial screens for untagged P1aABD and P1cABD/2α3α.
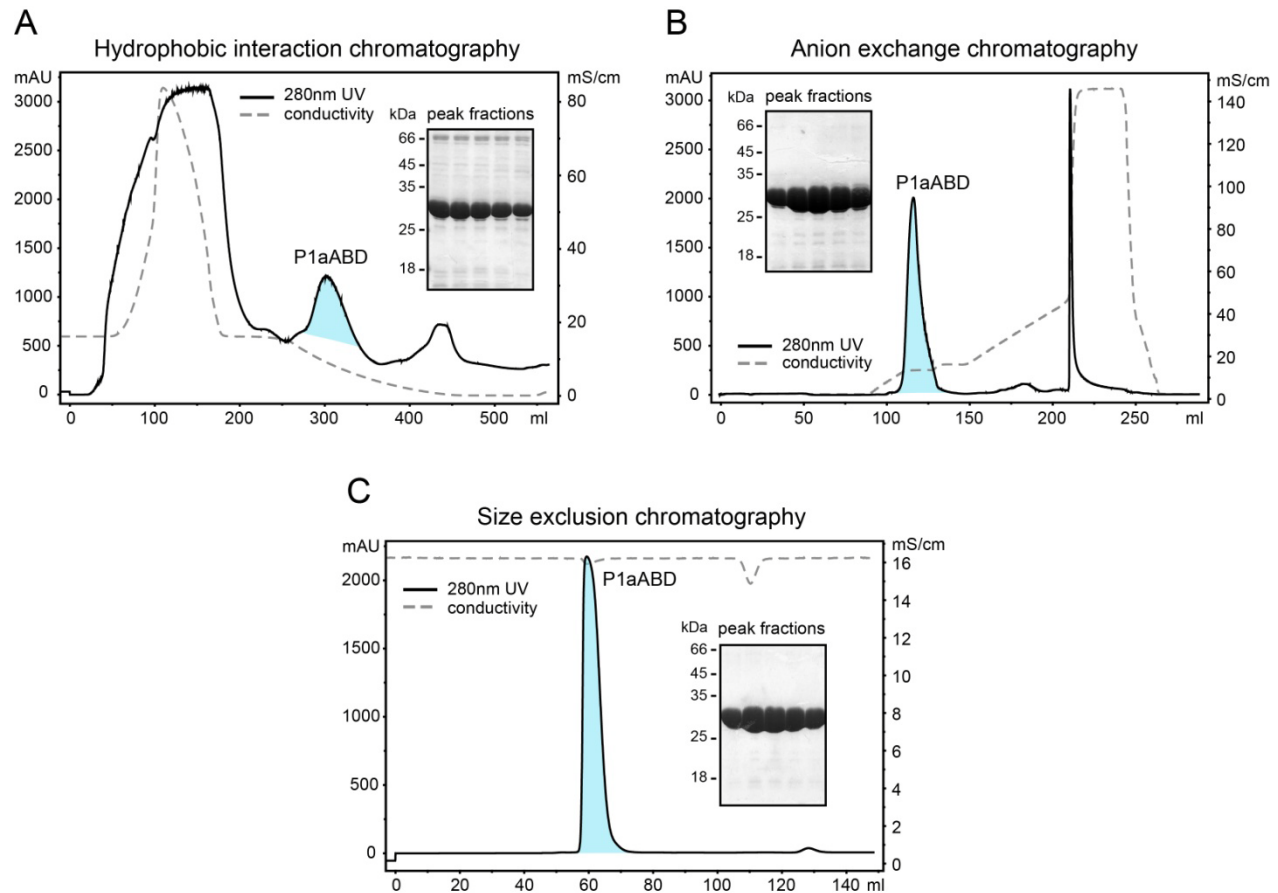
Figure 11. Isolation of untagged P1aABD using an orthogonal purification strategy. (*A*) After precipitation of unwanted proteins with ammonium sulphate, protein samples were clarified by centrifugation, and resulting supernatants applied on phenyl Sepharose columns. Proteins were eluted with a linear gradient of ethylene glycol (0-50 %) as described in Material and Methods. Typical chromatograms of a UV (OD$_{280nm}$, solid line) and conductivity (dashed line) traces obtained during purification are shown. Peak fractions (see OD$_{280nm}$, denoted in cyan) were analyzed for the presence of P1aABD by SDS-PAGE (shown in panel), and CBB staning. Position of molecular weight markers are shown on left side of the panel. (*B*) Selected peak fraction were pooled, dialyzed against column buffer B (20 mM Tris/HCl, 10 mM NaCl, 0.5 % glycerol, 0.5 mM DTT, pH 8.0), and applied on Sepharose Q columns equilibrated with the same buffer. Bound protein was eluted by a linear gradient of 10-300 mM NaCl in column buffer B. Collected fractions were analyzed and process as in *A*. (*C*) Fractions containing purified P1aABD were selected, pooled and concentrated before applying on HiLoad 16/600 Superdex 75 pg columns equilibrated with 20 mM Tris/HCl, 100 mM NaCl, 0.5 % glycerol, 0.5 mM DTT, pH 8.0. After analysis of eluted fractions (like in *A*), aliquots of highly pure protein samples concentrated to ~30 mg/ml were frozen in liquid nitrogen, and stored at -80°C until further use.

Despite of several hundred different conditions tested, crystal formation could not been observed, indicating that the flexible parts of the first exon-encoded sequences were indeed present and might have hindered crystal growth. However, under some conditions (for details see Materials and Methods) sphere-like particles with birefringent properties (indicative of crystal formation) appeared after several days (**Figure 12, A and C**).
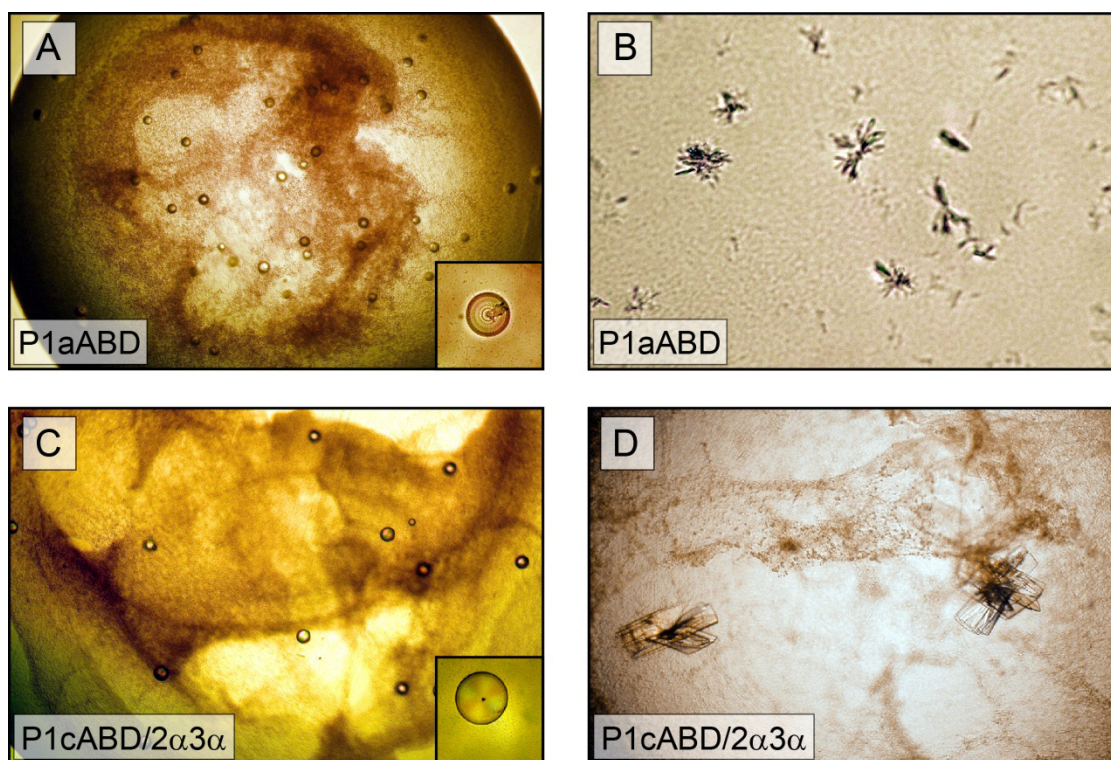
Figure 12. Crystallization of untagged P1aABD and P1cABD/2α3α. Initial crystallization trials with P1aABD (*A*) and P1cABD/2α3α (*C*), led to formation of sphere-like particles, appearing from protein precipitates after several days. In subsequent optimization attempts, conditions were found from which, needle- and plate-like crystal of P1aABD (*B*) and P1cABD/2α3α (*D*), respectively, were obtained., Boxed areas (bottom right corners of *A* and *C*) show magnified views of selected particles shown in *B* and *D*.

Further optimization of these conditions resulted in small needle- and plate-like crystals in the cases of P1aABD, and P1cABD/2α3α, respectively (**Figure 12, B and D**). Despite of an apparent partial improvement, results were not reproducible, and neither the size, nor the quality of the crystals obtained were increased. Furthermore, the diffraction capacity of the crystals was limited and all further attempts to prepare crystals suitable for data collection failed. In all, we were unable to obtain any structural information about P1a- and P1c-isoform-specific peptides.

Although our main goal remained unfulfilled, we established a novel protocol for the purification of untagged plectin fragments, which turned out to be particularly useful for the production of proteins required for my further biochemical in vitro studies (see below). Finally, the surprisingly high specificity observed for thrombin removal from plectin's exon 1a- and 1c-encoded sequences, implicate the intriguing possibility that thrombin may have a role in the regulation of plectin in vivo.

PART 2 - Interaction of plectin's ABD with non-filamentous vimentin

As obvious from the results of the first part of this thesis, we were not able to gather any structural information about plectin isoforms-specific sequences, mainly because of their conformational flexibility. However, many disordered proteins form ordered conformations and/or become stabilized upon binding to other proteins. In the case of plectin, such proteins might specifically interact with the first exon-encoded sequences and/or the neighbouring ABD of plectin. No isoform-specific binding partners of plectin had previously been described for plectin. Therefore, in the second part of my thesis, I tried to identify and characterize new binding partners of plectin`s ABD, potentially involved in the structural stabilization of plectin's first exon-encoded sequences. First, I investigated structural and functional relationships of plectin's ABD with other CH protein family members. Comparison of plectin's ABD with ABDs of other CH protein family members revealed a structural similarity between the ABD of plectin and that of fimbrin (Ševčík, *et al.*, 2004). Interestingly, aside from binding to F-actin, the first (N-terminal) of fimbrin's two ABDs, has been reported to specifically interact with the intermediate filament (IF) protein vimentin (Correia, *et al.*, 1999). In light of the extensive structural resemblance of fimbrin and plectin ABDs, we therefore decided to assess the IF-binding activity of plectin's ABD.

Plectin interacts with vimentin via the N-terminal part of its ABD

To assess ABD-vimentin interactions, we performed in vitro overlay assays. P1aABD (purified without any tag), plectin's ABD/2α and a truncated versions of plectin's ABD missing half of the CH1 domain (fragment encoded by plectin exons 4-8, P4-8), or the complete CH1 domain (fragment encoded by plectin exons 6-9, P6-9) were immobilized on nitrocellulose

membranes and overlaid with recombinant full-length vimentin (**Figure 13**) (Ševčík, *et al.*, 2004). In agreement with previously reported findings for fimbrin's ABD (Correia, *et al.*, 1999) all proteins, except the one missing the entire CH1 domain (P6-9) and the negative control (BSA), showed binding to vimentin, similar to the positive control, a recombinant plectin repeat domain 5 (**Figure 13**) (Ševčík, *et al.*, 2004). Thus only the CH1, but not the CH2 domain of plectin's ABD was found capable of binding to vimentin (Ševčík, *et al.*, 2004).
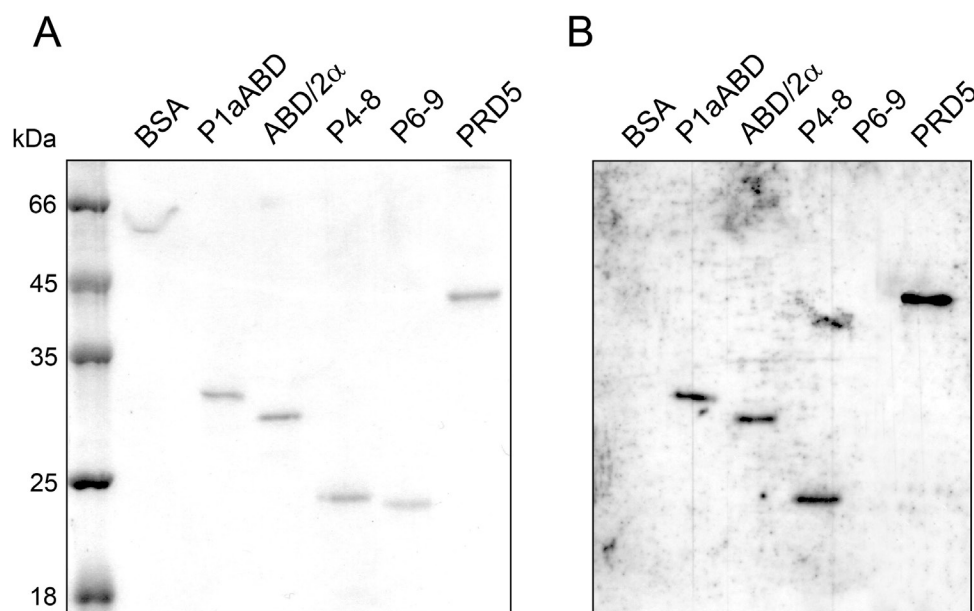
Figure 13. Overlay of various plectin ABD versions with full-length vimentin. Recombinant versions of plectin's ABD starting with exon 1a-encoded sequences (P1aABD), or starting with exon 2-encoded sequences and containing 2α-encoded sequences (ADB/2α), or lacking part of (P4-8), or the whole CH1 domain (P6-9), as well as a fragment corresponding to the repeat 5 domain of plectin (PRD5; positive control), and BSA (negative control) were subjected, in duplicate, to SDS-PAGE. Proteins on one gel were blotted onto a nitrocellulose membrane and overlaid with recombinant full-length mouse vimentin (*B*), proteins on a second gel were stained with CBB (*A*). All proteins, except for P6-9 and BSA, showed significant binding to vimentin. Molecular masses are indicated. The figure was modified from (Ševčík *et al.*, 2004).

To specify the subdomain of vimentin that bound to plectin's ABD, several truncated versions of vimentin (covering all functional subdomain of the protein; for details see Materials and Methods section and **Figure 14**) were expressed in *E. coli* and subjected to overlay assays (Ševčík, *et al.*, 2004). The ABD version used in these experiments contained the preceding 66 amino acid residues-long sequence specific for P1c, enabling detection of bound protein with P1c-specific antibodies. Interestingly, this fragment showed strong binding to full-length

vimentin and to VimNR, a truncated version of vimentin containing its N-terminal domain and its central rod domain, but lacking the C-terminal domain (**Figure 14**) (Ševčík, *et al.*, 2004). Only very weak interactions were observed with vimentin fragments corresponding to the N-terminal (VimN), or rod domains alone (VimR), or to the rod in conjunction with the C-terminal domain (VimRC) (Ševčík, *et al.*, 2004). These data suggested that the binding site of vimentin for plectin's ABD was contained in the N-terminal part of the molecule comprising the head domain and possibly parts of the rod (**Figure 14, A and B**) (Ševčík, *et al.*, 2004). Thus in the first type of overlay assays, P1aABD showed binding to vimentin, while in the second type P1cABD/2α interacted with specific fragments of vimentin indicating that binding of plectin's ABD to vimentin is most likely isoform-independent and mediated mainly by the CH1 domain of plectin.
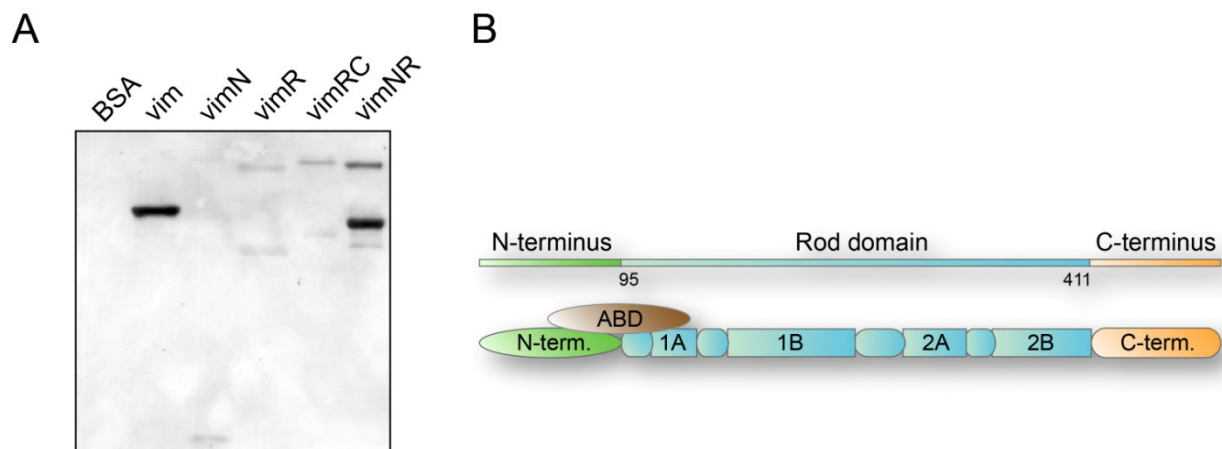
Figure 14. Overlay of recombinant vimentin fragments with plectin's ABD. (*A*) Recombinant versions of vimentin subdomains were immobilized on nitrocellulose membranes as described in **Figure 13**, and overlaid with the His-P1cABD/2α. Vim, full-length vimentin; VimN, N-terminal domain; VimR, rod domain; VimRC, vimentin without N-terminal domain; VimNR, vimentin without C-terminal domain. To detect vimentin-bound plectin ABD, P1c-specific antibodies were used. Note the strong binding of plectin's ABD to the full-length vimentin and VimNR, but only weak or no binding to other vimentin fragments. (*B*) Schematic cartoon shows binding of His-P1cABD/2α (ABD, brown) to the region of vimentin found based on results presented in *A*. Domains of vimentin corresponding to vimentin fragments as used in *A* are depicted in green (N-terminal domain), blue (rod domain), orange (C-terminal domain). Four helical (coil) segments of vimentin rod domain (1A, 1B, 2A and 2B) are labeled. Numbers of amino acids at the domain borders are shown. The figure was modified from (Ševčík *et al.*, 2004).

Plectin's ABD does not bind to filamentous vimentin

By using of overlay assays we identified vimetin as a new interaction partner of plectin's ABD, and mapped interaction sites on both, plectin's ABD and vimentin, too. In order to further

characterize and quantify this interaction, in vitro Eu^{3+}-protein binding assays using plectin's ABD without alternatively spliced exon 2α encoded sequences (ABD) were performed. Recombinant full-length vimentin, was labelled with Eu^{3+} using a standard protocol (for details see Materials and Methods), and used in overlay assays, where plectin's ABD, plectin repeat domain 5 (PRD5), and BSA were coated onto microtiter plates, with BSA being used as negative control, and PRD5 as positive control. As expected, vimentin showed strong binding to PRD5, but not to BSA (**Figure 15**).
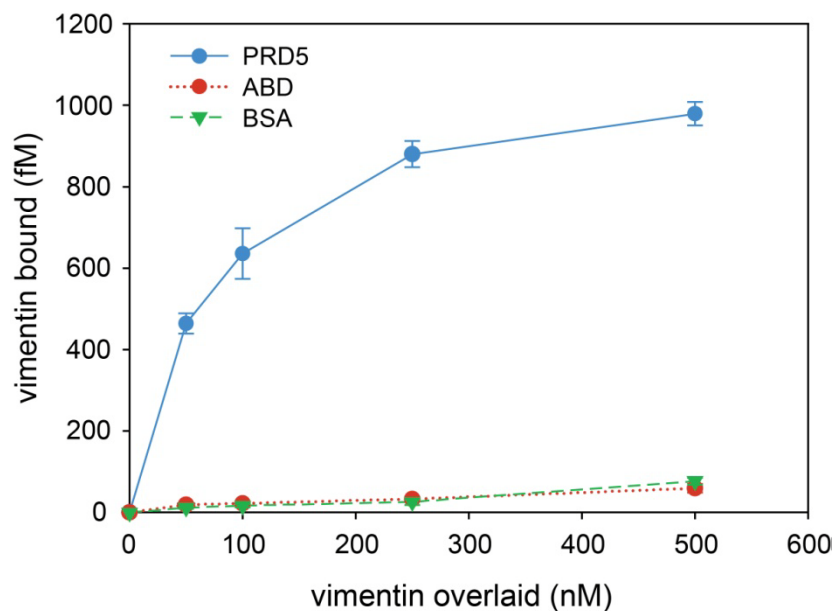
Figure 15. Binding of the Eu^{3+}-labeled full-length vimentin to plectin's ABD. Increasing concentrations (0-500 nM) of full-length, Eu^{3+}-labeled vimentin were incubated with proteins (100 nM) coated onto microtiter plates: PRD5 (positive control), ABD, and BSA (negative control). Note weak, unspecific binding of plectin's ABD to vimentin, similar to BSA. Data are represented as the mean (± S.E.) of triplicate determinations.

Interestingly, plectin's ABD failed to show any specific binding to vimentin, exhibiting binding levels similar to BSA (**Figure 15**). This finding was inconsistent with our previous observation, probably due to different conditions used in both experiments. First, in the previous overlay assays, proteins were partially denatured and separated by SDS-PAGE before being blotted onto nitrocellulose membrane, indicating that some conformational changes in plectin's ABD might have been necessary for proper binding. Second, labelling of vimentin with Eu^{3+} might decrease its binding affinity to an extent, where only strongly (*e.g.* PRD5), but not weakly (*e.g.* ABD) interacting proteins can be detected by the Eu^{3+} protein interaction assay.

To assess, plectin's ABD-vimentin interaction using assays not involving the immobilization of proteins on solid matrices, in my next experiments vimentin-binding to plectin's ABD was measured by in solution-cosedimentation of ABD/2α and PRD5 with IFs assembled from recombinant vimentin in vitro. After incubation of mixtures containing vimentin and ABD/2α, or PRD5 proteins (at molar ratios of 1:1 to vimentin), filaments were sedimented, and supernatant and pellet fractions analyzed by SDS-PAGE (**Figure 16**). Control samples containing just vimentin, ABD/2α, and PRD5 (without corresponding binding partner), were processed under similar conditions. As expected, PRD5 sedimented with filamentous vimentin, except for a minor apparently self-aggregating fraction that was found in the control (without vimentin) pellet fraction (**Figure 16**). In contrast to PRD5, ABD/2α did not cosediment with vimentin, although a slight self-precipitation was observed in the absence of vimentin (**Figure 16**). Thus results from both, Eu^{3+}-protein interaction assay and the vimentin cosedimetation assay were consistent, indicating that plectin's ABD (with or without the exon 2α-encoded sequence) does not interact with filamentous vimentin.
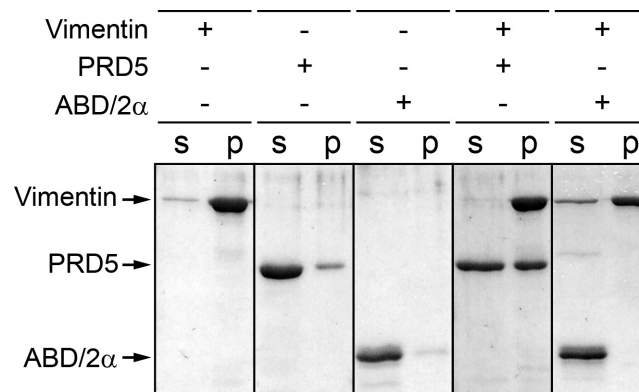
Figure 16. Co-sedimentation of full-length vimentin with plectin ABD. Polymerized vimentin was mixed equimolarly with plectin repeat domain 5 (PRD5) or ABD (ABD/2α). Vimentin filaments and proteins bound were sedimented by centrifugation, and equal amounts of supernatant (*s*) and pellet (*p*) fractions were subjected to SDS-PAGE. Separated proteins were visualized by CBB staining. Presence (+), or absence (-) of particular protein in the mixture is indicated.

Plectin interacts with oligomeric (tetrameric) forms of vimentin

The head domain of vimentin had previously been shown to harbor the binding site(s) for the CH1 subdomain of fimbrin's N-terminal ABD (Correia *et al.*, 1999), whereas desmin, an IF

protein of similar type, was found to interact with the corresponding domain of calponin via the N-terminal part of its rod domain (Fujii *et al.*, 2000). Interestingly, fimbrin and calponin have been found to interact with tetrameric forms of soluble vimentin and desmin. As recombinant ABD/2α and ABD of plectin were unable to interact with filamentous vimentin in sedimentation and Eu^{3+}-protein interaction assays, respectively, we tested the hypothesis that the plectin's ABD, too, interacts only with soluble forms of vimentin.
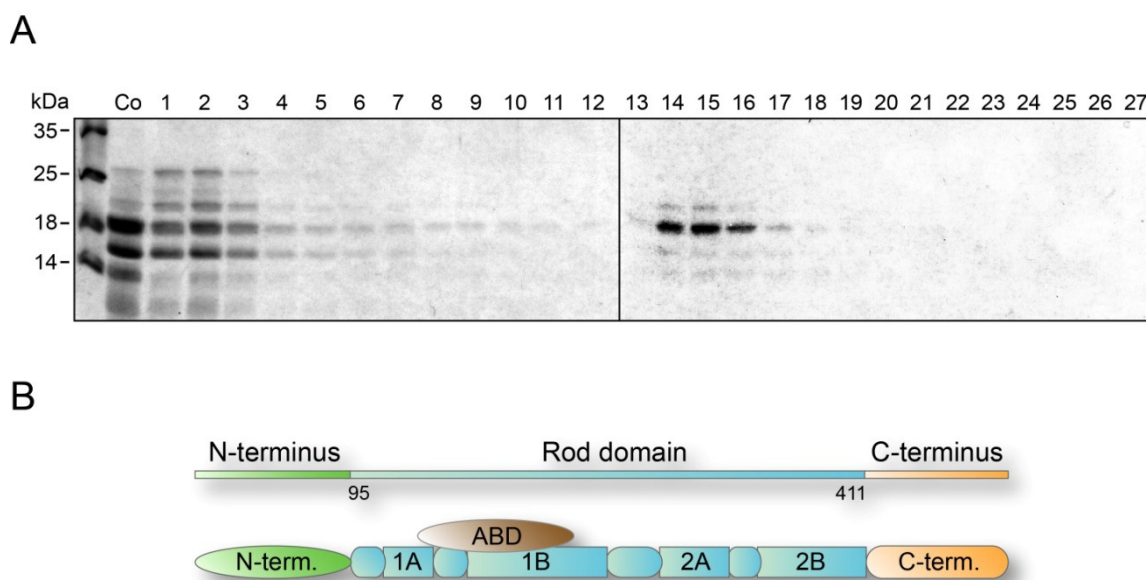
Figure 17. Affinity-binding of proteolytically derived fragments of vimentin to ABD/2α. (*A*) Partial chymotryptic digestion of vimentin followed by affinity-chromatography of resulting vimentin fragments on a ABD/2α-Sepharose column was carried out as described in the text. SDS-PAGE of eluted fractions stained with CCB is shown. Lanes 1-11, wash fractions; 12-27, salt-gradient elution of bound proteins. Co, sample loaded onto column. The molecular mass of size markers run in left-most lane is indicated. The ~18 kDa fragment of vimentin binding to ABD/2α mapped to the N-terminal part of the vimentin rod domain, as determined by MALDI-TOF mass spectrometry. (*B*) Schematic cartoon shows binding of ABD/2α (ABD, brown) to the 'Coil 1' segment of vimentin found based on results presented in *A*. Vimentin`s domains were colored and labeled as described in **Figure 14**. The figure was modified from (Ševčík *et al.*, 2004).

To confirm the specificity of ABD/2α-vimentin binding and to more precisely map vimentin's binding site to plectin's ABD, vimentin purified in urea was kept in its soluble (tetrameric) form by dialysis into 10 mM Tris/acetate, pH 8.3, 0.1 mM EDTA, 5 mM β-mercaptoethanol (Ševčík, *et al.*, 2004). The protein was than subjected to limited chymotryptic digestion and fragments generated were applied to a ABD/2α-Sepharose affinity column (Ševčík,

et al., 2004). Elution and SDS-PAGE analysis of bound proteins revealed that a single major fragment of approximately 18 kDa was retained on the column (**Figure 17A**) (Ševčík, *et al.*, 2004). This fragment could be mapped to 'Coil 1', an N-terminal segment of the vimentin rod domain, using MALDI-TOF mass spectrometric sequence analysis (**Figure 17B**) (Ševčík, *et al.*, 2004). This result confirmed the in vitro interaction of plectin's ABD with vimentin. However, the ABD of plectin was found to interact with a part of vimentin different from that identified in overlay assays (see above). In addition, the affinity chromatography results suggested that the ABD of plectin does not bind to filamentous vimentin, but rather to its soluble tetrameric species. Vimentin`s very high insolubility, tendency for filament formation, and monomeric state of truncated vimentin fragments precluded further experiments. As the nature of the plectin ABD-vimentin interaction was not completely understood and the interaction seemed to be plectin isoform-independent, at the end it was decided that vimentin was not the candidate to be used in further structural studies of plectin isoform-specific sequences.

PART 3 - Plectin isoform 1a-specific interaction with calmodulin

In the third part of my thesis I set out to identify and characterize isoform-specific binding partners of P1a, one of the two major isoforms expressed in keratinocytes (the other being P1c). In this case the biological significance of the interaction, rather than its structural implications was of foremost importance.

Ca^{2+}-induces a redistribution of plectin 1a in differentiating keratinocytes

Studies in cultured keratinocytes have demonstrated that the association of integrin α6β4 with P1a via the integrin β4 subunit and their clustering is crucial for the formation of HDs (Andrä *et al.*, 2003). In the early stages of keratinocyte differentiation (as well as of wound healing) HD components, such as integrin α6β4 and BPAG2, show a redistribution from HDs to other cell compartments (Kitajima *et al.*, 1992; Gipson *et al.*, 1993). To examine the fate of HD-associated P1a during calcium induced differentiation of keratinocytes, confluent cultures of primary mouse keratinocytes were subjected to differentiation by exposure to 1.3 mM $CaCl_2$ for up to 8 h (**Figure 18A**) (Kostan, *et al.*, 2009). Of note, the data presented in this chapter (**Figure 18**) were provided by Dr. Martin Gregor (group Prof. G. Wiche); they are presented here to better illustrate the physiological relevance of the in vitro data shown thereafter.
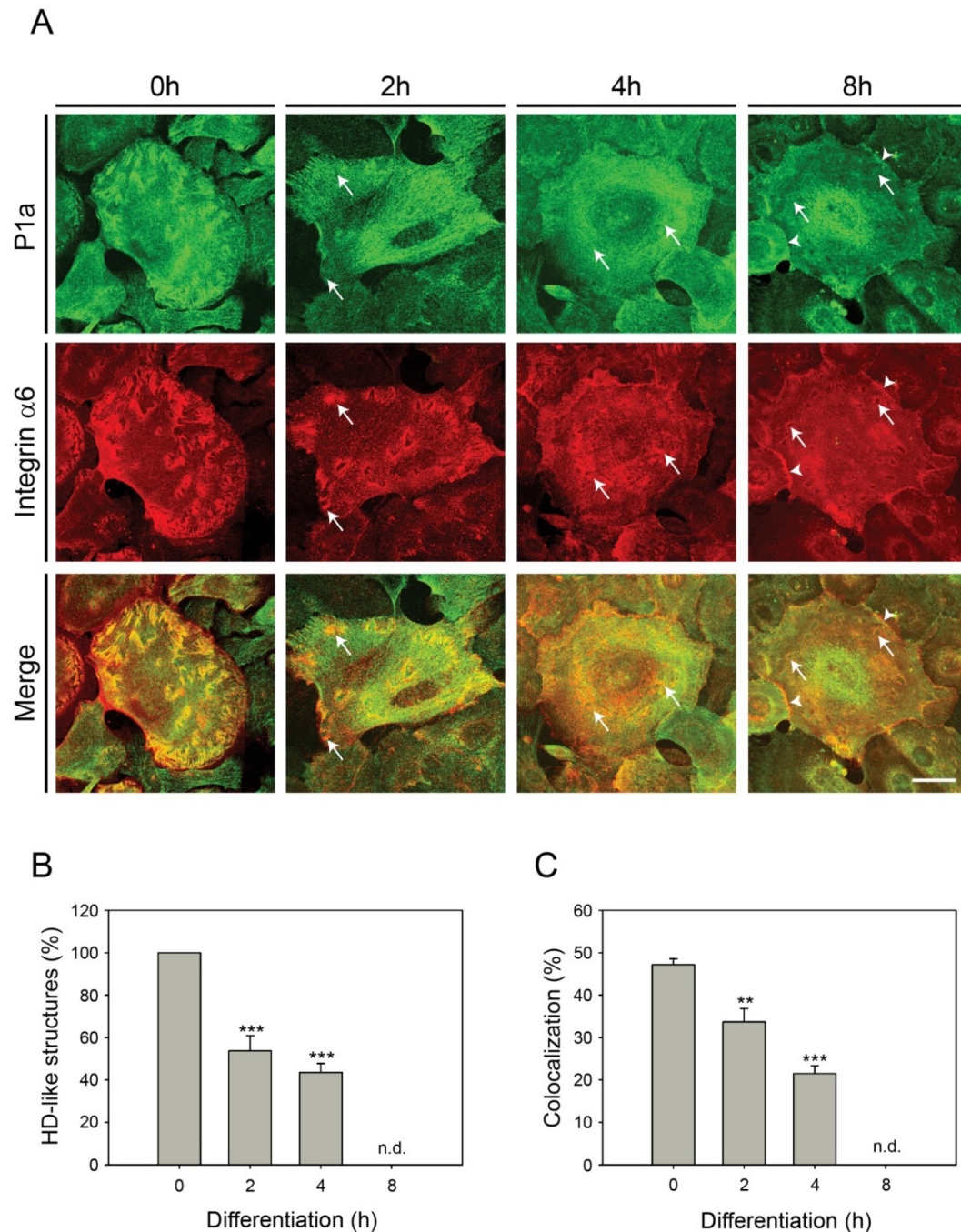
Figure 18. Redistribution of P1a in the early stages of Ca^{2+}-induced keratinocyte differentiation. (*A*) Cultures of primary keratinocytes, exposed to Ca^{2+} for 0, 2, 4, and 8 h, were subjected to immunofluorescence microscopy using antibodies indicated. Arrows point to areas where P1a staining does not coincide with integrin α6-positive HD-like structures. Arrowheads denote areas at the cell periphery with accumulation of P1a. Note, wedge-like patterns typical of HD-like structures in primary keratinocytes. Bar, 20 μm. (*B* and *C*) Bar diagrams representing statistical quantitation of HD-like (integrin α6-positive) structures (*B*) and colocalization of plectin 1a with integrin α6 (*C*) in primary keratinocytes during Ca^{2+}-induced differentiation. Data shown in *B* and *C* represent mean values (± S.E.). 15 cells of the type shown in *A* from three different experiments were analyzed; ** and ***, P < 0.01 and P < 0.001, respectively. n.d., not determined. Note, reduction of HD-like structures, as well as decreasing colocalization of P1a with integrin α6 in the course of differentiation. The figure was modified from (Kostan *et al.*, 2009).

Prior to differentiation (0 h), P1a was found associated with prominent integrin α6-positive wedge-like structures (Kostan, *et al.*, 2009). Of these, 47% were also positive for P1a, reflecting heterogeneity of HD-like structures caused most likely by differences in their assembly state (Kostan, *et al.*, 2009). Similarly to integrin α6β4 and BPAG2, upon Ca^{2+}-induced differentiation of primary keratinocytes, a remarkable redistribution of P1a was observed (**Figure 18A**) (Kostan, *et al.*, 2009). Already within the first 2-4 h of differentiation, the P1a signal became less prominent at HD-like structures. At the same time P1a became diffusely distributed within the cell, showing an accumulation in peripheral cell-cell contact areas as well as in perinuclear regions, as differentiation proceeded (**Figure 18A**) (Kostan, *et al.*, 2009). Integrin α6 showed a similar redistribution to the cell margins, accompanied by a reduction of HD-like structures in the cell interior (**Figure 18, A and B**) (Kostan, *et al.*, 2009). A quantitative analysis revealed that already 2 h after addition of Ca^{2+}, the amount of HD-like structures was reduced to 53% of control values (0 h), with a further drop to 43% after 4 h of differentiation (**Figure 18B**) (Kostan, *et al.*, 2009). HD-like structures, which were still noticeable at later stages of Ca^{2+} treatment (8 h), in general were P1a-negative (**Figure 18A**). The amount of P1a/integrin α6-costained structures after 4 h of Ca^{2+} treatment was reduced to less than half compared with untreated cells (0 h) (**Figure 18C**), implying dissociation of plectin 1a from integrin α6β4 and HD-like structures during the differentiation process (Kostan, *et al.*, 2009).

Association of calmodulin with P1a upon Ca^{2+}-triggered differentiation of keratinocytes

Calmodulin (CaM) is a ubiquitous, calcium-binding protein that can bind to and regulate a multitude of different protein targets, thereby affecting many different cellular functions. It mediates processes such as inflammation, metabolism, apoptosis, muscle contraction, intracellular movement, short-term and long-term memory, nerve growth and the immune response. As the phosphorylation of integrin β4 by PKCα caused only a partial disassembly of HDs (Wilhelmsen *et al.*, 2007; Rabinovitz *et al.*, 2004), we speculated that additional mechanism(s) might be required for their complete disassembly (Kostan, *et al.*, 2009). The PKCα activator Ca^{2+} also activates CaM that is known to modulate some of the functions of dystrophin, utrophin, and filamin through its direct binding to their highly conserved ABDs (Bonet-Kerrache *et al.*, 1994; Winder and Kendrick-Jones, 1995; Nakamura *et al.*, 2005).

Since plectin (as mention above) shares with these proteins a similar ABD (Ševčík *et al.*, 2004), it was of interest, whether P1a, too, bound to CaM, and whether such an interaction could affect plectin-mediated IF network anchorage at HDs. To address these issues, I first prepared 1% Triton X-100 soluble and insoluble (cytokeratin-enriched) subcellular fractions from differentiating cultured keratinocytes, and subjected them, along with total cell lysates, to immunoblotting using antibodies to integrin β4, P1a, CaM, PKCα/βII, and keratin 5 (K5), or K5, K6, and K18 (pan-keratin) (**Figure 19, A and B**) (Kostan, *et al.*, 2009). The relative amounts of detectable keratins and phosphorylated (activated) PKCα/βII served as controls for equal loading and as differentiation marker, respectively. The analysis of total cell lysates at various time points revealed hardly any differences in the expression profiles of these proteins during Ca^{2+}-induced differentiation (**Figure 19A**) (Kostan, *et al.*, 2009). As expected, the relative distribution of cytokeratins, most of which were found in the insoluble fractions, was hardly altered during the early stages of differentiation (**Figure 19B**) (Kostan, *et al.*, 2009). As revealed by densitometric analysis, integrin β4 became more prominent in the soluble fraction with continuing differentiation (**Figure 19, B and C**) (Kostan, *et al.*, 2009), probably as a result of increased phosphorylation by PKCα leading to its reduced association with the keratin filaments. Unlike integrin β4, P1a was found predominantly in the cytokeratin-enriched fraction during the first 4 h of differentiation while becoming more soluble only after 8 h (**Figure 19, B and C**) (Kostan, *et al.*, 2009). This suggested that plectin, in contrast to integrin β4, remained associated with insoluble keratin filaments, at least during the early phases of differentiation. The same seemed to apply to CaM, as it, too, was found to codistribute with the insoluble cytokeratin fraction, especially at the 2 and 4 h time points of keratinocyte differentiation (**Figure 19, B and C**) (Kostan, *et al.*, 2009). Thus, increased codistribution of CaM with P1a in the early phases of differentiation indicated, at least an indirect interaction of these two proteins.

Using an alternative assay, plectin and CaM, were partially co-immunoprecipitated from lysates of wild-type keratinocytes differentiated for 4 h when incubated with anti-pan-plectin antibodies and protein A-Sepharose beads (**Figure 20**, *+/+, 4 h*) (Kostan, *et al.*, 2009). In corresponding fractions from undifferentiated keratinocytes (**Figure 20**, *+/+, 0 h*), or from plectin^{-/-} cells (**Figure 20**, *-/-, 4 h*), CaM could not be detected (Kostan, *et al.*, 2009). Thus, subcellular fractionation, and coimmunoprecipitation data combined, provided evidence for Ca^{2+}-induced association of plectin with CaM during the initial period of keratinocyte

differentiation (Kostan, *et al.*, 2009). As anti-pan-plectin antibodies had been used for immunoprecipitation these data did not provide information about possible isoform specificity in binding.
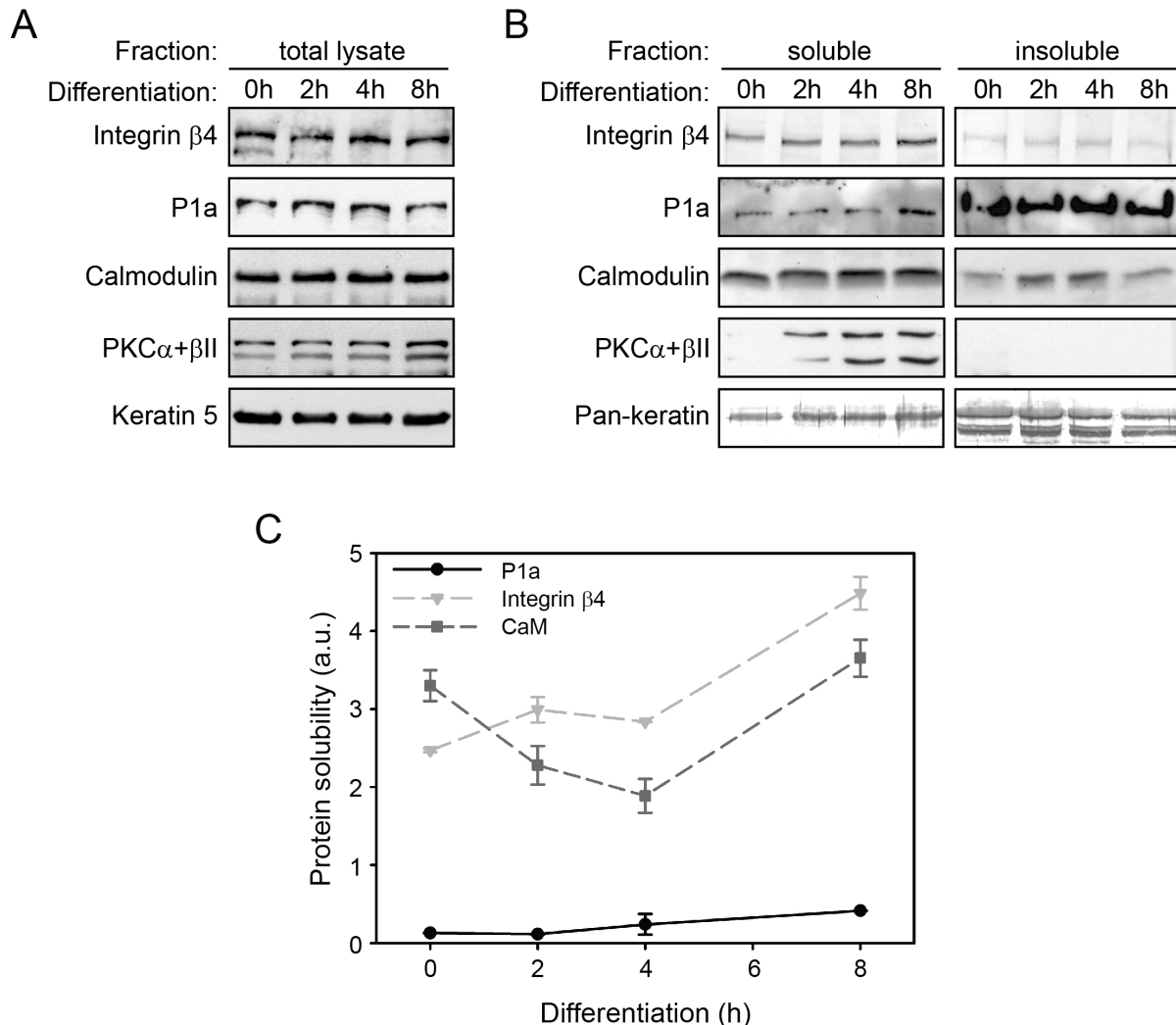
Figure 19. Increased association of CaM with the insoluble cytokeratin fraction in the course of Ca^{2+}-induced keratinocyte differentiation. Immortalized mouse keratinocytes were grown on collagen I and either left untreated (0 h), or stimulated with CaCl$_2$ for 2, 4, and 8 h. (*A*) Cells were lysed without extraction (total lysate) and analyzed by immunoblotting using antibodies to proteins indicated. (*B*) Cells were sequentially extracted to obtain Triton-soluble (soluble) and cytokeratin-enriched (insoluble) fractions, and analyzed as in *A*. Keratin levels assessed by keratin 5 (*A*), or anti-pan-keratin (*B*) antibodies, served as loading controls. (*C*) Quantitation of protein solubility at different time points of differentiation. Signal intensities of P1a, integrin β4, and CaM in soluble and insoluble fractions were quantified by densitometry of gels, including the one shown in *A*. Data points represent ratios between amounts of protein in soluble versus insoluble fractions. Mean values (± S.E.) of three independent experiments are shown. In some cases, error bars do not extend outside of data point symbols. Note, decrease of CaM solubility within 2 and 4 hours of differentiation. The figure was modified from (Kostan *et al.*, 2009).
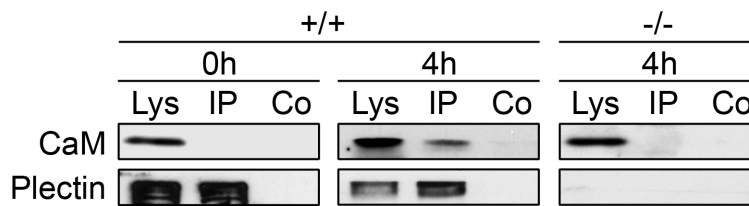
Figure 20. Direct interaction of CaM with plectin during Ca^{2+}-induced keratinocyte differentiation. Lysates (Lys) from undifferentiated (0 h) or differentiated (4 h) immortalized mouse wild-type (+/+) and plectin-null (–/–) keratinocyte cultures were incubated with anti-pan plectin (#46) antibodies (IP), or without antibodies (Co). Immunocomplexes formed were sedimented using protein A beads and the precipitates subjected to immunoblotting using antiserum to plectin 1a or CaM. Note, partial co-sedimentation of CaM with plectin only in lysates from differentiated wild-type keratinocytes. The figure was modified from (Kostan *et al.*, 2009).

Plectin interacts with calmodulin via its CH1 domain in a Ca^{2+}- and isoform-dependent manner

Based on in silico predictions of CaM-binding amphiphilic α-helices, pull-down experiments (filamin A), and overlay assays (dystrophin), the putative CaM-binding site of dystrophin, utrophin, and filamin A were assigned to a region lying within the CH1 domains of their ABDs (Winder and Kendrick-Jones, 1995; Nakamura *et al.*, 2005; Jarrett and Foster, 1995).

To test, whether plectin interacts with CaM via a similar domain, I performed pull-down assays, with Sepharose-bound CaM (CaM-S) and recombinant versions of plectin's ABD (MBP-ABD), or its CH1 domain (encoded by plectin exons 2-5; MBP-CH1) domain, both N-terminally fused to maltose-binding protein (MBP); MBP alone and Sepharose beads without bound CaM (S) were used as controls (Kostan, *et al.*, 2009). When tested in the presence of either 2 mM $CaCl_2$, or 5 mM EGTA, neither plectin's ABD, nor MBP alone showed binding to CaM-Sepharose (**Figure 21A**) (Kostan, *et al.*, 2009). In contrast, the CH1 domain of plectin showed strong binding to CaM in the presence of Ca^{2+}, but not in its absence (**Figure 21A**) (Kostan, *et al.*, 2009). No binding of the CH1 fusion protein to Sepharose beads without bound CaM was observed. Furthermore, in the presence of W7, a specific inhibitor of CaM, binding of the CH1 fusion protein to CaM-Sepharose was substantially diminished (Kostan, *et al.*, 2009). These experiments confirmed CaM's Ca^{2+}-dependent association with plectin detected in vivo. The observation that the ABD of plectin did not show CaM-binding (albeit containing the CH1 domain), while the CH1 domain alone did, suggested that the CaM-binding site residing in the

MBP-ABD fusion protein was inaccessible, and a conformational change of plectin's ABD was probably required for CaM-binding.

Next we wanted to examine, whether the various first exon-encoded sequences affect the binding activities of the ABD. To test this, I subjected N-terminal fragments of plectin comprising the ABD, and the preceding isoform-specific sequences of either P1a (P1aABD), P1c (P1cABD), or P1f (P1fABD), together with the ABD without any preceding sequence (ABD), to
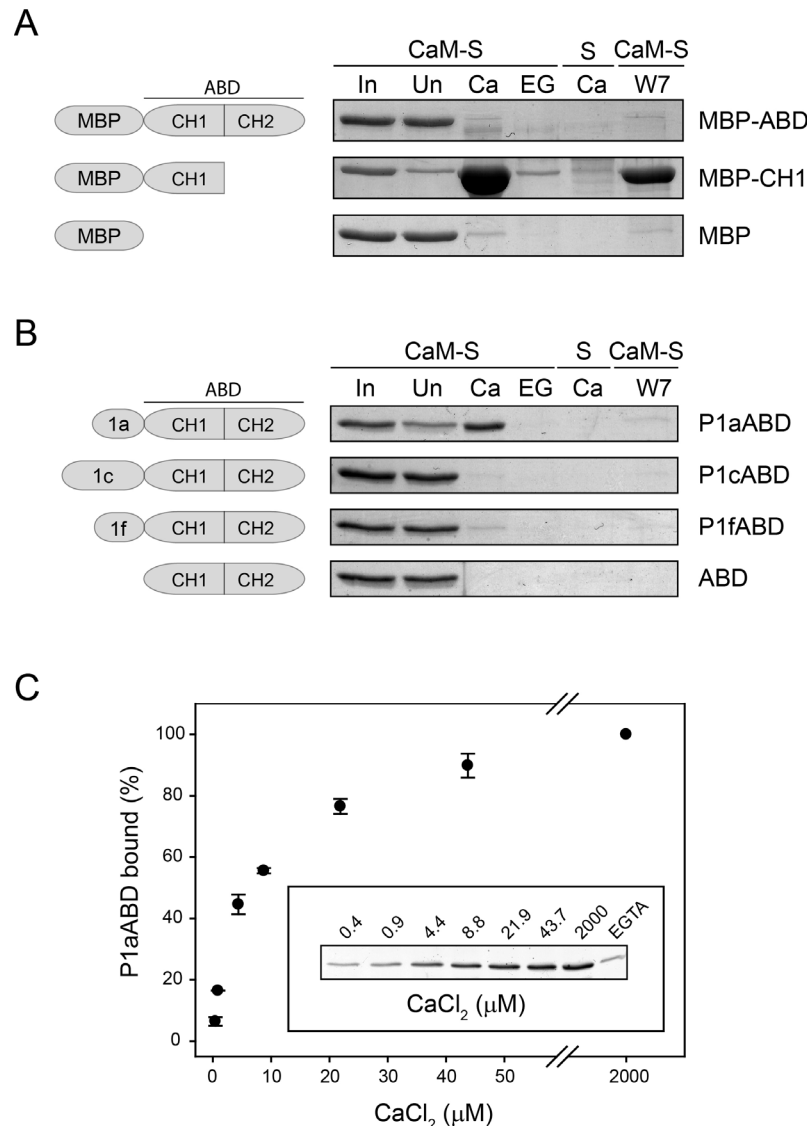
Figure 21. Ca^{2+}- and isoform-dependent interaction of plectin with CaM. (*A*) Fusion proteins of MBP with plectin's ABD (MBP-ABD), or N-terminal CH1 domain (MBP-CH1), or MBP alone (MBP), were incubated with CaM-Sepharose beads (CaM-S), or empty beads (S), in the presence of 2 mM $CaCl_2$ (Ca), or 5 mM EGTA (EG), or a mixture of 2 mM $CaCl_2$ and 80 µM W7 (W7). After washing of beads, proteins bound were analyzed by SDS-PAGE. ~3% of input (sample supplemented with 2 mM $CaCl_2$ before addition of CaM-Sepharose beads) and of unbound protein fractions (after pull-down) were analyzed in lanes *In* and *Un*, respectively. Proteins were visualized by staining with CBB. (*B*) as *A*, using untagged versions of plectin's ABD, preceded by plectin isoform 1a-, 1f-, and 1c-specific sequences, and of the ABD alone, instead of MBP fusion proteins. Note, that only MPB-CH1 and P1aABD showed binding to Ca^{2+}/CaM. Schematic representations in *A* and *B* show protein fragments used in the assays. (*C*) Ca^{2+}-dependent binding of P1aABD to CaM-Sepharose. Pull-down assays with P1aABD were performed as in *B*, except that increasing concentrations of $CaCl_2$ were used as indicated. The relative amount of P1aABD that bound to CaM was determined by densitometry, and plotted subtracting the amount of protein sedimented in the presence of 5 mM EGTA (EGTA). Data are presented as percentage of binding compared to maximum (100%) P1aABD-binding in the presence of 2 mM $CaCl_2$. Mean values (± S.E.) of three independent experiments are shown. The figure was modified from (Kostan *et al.*, 2009).

pull-down assays using CaM-Sepharose (Kostan, *et al.*, 2009). Interestingly, only fragment P1aABD showed binding to CaM-Sepharose beads, while no, or hardly any, binding was observed for the other fragments (**Figure 21B**) (Kostan, *et al.*, 2009). CaM-binding of P1aABD was specific, as demonstrated by its dependence on Ca^{2+}, lack of binding to Sepharose without bound CaM, and abolishment of binding in the presence of W7 (Kostan, *et al.*, 2009). Cells under physiological conditions maintain a large concentration gradient between extracellular and intracellular calcium. Normal extracellular concentrations of calcium are in the 1-3 mM range, while intracellular concentrations are in the micromolar range (0.1 to 0.2 μM). In most of the in vitro experiments presented here, I used calcium at 2 mM (Kostan, *et al.*, 2009). Therefore, I wanted to investigate next, whether P1aABD-CaM interaction will take place at lower, more physiological concentrations of calcium as well. The calcium dependence of P1aABD-binding to CaM was tested using CaM-pulldown assays (Kostan, *et al.*, 2009). At differing calcium concentrations (0.4 μM to 2 mM $CaCl_2$), a constant amount of P1aABD was incubated with CaM-Sepharose, and the amount of bound plectin was quantified using SDS-PAGE. 5mM EGTA was used as control to determine the level of unspecific binding (**Figure 21C**) (Kostan, *et al.*, 2009). As expected, binding of P1aABD to CaM-Sepharose was observed even at the lowest calcium concentration tested and remained higher then unspecific binding observed in the absence of Ca^{2+} (**Figure 21C**) (Kostan, *et al.*, 2009). In fact, very similar dose-response data were reported for filamin A-binding to CaM using in vitro binding assays under conditions similar to those used in our study (Nakamura *et al.*, 2005).

Ca^{2+}/CaM regulates the binding of P1a, but not of P1f or P1c, to F-actin

As a transducer of cytosolic Ca^{2+} signals regulating the activities of proteins, CaM plays a crucial role in a variety of Ca^{2+}-dependent signaling pathways. Investigating the physiological aspects of CaM's specific interaction with plectin 1a, I next examined the effects of CaM on the binding of plectin to filamentous actin (F-actin) using a cosedimentation assay (Kostan, *et al.*, 2009). For this, I tested three isoform-specific fragments of plectin that had shown distinct CaM-binding properties, P1aABD, P1fABD and P1cABD, in CaM-Sepharose pull-down assays (Kostan, *et al.*, 2009). Prior to cosedimentation with polymerized F-actin, samples were mixed with increasing concentrations of CaM, in the presence of either 2 mM $CaCl_2$, or 5 mM EGTA. The analysis of supernatant and pellet fractions by SDS-PAGE showed that CaM, in a

concentration- and Ca^{2+}-dependent manner, strongly inhibited F-actin binding of P1aABD, but had only minor effects in the absence of Ca^{2+} (**Figure 22, A and B**) (Kostan, *et al.*, 2009). In the case of P1fABD and P1cABD, CaM reduced P1fABD- and P1cABD-F-actin binding only moderately and independently of Ca^{2+}, suggesting that this interaction was unspecific (**Figure 22, C, D, E, and F**) (Kostan, *et al.*, 2009). Interestingly, I found that the difference in the inhibitory effect of CaM on plectin-F-actin interaction in the presence (2 mM $CaCl_2$) and absence of calcium (5 mM EGTA) was more pronounced in the case of P1cABD compared to P1fABD (**Figure 22, D and F**). Nevertheless, as obvious from the graphical evaluation (**Figure 22, B and F**), this difference was not as significant as in the case of P1aABD-F-actin binding, indicating that the regulation of plectin-F-actin interaction by CaM is P1a isoform specific (Kostan, *et al.*, 2009). This was also consistent with the data from pull-down assays where only P1aABD, but not P1fABD or P1cABD, showed binding to CaM (**Figure 21B**) (Kostan, *et al.*, 2009).

Plectin and other members of the plakin protein family (for review see Jefferson *et al.*, 2004) posses a conserved region called the plakin domain, which is located near their N termini. In plectin, the plakin domain (encoded by exons 9-30) is located between the ABD and the rod domain. Consisting of nine consecutive spectrin repeats organized in an array of tandem modules, this domain required for the efficient binding of plectin to HD-associated integrin α6β4. It has been demonstrated that dystrophin and utrophin, members of the spectrin protein family that share homologous ABDs with plectin, undergo lateral association with F-actin through interaction of their spectrin-like repeats, suggesting that these modules enable at least some members of the plakin protein family to laterally bind and stabilize F-actin (Rybakova *et al.*, 2002 and 2006). So far, the binding of plectin to F-actin via its plakin domain has not been investigated. To find out whether plectin's plakin domain has an impact on CaM-regulated plectin-F-actin binding, I purified a tag-less plectin fragment (encoded by exon 1a-24, P1a-24) comprising a major part of plectin's plakin domain (using a similar purification strategy as described in part 1 of this thesis) and subjected it to F-actin cosedimentation assay upon incubation with increasing concentrations of CaM both in the presence (2 mM $CaCl_2$) and in the absence of calcium (5 mM EGTA). Similar to the case of P1aABD, CaM was found to inhibit the binding of P1a-24 to F-actin in the presence of Ca^{2+} (**Figure 23, A and B**). As expected, in the presence of EGTA, only a slight decrease in F-actin- binding to P1a-24 was observed up to
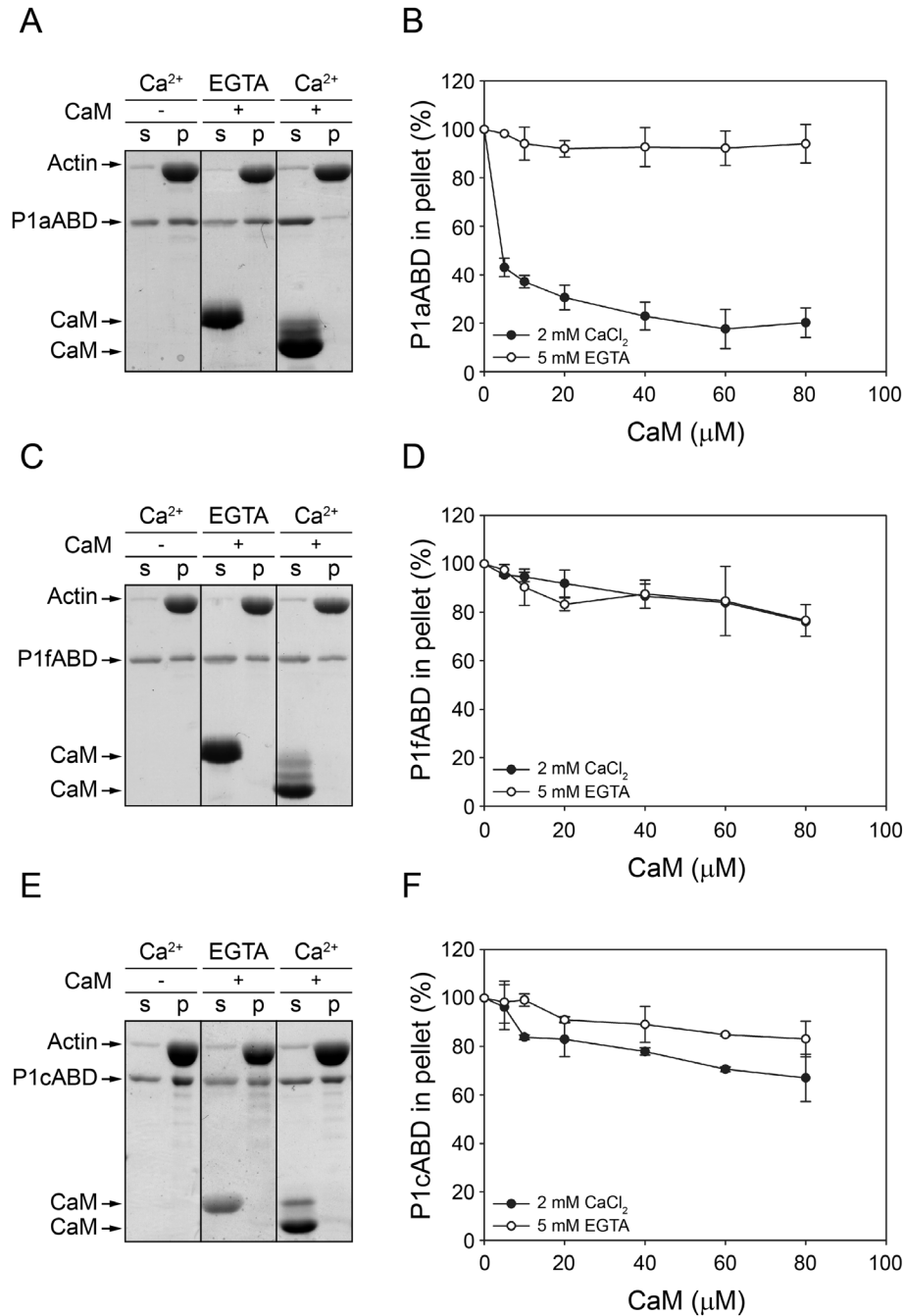
Figure 22. **Differential modulation of P1aABD-, P1fABD- and P1cABD–F-actin binding by CaM.** Mixtures of recombinant plectin fragments P1aABD (*A*), P1fABD (*C*), or P1cABD (*E*), with or without CaM, were incubated, with preassembled F-actin, in the presence of Ca^{2+}, or EGTA. Actin filaments and proteins bound were sedimented by centrifugation and equal amounts of supernatant (s) and pellet (p) fractions were subjected to SDS-PAGE; separated proteins were visualized by CBB staining. (*B, D* and *F*) Densitometric quantitation of gel bands, obtained in experiments run under conditions similar to those of *A, C* and *E*, except that increasing concentrations of CaM were present in the reaction mixtures. Data are presented as percentage of binding compared to maximum (100%) F-actin-binding in the absence of CaM. Mean values (± S.E.) of three independent experiments are shown. The figure was modified from (Kostan *et al.*, 2009).

the highest concentration of CaM tested. Interestingly, while binding of P1aABD to F-actin was reduced by CaM to 20% of the binding determined in the absence of CaM (100%) (for details see **Figure 22B**), at a similar concentration of CaM, P1a-24 binding to F-actin was reduced to less than 40% (**Figure 23B**). This suggests that plectin, similarly to dystrophin and utrophin, might interact with F-actin via its plakin domain, and thus reduce the effect of CaM on plectin-F-actin complex disruption. However, to support this notion, as well as to produce statistically significant results further experiments need to be performed. In conclusion, P1a-24 (a larger fragment of plectin resembling the full-length protein) exhibited a Ca^{2+}/CaM dependent response similar to the shorter plectin version, P1aABD. This indicated that CaM activities are most-likely unaffected and thus independent of plectin sequences flanking the ABD C-terminally.
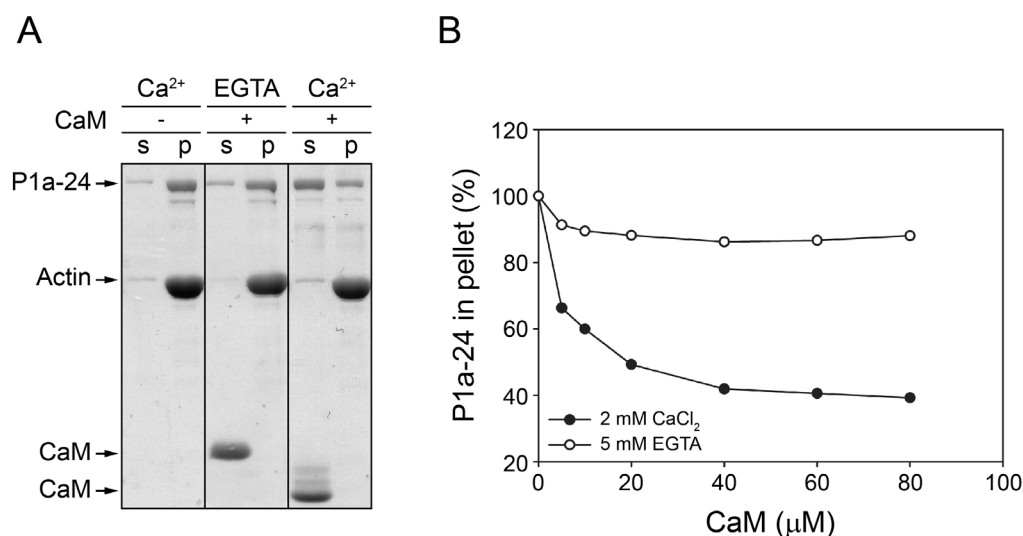
Figure 23. Ca^{2+}-**dependent inhibition of P1a-24–F-actin binding by CaM.** (*A*) Mixtures of recombinant plectin fragment P1a-24 with or without CaM, were incubated, with preassembled F-actin, in the presence of Ca^{2+}, or EGTA. Actin filaments and proteins bound were sedimented by centrifugation and equal amounts of supernatant (s) and pellet (p) fractions were subjected to SDS-PAGE; separated proteins were visualized by CBB staining. (*B*) Densitometric quantitation of gel bands, obtained in experiments run under conditions similar to those of *A,* except that increasing concentrations of CaM were present in the reaction mixtures. Data are presented as percentage of binding compared to maximum (100 %) F-actin-binding in the absence of CaM.

Binding affinity of P1aABD, P1cABD, and P1fABD to F-actin

To support the results obtained by pull-down assays (see above) and to confirm that the inhibition of plectin-F-actin binding is independent of binding affinities of particular plectin

isoforms for F-actin, we determined actin-binding dissociation constants (*Kd* values) of P1aABD, P1cABD and P1fABD in the absence of CaM, using cosedimentation assays. Here, constant amounts of F-actin (4 µM) were mixed with increasing amounts of protein (0 - 65 µM), and subjected to high speed ultracentrifugation (217000 *g*). Densitometry of stained gel bands corresponding to supernatant and pellet fractions was used to determine saturation levels, and calculate affinities of binding partners.

The resulting binding curves revealed that in all cases the dissociation constants were in the micromolar range (**Figure 24**). In fact, P1cABD bound to F-actin with a *Kd* of 9.09 µM, while for P1aABD and P1fABD *Kds* of 6.27 and 7.53 µM (Kostan, *et al.*, 2009), respectively, were measured, comparable to those of other actin-binding proteins (Sawyer *et al.*, 2009). It should be noted that the affinity of P1cABD to F-actin was found to be slightly lower compared to that of P1aABD indicating that in the presence of CaM, binding of P1cABD to F-actin, would be reduced more than that of P1aABD (compare **Figure 22, B and F**).
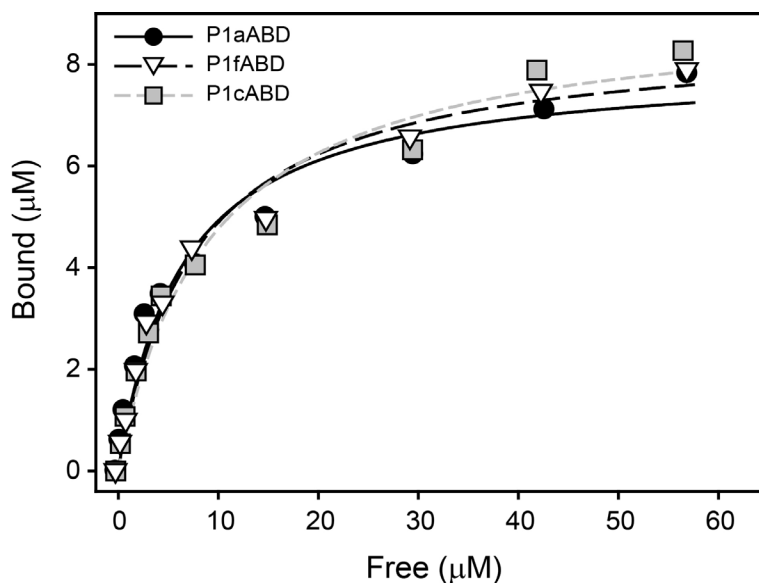
Figure 24. Binding of P1aABD, P1fABD and P1cABD to F-actin. Various amounts of P1aABD, P1fABD or P1cABD were incubated with 4 µM F-actin and subsequently centrifuged at 217000 *g*. The amounts of free and bound proteins were determined by densitometry of CBB-stained SDS-polyacrylamide gels loaded with equal volumes of supernatant and pellet fractions similar to those shown in **Figure 22**. Data represent mean values of three independent experiments. Nonlinear regression analysis yielded average apparent *Kd* values of 6.27, 7.53 and 9.09 µM for P1aABD-, P1fABD- and P1cABD-binding to F-actin, respectively. The figure was modified from (Kostan *et al.*, 2009).

However, such an effect has not been observed. Finally, our results showed that the differences observed in Ca^{2+}/CaM regulation of P1aABD, P1cABD and P1fABD binding to F-actin are not caused by different F-actin–binding affinities of these fragments (Kostan, *et al.*, 2009).

Binding of CaM to P1a prevents association of plectin with integrin β4

In light of CaM's ability to regulate plectin 1a-F-actin binding, it was of interest to assess whether it could also influence plectin's interaction with integrin β4, and thus could play a role in the assembly and/or disassembly of HDs. In fact, in previous studies, a binding site for integrin β4 has been mapped to the CH1 domain of plectin and binding of integrin β4 and of F-actin to plectin was shown to be mutually exclusive (Geerts *et al.*, 1999). In addressing this issue, I used untagged N-terminal plectin fragments (Kostan, *et al.*, 2009), as artificial sequences originating from fused tags may influence the conformational flexibility of these fragments with consequences for their binding properties. In a first series of experiments, a panel of soluble integrin β4 fragments (Rezniczek *et al.*, 1998; see also **Figure 25, A and B**) was immobilized on nitrocellulose membranes and overlaid with P1aABD labeled with Alexa Fluor 680 (Kostan, *et al.*, 2009). Infrared imaging revealed that P1aABD bound strongly to $β4-F_{1,2}LF_{3,4}C$, $β4-F_{1,2}L'$, and $β4-F_{1,2}L$, but not to any of the other integrin β4 fragments tested (**Figure 25A**) (Kostan, *et al.*, 2009). These data were in accordance with previous studies, showing that the first pair of fibronectin type III domains and part of the connecting segment of β4 were the minimal region required for the interaction of plectin's ABD with integrin β4 (Geerts *et al.*, 1999). Next, untagged P1aABD immobilized on CnBr-activated Sepharose beads was used to pull-down the integrin β4 fragment $β4-F_{1,2}LF_{3,4}C$, in the presence of increasing concentration of Ca^{2+}-bound, or Ca^{2+}-free forms of CaM (Kostan, *et al.*, 2009). As in the case of F-actin, CaM inhibited the association of integrin β4 with P1aABD in a concentration- and strictly Ca^{2+}-dependent manner (**Figure 26A**) (Kostan, *et al.*, 2009).

A quantitative analysis revealed that suppression of integrin β4-P1aABD binding by CaM reached 60% under these conditions (**Figure 26D**) (Kostan, *et al.*, 2009). Furthermore, when the integrin β4 fragment was allowed to preform a complex with Sepharose bead-immobilized P1aABD during a 30-min incubation before activated CaM was added, CaM effected a similar disruption of the plectin-integrin complex (**Figure 26, B and D**) (Kostan, *et al.*, 2009). Control experiments, showed no binding of $β4-F_{1,2}LF_{3,4}C$ to empty beads, nor of $β4-F_{1,2}$ (an integrin β4
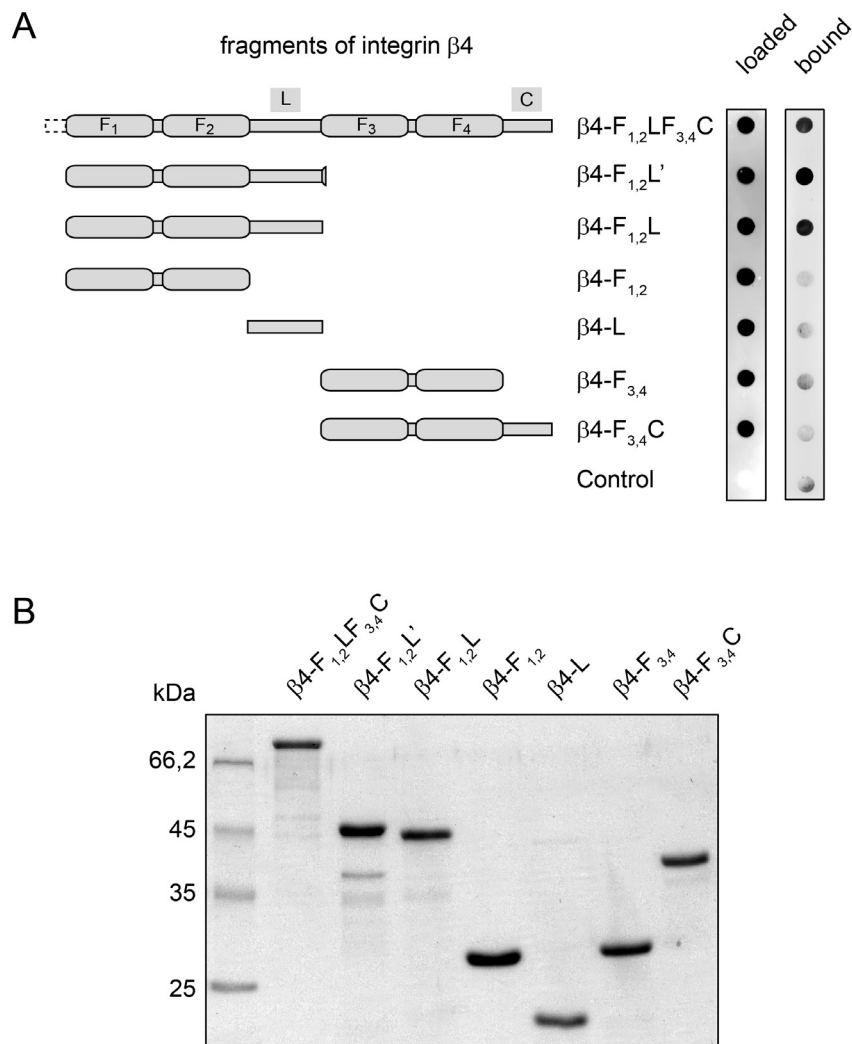
Figure 25. Binding of P1aABD (Alexa Fluor 680-labeled) to recombinant fragments of integrin β4. (*A*) Purified His-tagged recombinant proteins, representing the schematically indicated fragments of integrin β4 (for details see Rezniczek *et al.*, 1998), were spotted in duplicates (4 μg each) onto nitrocellulose membranes; solution P (for details see Materials and Methods section) served as control for unspecific binding and/or background fluorescence (control). One set of membrane-immobilized proteins was stained with CBB as a loading control (loaded), the other (bound) was overlaid with P1aABD (3 μg/ml) and bound protein was analyzed in an Odyssey Infrared Imager. (*B*) SDS-PAGE (CBB staining) of integrin β4 fragments used in *A*. Sizes of molecular mass markers are indicated. The figure was modified from (Kostan *et al.*, 2009).

fragment that had not shown binding to P1aABD in dot blot assays) to Sepharose bead-immobilized P1aABD or empty beads (**Figure 26C**) (Kostan, *et al.*, 2009). CaM, showing no binding to empty beads, cosedimented with bead-immobilized P1aABD in a Ca^{2+}-dependent and W7-suppressible manner (**Figure 26C**) (Kostan, *et al.*, 2009). These data clearly established the specificity of the pull-down assay used for assessing competitive binding (**Figure 26, A and B**) (Kostan, *et al.*, 2009).

Measurements of the dissociation constants of CaM and of the integrin $β4-F_{1,2}LF_{3,4}C$ fragment to P1aABD Sepharose revealed that integrin bound to P1aABD Sepharose with slightly higher affinity (*Kd* 0.05 μM) than CaM (*Kd* 0.16 μM; **Figure 26E**) (Kostan, *et al.*, 2009). Even though the dissociation constants measured under these in vitro conditions were within a similar range, a locally higher concentration of CaM (compared to plectin) would provide a basis for the
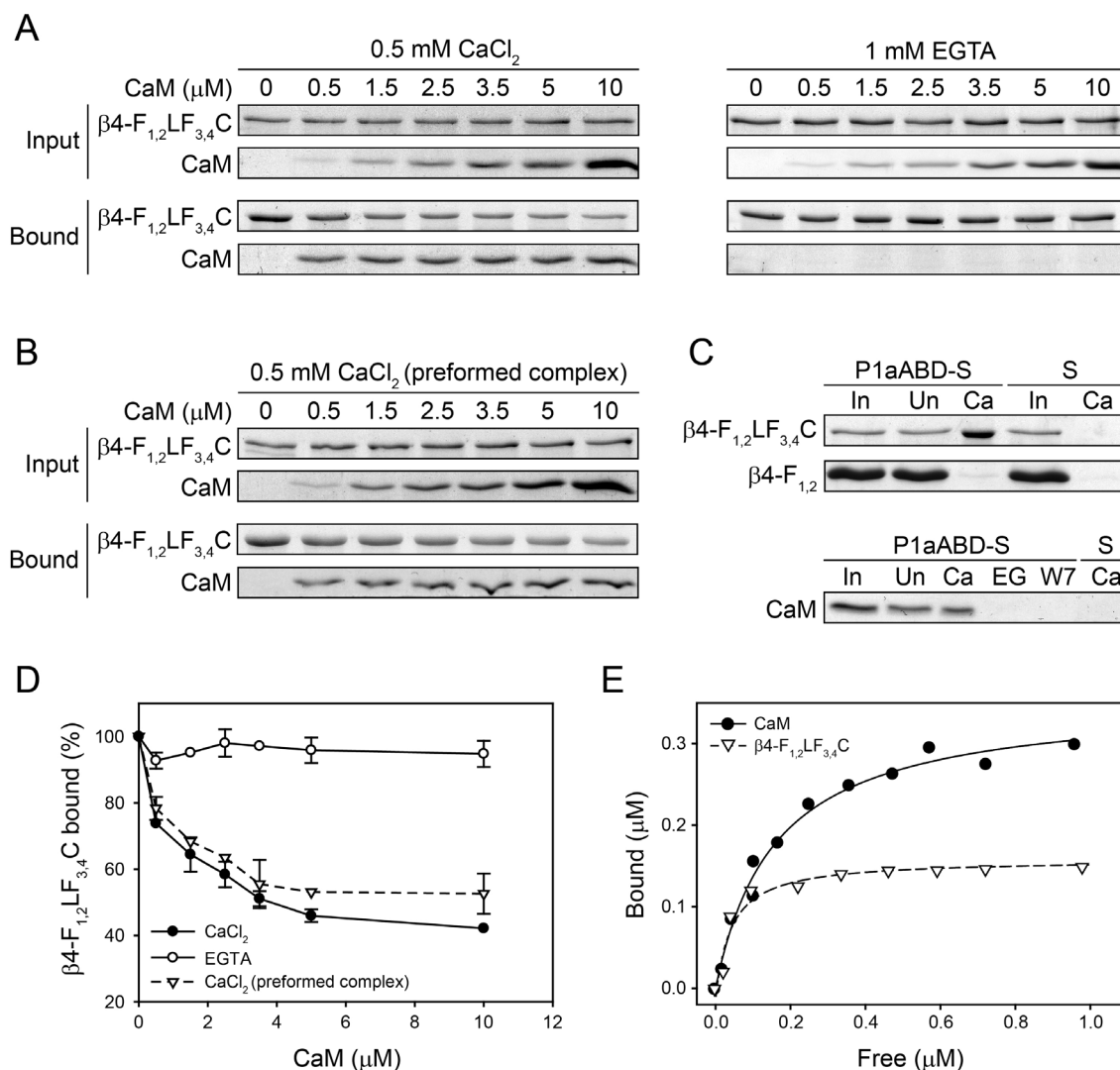
Figure 26. CaM-dependent binding of integrin β4 to Sepharose bead-immobilized plectin fragment P1aABD.
(*A*) Mixtures of integrin β4 fragment β4-F$_{1,2}$LF$_{3,4}$C (1.5 μM) and Sepharose bead-immobilized P1aABD were incubated with increasing amounts of CaM (0-10 μM), in the presence (0.5 mM CaCl$_2$) or absence (1 mM EGTA) of Ca^{2+}. Proteins bound were analyzed by SDS-PAGE and visualized by CBB staining (bound). Aliquots of reaction mixtures taken prior to incubation were run as loading controls (input). (*B*) As in *A,* except that intergrin/P1aABD mixtures were incubated for 30 min prior to addition of CaM to preform a complex. (*C*) Integrin β4 fragments β4-F$_{1,2}$LF$_{3,4}$C and β4-F$_{1,2}$ (upper rows), or CaM (lower row) were incubated with Sepharose bead-immobilized P1aABD (P1aABD-S) or empty beads (S) under the conditions indicated. Ca, 0.5 mM CaCl$_2$; EG, 1 mM EGTA; W7, 0.5 mM CaCl$_2$ and 80 μM W7. ~3% of reaction input (In) and of unbound protein (Un) were run as internal controls. Binding was analyzed as in *A*. (*D*) Ple1aABD-bound β4-F$_{1,2}$LF$_{3,4}$C fractions from *A* and *B* were determined by densitometric analysis of gels. Percent binding compared to that in the absence of CaM (100%) is shown. Data represent mean values (± S.E.) of three independent experiments. (*E*) Sepharose bead-immobilized P1aABD was incubated with increasing amounts of CaM, or β4-F$_{1,2}$LF$_{3,4}$C, in the presence of 0.5 mM CaCl$_2$. The amounts of free and bound proteins were determined by densitometric analysis of CBB-stained SDS-polyacrylamide gels loaded with supernatant and pellet fractions similar to those shown in *C*. Data represent mean values of three independent experiments. Nonlinear regression analysis yielded average apparent *Kd* values of 0.16 and 0.05 μM, for CaM- and β4-F$_{1,2}$LF$_{3,4}$C-binding to P1aABD-Sepharose, respectively. The figure was modified from (Kostan *et al.*, 2009).

successful displacement of plectin 1a from integrin in keratinocytes. The interaction of the plectin's ABD with the first pair of FnIII repeats and the N-terminal 35 amino acids of the linker segment (L) connecting the two pairs of the fibronectin type III (Fn) domains of integrin β4 (residues 1115-1355), is thought to be the initial step in HD assembly (Geerts *et al.*, 1999, Koster *et al.*, 2004, Rezniczek *et al.*, 1998). This is strengthened by additional interactions of plectin's plakin domain with the C terminus of the linker and the C-terminal tail of integrin β4. While plectin ABD-integrin β4 binding was found to be Ca^{2+}/CaM-dependent (Kostan, *et al.*, 2009), interaction of plectin's plakin domain with integin β4 is regulated by phosphorylations primarily occurring in the linker region of integrin β4. To assess, whether CaM-binding, too, could have some effect on interaction of plectin's plakin domain with integrin β4, plectin fragment P1a-24
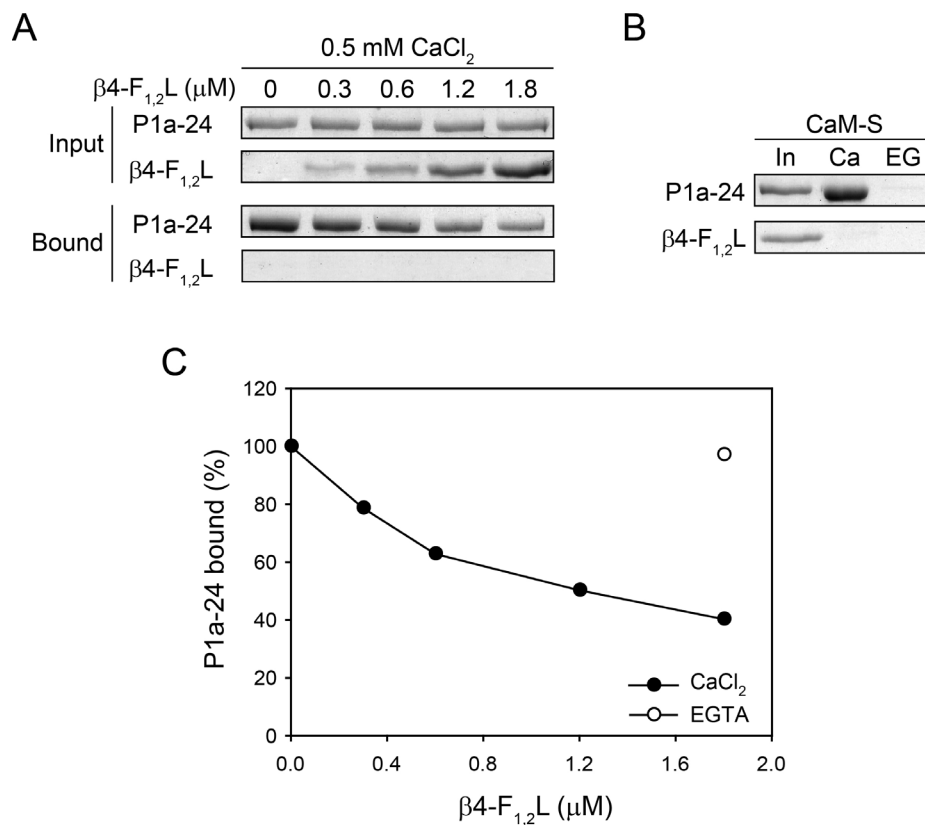
Figure 27. Integrin β4-dependent binding of P1a-24 to Sepharose bead-immobilized CaM. (*A*) Mixtures of P1a-24 (0.3 μM) and Sepharose bead-immobilized CaM were incubated with increasing amounts of integrin β4 fragment β4-$F_{1,2}$L (0-1.8 μM), in the presence (0.5 mM $CaCl_2$) or absence (1 mM EGTA; data not shown) of Ca^{2+}. Proteins bound were analyzed by SDS-PAGE and visualized by CBB staining (bound). Aliquots of reaction mixtures taken prior to incubation were run as loading controls (input). (*B*) P1a-24 (upper row), or integrin β4 fragment β4-$F_{1,2}$L (lower row) were incubated with Sepharose bead-immobilized CaM (CaM-S) under the conditions indicated. Ca, 0.5 mM $CaCl_2$; EG, 1 mM EGTA. ~3% of reaction inputs (In) were run as internal controls. Binding was analyzed as in *A*. (*C*) CaM-bound P1a-24 fractions from *A* were determined by densitometric analysis of gels. Percent binding compared to that in the absence of β4-$F_{1,2}$L (100%) is shown. Note that Ca^{2+}-dependence of P1a-24 binding to CaM-S in the presence of integrin β4-$F_{1,2}$L was tested at 1 mM EGTA, only for highest (1.8 μM) concentration of integrin used.

(comprising a major part of plectin's plakin domain) was subjected to a pull-down assay with CaM bound to Sepharose beads (CaM-S) in the presence of Ca^{2+} (0.5 mM $CaCl_2$) and increasing concentrations of an integrin β4 fragment (0-1.8 μM; β4-$F_{1,2}$L) harboring a second-plectin binding site (**Figure 27, A and B**). Interestingly, at increasing concentration of β4-$F_{1,2}$L, binding of P1a-24 to CaM was reduced, indicating that similar to the case of P1aABD, interactions of P1a-24 with integrin β4-$F_{1,2}$L is regulated be CaM. Quantitative analysis of these data revealed that suppression of CaM-P1a-24 binding by integrin β4 reached more than 60% under conditions used (**Figure 27C**). In addition, control experiments with integrin β4-$F_{1,2}$L and P1a-24 (**Figure 27B**), clearly showed specificity and calcium dependence of the interactions. In fact, while no binding of β4-$F_{1,2}$L to CaM was observed (neither in the presence of $CaCl_2$ nor of EGTA), P1a-24 was found to interact with CaM in a Ca^{2+}-dependent manner (**Figure 27B**). Thus, our results imply a role of CaM in the regulation of not only the first, but also the second integrin β4-binding site of plectin. However, this issue needs further clarification, as CaM was found to interact primarly with the CH1 domain of plectin, which is located distant to plectin's plakin domain. On the other hand, a direct interaction of CaM with plectin's plakin domain has never been investigated. Clearly, additional experiments are needed to explore the observed phenomenon, as well as to improve the quality and significance of these results.

Discussion

Cleavage of plectin isoforms-specific sequences by thrombin and its potential physiological relevance

The observation that plectin fragments purified without affinity tag did not become susceptible to degradation as in the case of plectin fragments isolated by using of fusion tag suggested that the factor responsible for "specific" loss of first exon-encoded sequences in our experiments was thrombin. Thrombin is an endoprotease that naturally functions as a blood clotting factor to convert fibrinogen to fibrin (Crawley *et al.*, 2007). Human thrombin is one of the most active site-specific proteases, which is an advantage because a very low mass ratio of enzyme to target protein is needed for efficient cleavage. Although no single consensus sequence describes the specificity of thrombin cutting, cleavage frequently occurs after the proline-arginine residue pair when properly exposed in a three-dimensional structure (Gallwitz *et al.*, 2012). Thrombin is a site-specific protease that exhibits very low non-specific cleavage under many conditions. However, its excess may result in unwanted proteolysis at secondary sites. In our case, prolonged incubation with thrombin could lead to such effects. Interestingly, neither uncleaved, full-length protein, nor other degradation products were observed upon analysis of lyophilized protein sample on SDS-PAGE, indicating that in this case, cleavage was specific and complete. As thrombin is thought to be a site-specific protease, secondary activity in our preparations could arise from other proteases present in the purchased thrombin. To exclude this possibility, effects of thrombin inhibitors on cleavage could be examined and/or additional purification of purchased thrombin (*e.g.* by ion exchange chromatography), could be performed. However, in our purification protocol, we did not include these approaches and rather focused on developing purification protocols excluding the usage of thrombin altogether.

Interestingly, limited (in situ) proteolysis with less specific proteases like *e.g.* trypsin, or chymotrypsin is used in crystallography to remove flexible parts of the protein in order to increase the probability of its crystallization (Dong *et al.*, 2007). Thus removal of the first exon-encoded sequences was on one hand beneficial for our successful crystallization (as we obtained crystal of the P1cABD lacking the residues removed by thrombin). On the other hand it indicated that this part of the protein is flexible and/or unstructured, it is not part of a compact domain, and therefore, prone to proteolytic removal. In addition, the question arises whether cleavage of

plectin by thrombin has a physiological relevance and is used in regulation of plectin functions in vivo.

During long term differentiation of keratinocytes expression of P1a was found to be subject to transcriptional as well as posttranscriptional regulation, similar to integrin α6β4 (Tennenbaum *et al.*, 1996). In our study (Kostan *et al.*, 2009), more rapid (faster) decrease of P1a protein content in comparison to its mRNA level within 5 days of differentiation was observed, suggesting that proteolytic cleavage of P1a is followed by repression of gene expression. Furthermore, plectin was shown to be regulated by proteases either as wild-type (Stegh *et al.*, 2000), or mutant (EBS-Ogna) protein (Walko *et al.*, 2011) suggesting that such regulation does indeed exist, although specific removal of the first exon-encoded sequences by protease has previously not been observed. Besides all its important effects for the initial phase of wound healing, thrombin has been found to induce proliferation of fibroblasts and keratinocytes (Chen and Buchanan, 1975; Algermissen *et al.*, 2000) during this process. However, thrombin exerts its activity by binding with high-affinity to protease-activated receptors 1, 3 and 4 (Coughlin, 1999), or thrombomodulin (Peterson *et al.*, 1999), a functional anticoagulant, both present on the surface of keratinocytes (Algermissen *et al.*, 2000; Peterson *et al.*, 1999). Thus thrombin, most likely does not facilitate degradation of plectin isoforms in vivo.

The idea about a regulation of first exon-encoded sequences by proteolytic cleavage is tempting, mainly because these sequences dictate plectin's function and play an important role for plectin's subcellular localization (Rezniczek *et al.*, 2003). Thus upon stimuli, proteolytic degradation of plectin's first exon-encoded sequences could lead to displacement of plectin from its specific location, and/or to its release from the binding partner, allowing further processing of the protein. In addition, protease-mediated removal of first exon-encoded sequences of plectin could have an effect on the binding properties of plectin's ABD which is succeeding them. In fact, plectin's ABD has been shown to interact with several binding partners (Rezniczek *et al.*, 2010), and the specificity of its binding to individual binding partners has been suggested to be regulated by plectin's first exon-encoded sequences (Kostan *et al.*, 2009).

Structure of plectin isoforms-specific sequences

After solving the structure of the mouse (Ševčík *et al.*, 2004) and human ABDs of plectin (García-Alvarez *et al.*, 2003), it became clear that some parts of plectin isoform specific

sequences have a propensity to become structured. In fact, the last 6 amino acid residues of the P1c-specific sequence were found to form an α-helix in the crystal structure of human plectin P1cABD (García-Alvarez *et al.*, 2003). This observation, together with growing evidence for functional variety of plectin isoforms, dictated by first exon-encoded sequences, led us to the idea to determine the 3D structure of P1a and P1c specific sequences fused to plectin's ABD. In the time course of my thesis, I did not obtained any structural information about P1a and P1c specific sequences, either because of the problems discussed in the previous paragraph (thrombin cleavage), or because of lack of diffraction quality crystals of P1cABD or P1aABD. Nevertheless, our results suggested that P1c and P1a specific sequence are most likely flexible and disordered as both sequences were proteolytically removed from the ABD upon treatment with thrombin. In agreement with this idea, in the structure of the P1cABD-integrin β4Fn12 complex (de Pereda *et al*, 2009), where the entire P1c-specific sequence was used for formation of the complex, the main part of the P1c-specific sequence was found to be disordered. In fact, there was no visible density found for most of the P1c-specific sequence and only two small regions of it became structured upon binding to integrin β4 (de Pereda *et al*, 2009). This would explain on the one hand, why it was difficult (almost impossible) to obtain crystals of P1cABD and P1aABD, and on the other hand it raised the question of wheter the P1c and P1a isoform-specific sequences needed to be unstructured.

Intrinsically disordered regions are typically involved in regulation, signaling and control pathways in which interactions with multiple partners and high-specificity/low-affinity interactions are often a requisite. Another unique functional faculty of intrinsically disordered proteins (IDPs) is that their open structure is largely preserved when they form a complex with their target (Dyson and Wright, 2005). Thus for plectin isoform-specific sequences being disordered could be beneficial and important for providing a disproportionately large binding surface and multiple contact points for a sequence of the given relatively small size. An additional prominent feature is that IDPs can adopt different structures upon different stimuli or with different partners, which enables their versatile interaction with various targets. This phenomenon, termed binding promiscuity (Kriwacki *et al.*, 1996) or one-to-many signaling (Dunker *et al.*, 2001), enables an exceptionally plastic behavior in response to the needs of the cell. In this respect plectin isoform-specific sequences could interact with multiple binding partners and adjust/regulate binding properties of whole plectin molecule. Finally, many

intrinsically disordered proteins undergo transitions to more ordered states or fold into stable secondary or tertiary structures on binding to their targets - that is, they undergo coupled folding and binding processes (Wright and Dyson, 2009). Thus, using of proper interaction partner could help to crystallize and obtain structural information about some of the plectin isoform-specific sequences, as it was already observed in the case of the P1cABD-integrin β4Fn12 complex (de Pereda *et al.*, 2009). Interestingly, in this case some parts of the P1c specific sequence became structured, although an improper interaction partner had been used; as P1a but not P1c was shown to colocalize specifically with HDs, where interaction between plectin and integrin β4 takes place (Andrä *et al.*, 2003). All together, we can assume that some plectin isoform-specific sequences have the propensity to be structured or disordered as determined by their sequence. As there is no sequence homology between different plectin isoform-specific sequences and plectin isoforms display diversity in their sub-cellular localization, binding partners, and binding modes, structural characteristics of plectin isoform specific sequences and their possible effects on binding activities of plectin's ABD will be most likely unique for each of them and need to be elucidated on case-to-case basis.

Plectin's ABD interacts with non-filamentous vimentin

Although CH domains forming a canonical ABD seem to be structurally highly conserved, the plethora of existing data are pointing towards functional diversity of CH1 and CH2 subdomains (Gimona *et al.*, 2002). In our study we were able to identified vimetin as a new interaction partner of plectin's ABD and mapped its binding to the first, more N-terminal CH domain of plectin (Ševčík, *et al.*, 2004). It was reported that proteins containing either single CH subdomains (calponin), or more complex ABDs (fimbrin, dystrophin) can interact with IF proteins. Calponin binds to desmin, the major IF protein in smooth and skeletal muscle (Wang and Gusev, 1996; Mabuchi *et al.*, 1997; Fujii *et al.*, 2000), fimbrin interacts with and colocalizes with vimentin in filopodia, retraction fibres, and podosomes at the ventral surface of cultured macrophages (Correia, *et al.*, 1999), and dystrophin binds directly and specifically to keratin 19 at the costameres of striated muscle (Stone *et al.*, 2005). While in the case of fimbrin and calponin there is evidence that binding occurrs to IF subunit proteins in their nonfilamentous state (Wang and Gusev, 1996; Mabuchi *et al.*, 1997; Fujii *et al.*, 2000; Correia, *et al.*, 1999), binding of dystrophin to filamentous keratins was observed (Stone *et al.*, 2005). Fimbrin was unable to

bind to polymerized vimentin in cosedimentation assays and binding occurred at a stoichiometry of 1:4, suggesting that the IF protein was in its tetrameric form (Correia, *et al.*, 1999). As one may expect on the basis of their structural similarity (Ševčik *et al.*, 2004), the ABDs of fimbrin and plectin apparently also have a number of functions in common, including binding to vimentin (Ševčík, *et al.*, 2004). Similar to fimbrin (Correia, *et al.*, 1999) the ABD of plectin failed to associate with vimentin filaments, as assessed by our vimentin cosedimentation and in vitro Eu^{3+}-protein binding assays, suggesting that it, too, interacted with soluble IF protein subunits rather than with their filamentous polymers. Binding assays revealed that the major vimentin-binding interface was localized within the CH1 subdomain of plectin (Ševčik *et al.*, 2004). Since P4-8 (plectin's ABD/2α lacking half of the CH1 domain) bound to vimentin, sequences preceding those encoded by exon 4 apparently did not contribute to this interaction (Ševčik *et al.*, 2004). However, as fragments corresponding to the first half of plectin's CH1 domain (exons 2-4) have not been examined in our studies (Ševčik *et al.*, 2004), a role of this part in vimentin-binding can not be fully excluded. Using an overlay assay we found strong binding of plectin's ABD to a fragment of vimentin comprising the rod and its N-terminal domains, but when examined individually, both of these domains showed only weak binding (Ševčik *et al.*, 2004). Using a similar method, it had been shown that a vimentin fragment lacking the C terminus (N410/VimNR) was capable of binding to fimbrin, contrary to a fragment lacking the initial 102 amino acid residues (102C/VimRC), suggesting that the fimbrin-binding site was located in the N-terminal head domain of vimentin (Correia, *et al.*, 1999). The N-terminal vimentin fragment (VimN) and the rod fragment (VimR) used in our experiments ended and started at Phe95, respectively (Ševčík, *et al.*, 2004). Consequently, the rod-containing fragment used in our experiments and the N-terminal fragment N410/Vim-NR used in (Correia, *et al.*, 1999) overlapped by a few amino acid residues. With this consideration, the results of our overlay assay were consistent with the findings reported in (Correia, *et al.*, 1999). Using, as an alternative method, affinity-binding of proteolytic fragments of vimentin in combination with mass spectrometry, we found that plectin bound to a ~18 kDa fragment (Ševčik *et al.*, 2004) corresponding to "Coil 1" (Strelkov *et al.*, 2003), the N-terminal part of the α-helical rod domain of vimentin. This is in agreement with similar experiments in which the calponin-binding site was restricted to the N-terminal part of the desmin rod domain (Fujii *et al.*, 2000). However, in the overlay assay, the rod domain of vimentin (VimR) alone showed little binding to plectin (Ševčik

et al., 2004). As fragments obtained by partial proteolytic digestion of properly folded full-length vimentin are more likely to preserve the structure of the native protein than recombinantly prepared fragments, we assume the true plectin ABD-binding site of vimentin to be localized in the N-terminal part of its rod domain (Ševčik *et al.*, 2004). Binding to the evolutionary highly conserved CH domains could be a common feature of IF proteins in general. Likewise, considering that the α-helical coiled-coil structure of vimentin's rod domain is highly conserved in all IF protein family members, plectin's ABD may bind also to other IF proteins, such as desmin or keratins.

The functional significance of plectin ABD-vimentin interaction

The functional significance of the plectin ABD-vimentin interaction remains elusive. The primary activity of the ABD supposedly is actin-binding, a function demonstrated for fimbrin, plectin, and dystrophin (Andrä *et al.*, 1998; Glenney *et al.*, 1981; Way *et al.*, 1992b). The CH domain of calponin, on the other hand, does not seem to be required for actin-binding as calponin interacts with actin via its C-terminal domain (Gimona and Mital, 1998). Thus, with an IF protein-binding site residing in their N-terminal CH domains in addition to their genuine actin-binding activities, fimbrin, dystrophin, plectin and calponin, might influence the assembly and organization of both actin and IF cytoskeletal networks. The interaction of fimbrin's ABD with vimentin has been shown to be adhesion dependent and it has been suggested that this complex is a transient structure involved in early cell adhesion (Correia, *et al.*, 1999). In smooth muscle cells calponin may be an integral component of desmin IFs in the vicinity of dense bodies (Mabuchi *et al.*, 1997). The interaction between IF proteins, such as desmin or vimentin, and proteins containing one or more CH domains could represent a highly conserved function related to the establishment of cell adhesion structures. By sequestering soluble vimentin at certain sites, such as focal adhesion contacts, plectin may favor and/or initiate IF network formation at these sites by locally increasing IF protein concentrations. Once filament assembly has been initiated, plectin may stabilize and anchor the filaments at these sites via its alternative C-terminal IF-binding site. Future experiments should show whether this model can be verified.

The ABD of plectin turned out to be multifunctional, binding not only to vimentin (Ševčik *et al.*, 2004), but also to other proteins like actin (Fuchs *et al.*, 1999), integrin β4 (Geerts *et al.*, 1999; Rezniczek *et al.*, 1998), and nesprin 3 (Wilhelmsen *et al.*, 2005), to name a few. In

addition, binding of F-actin and integrin β4 to the ABD of plectin has been shown to be mutually exclusive (Geerts *et al.*, 1999; Litjens *et al.*, 2003). Similarly, binding of vimentin to the CH1 domain of plectin would most likely interfere with binding of other interaction partners of plectin's ABD; a property that has not been investigated, yet (Ševčik *et al.*, 2004).

Differential splicing of the plectin gene leads to generation of several plectin isoforms, distinguished from each other by the sequence and length of their N termini encoded by alternative first exons (Fuchs *et al.*, 1999). The role of plectin isoform-specific sequences in the binding of plectin's ABD to vimentin has not yet been tested. In our experiments we used P1aABD and P1cABD/2α proteins, both of which showed binding to vimentin (Ševčik *et al.*, 2004), however no further quantification and comparison of these interactions has been done. The large number of overlapping binding sites present on plectin's ABD speaks for the existence of mechanisms regulating the selectivity of the ABD for different binding partners. This role could be mediated by plectin isoform-specific sequences adjacent to the ABD. In this respect, some plectin isoform-specific sequences could stabilize or prevent binding of the ABD to vimentin and/or change the specificity of plectin's ABD for binding to other IF proteins. Thus the ABD of P1d, the only isoform of plectin that is specifically expressed in skeletal and cardiac muscle (Fuchs *et al.*, 1999) and is responsible for the recruitment and anchorage of desmin IFs to Z-disks (Konieczny *et al.*, 2008), could interact with desmin. In the same view, the ABD of P1a, the major plectin isoform expressed in basal keratinocytes (Andrä *et al.*, 2003) could specifically interact with cytokeratins, similarly to the ABD of dytrophin. Although further work will be needed to understand how plectin controls IF assembly at the molecular level, our observations supports a general role for plectin in regulating IF networks.

CaM-plectin binding is regulated by first exon-encoded sequences of plectin

The difference in CaM binding of plectin's entire ABD compared with its CH1 domain (Kostan, *et al.*, 2009) could be explained by distinct conformational states of the ABD, with the conformation adopted by plectin isoform 1a being optimal for CaM binding. In fact, two conformational stages of the ABD of plectin and a model for the transition from one stage to the other upon binding to F-actin, have previously been proposed (García-Alvarez *et al.*, 2003). Similarly, a recombinant version of the CH1 domain of filamin A, but neither the full-length protein nor its CH1 domain-containing full-length ABD were found to bind to CaM in the

absence of F-actin, suggesting that filamin, too, harbors a cryptic CaM-binding site in its CH1 domain, which becomes exposed upon binding to F-actin (Nakamura *et al.*, 2005). Based on our data it is conceivable that sequences encoded by plectin's first exons mediate the conformational change of the ABD required for CaM binding, thereby modulating the function of plectin. In support of this model, we found that an N-terminal fragment of plectin, containing the ABD preceded by exon 1a-encoded sequences, associated with CaM, whereas similar fragments containing plectin 1f- and plectin 1c-specific sequences showed no, or only weak interaction with CaM (Kostan *et al.*, 2009). Furthermore, our data showed that CaM regulated actin-binding of the plectin 1a fragment in an isoform-dependent manner, whereas actin-binding in the absence of CaM appeared to be isoform-independent (Kostan *et al.*, 2009). In fact, P1cABD bound to F-actin with a *Kd* of 9.09 μM, while for P1aABD and P1fABD the *Kd* was 6.27 and 7.53 μM, respectively (Kostan, *et al.*, 2009). Moreover, full-length P1f showed substantially reduced co-localization with CaM compared with P1a when expressed in plectin-deficient keratinocytes (Kostan *et al.*, 2009).

ABD-preceding residues corresponding to plectin isoforms 1a and 1c have previously been suggested to affect the binding of the ABD of plectin to integrin β4, because P1c fragments were found to bind to integrin β4 more efficiently than the corresponding fragments of P1a in yeast two hybrid assays (Litjens *et al.*, 2003). However, these results were inconclusive insofar as only P1a, but not P1c, is recruited to HDs in basal keratinocytes (Andrä *et al.*, 2003), suggesting that the regulation of the interaction of plectin with integrin β4 by CaM may be restricted to P1a in the vicinity of HDs. Interestingly, the two-orders-of-magnitude difference in P1aABD binding affinities to actin and integrin could explain why P1a in keratinocytes shows preferential binding to integrin (Kostan *et al.*, 2009). Thus, in addition to their proposed targeting function (Rezniczek *et al.*, 2003), some of plectin's first exon-encoded sequences might regulate the structural flexibility of the ABD of plectin, mediating conformational transitions required for its binding to various proteins, CaM included. In fact, the ABD of plectin modulated in that way may acquire specific binding properties that distinguishes it from other isoforms. It remains to be shown in future experiments whether and how first exon-encoded sequences effect conformational changes of the ABD of plectin.

Implications of CaM-binding for plectin-F-actin interaction

Although CaM-binding to the ABD of P1a is likely to be of importance for the disassembly of HDs during keratinocyte differentiation (by preventing interaction with integrin

---

β4), it remains to be seen whether CaM inhibition of actin-binding has a biological function in this process as well. However, CaM-mediated regulation of this interaction may play a role in migration and terminal differentiation of keratinocytes. For instance, prevention of plectin-actin association by CaM could be a mechanism regulating actin reorganization and remodeling, which are required for the formation of cell protrusions during migration. Consistent with such notion, it has been shown that plectin-deficient keratinocytes, lacking keratin-integrin α6β4 anchorage, have an elevated migration potential (Osmanagic-Myers *et al.*, 2006). PKC phosphorylation has been identified as another mechanism for the mobilization of integrin α6β4 from HDs and its association with F-actin in cellular protrusions of squamous carcinoma-derived A431 cells (Rabinovitz *et al.*, 1999). Because we found CaM to associate with P1a in the early stages of keratinocyte differentiation (Kostan *et al.*, 2009), prevention of plectin-actin interaction involving CaM might be important not only for actin remodeling, but also for modulating competitive actin-binding of plectin and integrin. In addition, in line with recent studies revealing a role of plectin as a scaffolding platform for proteins involved in signaling, the release of plectin from HDs and actin filaments mediated by PKC/CaM may be important for proper localization of signaling molecules involved in actin reorganization and remodeling during cell migration, particularly as P1a was found to co-localize with CaM in cell protrusions after Ca^{2+} treatment of subconfluent keratinocytes culture (Kostan *et al.*, 2009). In confluent cultures, the release of plectin from HDs, along with inhibition of plectin-actin binding could possibly favor association of plectin with desmosomes, whose formation in keratinocytes is stimulated by Ca^{2+}. In fact, in confluent monolayers of differentiating keratinocytes our data showed redistribution of plectin 1a from HDs to the cell periphery in areas of cell-cell contacts (Kostan *et al.*, 2009). In line with this, plectin was found to be involved in the anchorage of IFs at desmosomes and the submembrane skeleton in polarized MDCK cells (Eger *et al.*, 1997). More experiments will be necessary to fully explore this process.

Recruitment of CaM interferes with P1a-integrin β4 binding

It has been shown previously that EGF-triggered phosphorylation of integrin α6β4 by PKCα (Rabinovitz *et al.*, 2004, Wilhelmsen *et al.*, 2007) and/or Fyn (Mariotti *et al.*, 2001) promotes the disassembly of HDs. Based on these observations, a mechanism of phosphorylation-induced HD disruption has been proposed (Litjens *et al.*, 2006). In our study
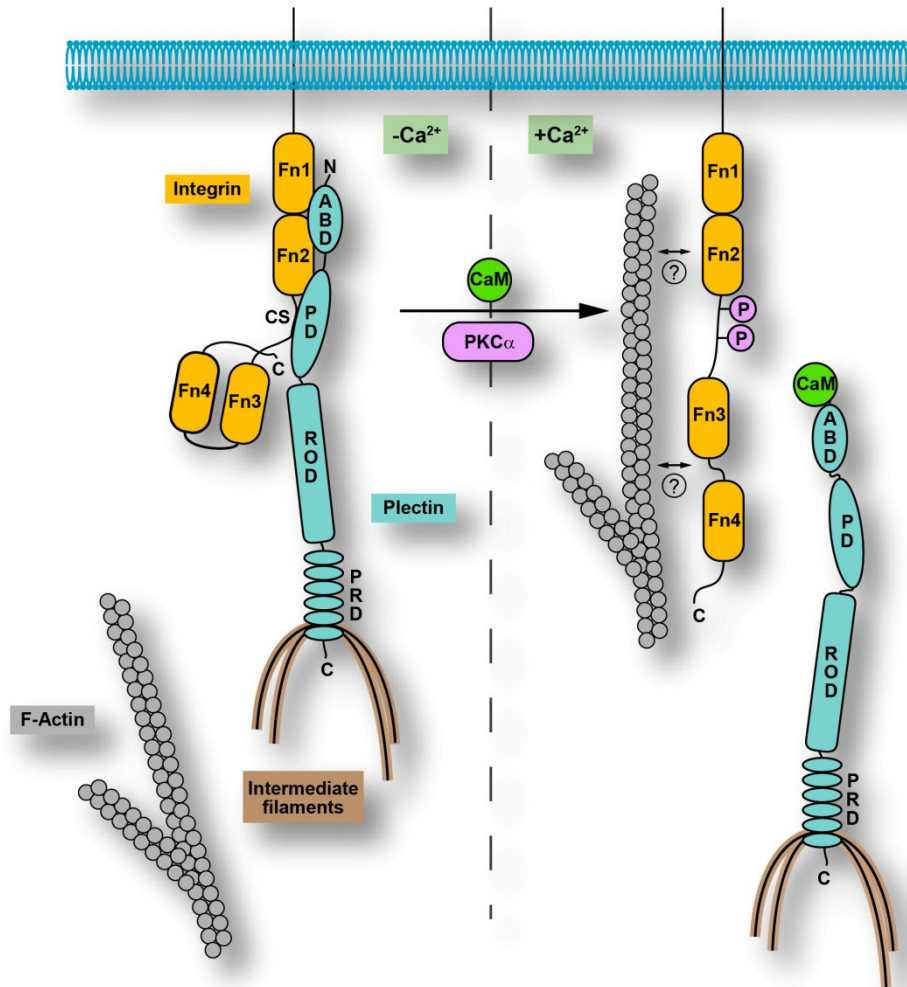
Figure 28. Model of integrin-keratin linkage via plectin 1a in undifferentiated and Ca^{2+}-differentiated keratinocytes. Under normal conditions ($-Ca^{2+}$), plectin 1a anchors IFs to HDs via association of its plakin domain (*PD*) with the connecting segment (*CS*) of integrin β4 and of its ABD with the first pair of the fibronectin type III (*Fn1* and *Fn2*) domains of integrin β4. When the concentration of Ca^{2+} in the cell increases ($+Ca^{2+}$), activation of PKCα or other kinase (e.g. ERK1/2, for details see Frijns *et al.*, 2010) leads to phosphorylation of serines within the CS domain of integrin, while CaM in its Ca^{2+}-bound form interacts with the isoform specific sequence of plectin 1a (Jaegeun Song unpublished results). Both events cause the dissociation of plectin from membrane- bound integrin and a redistribution of both proteins to actin-rich peripheral protrusions (and to perinuclear regions in the case of plectin). While integrin β4 might interact (directly or indirectly) with F-actin in such protrusions, as suggested by previous studies (Rabinovitz *et al.*, 1999), the role of CaM remaining bound to the ABD of plectin could be to prevent it from interacting not only with integrin but also with F-actin, thereby disconnecting IFs from the membrane. Furthermore, with progressing differentiation, down-regulation of plectin 1a and integrin α6β4 expression occurs. Note that the previously reported interactions of plectin's C-terminal domain with the CS and tail domains of integrin β4 (for details see Rezniczek *et al.*, 1998) are not shown (regulatory mechanisms involved in these interactions are unknown; however, CS phosphorylation might lead to destabilization of these interactions as well). The figure was modified from (Kostan *et al.*, 2009)

Discussion   71

an additional mechanism involved in this process has been uncovered, where Ca^{2+}-triggered binding of CaM to the ABD of plectin prevents its association with integrin β4 (Kostan *et al.*, 2009). Taking both mechanisms into account, we propose a new model for the disassembly of the plectin-integrin α6β4 complex during keratinocyte differentiation (**Figure 28**) (Kostan, *et al.*, 2009). In this model, Ca^{2+}-trigged CaM binding to plectin and phosphorylation of integrin β4 by Ca^{2+}-activated PKCα play complementary roles (Kostan, *et al.*, 2009). Thus, upon exposure of keratinocytes to Ca^{2+} during differentiation, both mechanisms are activated contributing to efficient disassembly of the plectin-integrin α6β4 complex and a redistribution of both subcomponents to actin-rich protrusions. There, integrin may be associated with actin filaments (Rabinovitz *et al.*, 1999), whereas plectin-actin interaction is prevented by CaM (Kostan, *et al.*, 2009). Whether phosphorylation of integrin β4 precedes and/or is important for CaM-binding to plectin, or whether additional regulatory factors are involved, remains to be shown. PKCα and CaM may act sequentially, or synergistically, one enhancing the effect of the other. Regulation could even be more complex, considering that PIP_2, which was found to inhibit the interaction of the ABD of plectin with actin (Andrä *et al.*, 1998), binds to the CH2 domain of plectin, which in turn has been shown to be involved in plectin interaction with integrin β4 (Geerts *et al.*, 1999, Litjens *et al.*, 2006). However, the role of PIP_2 in regulating plectin-integrin interaction has not been elucidated thus far.

In conclusion, I was able to identify and characterize CaM, as an isoform-specific binding partner of plectin's ABD that regulates the interaction of plectin not only with integrin β4, but as also with F-actin (Kostan, *et al.*, 2009) , thus playing a potentially very important role in HD disassembly. These mechanisms have important implications for keratinocyte differentiation, wound healing, and cell migration. Moreover, this study provided new insights into the molecular mechanism of how first exon-encoded sequences of plectin can modulate the functions of this unusually versatile cytolinker protein. The effects of ABD-bound CaM on the stability and flexibility of the exon 1a-encoded sequence, have still to be tested. Taking into account the possibility of heterologous over-expression, its relatively high solubility, compact fold, and known structure, CaM seems well suited for further structural studies

Materials and Methods

Common materials, buffers, solutions and growth media

Commonly used buffers and solutions

TAE (Tris-acetate-EDTA)

40 mM Tris/acetate, 2 mM EDTA, pH 8.2

TE (Tris-EDTA)

10 mM Tris/HCl, 1 mM EDTA, pH 8.0

PBS (phosphate buffered saline)

137 mM NaCl, 2.7 mM KCl, 8.1 mM Na_2HPO_4, 1.76 mM KH_2PO_4, pH 7.4

PBS-T

PBS containing 0.1% Tween-20

TBS (Tris buffered saline)

20 mM Tris/HCl, 137 mM NaCl, 2.7 mM KCl, pH 7.5

Bacterial strains and growth media

Bacterial strains

E. Coli strain DH5α (deo^R, endA1, gyrA96, hsd R17(rk$^-$, mk$^+$), recA1, relA1, phoA, supE44, thi^{-1}, Δ(lacZYA-argF)U169, Φ80lacZΔM15, F$^-$, λ$^-$) were used for al cloning purposes. For expression of recombinant proteins either *E.coli* strain BL21-CodonPlus(DE3)-RIL (F$^-$, ompT, hsdS(r$_B^-$ m$_B^-$), dcm$^+$, Tet^r, gal, λ(DE3), endA, Hte [argU ileY leuW Cam^r]), or *E.coli* strain BL21(DE3) (F$^-$, ompT, hsdS(r$_B^-$ m$_B^-$), dcm$^+$, gal, λ(DE3)) was used.

LB (Lysogeny Broth)

Tryptone…………………………………………….10 g/l
Yeast extract ……………………………………..5 g/l
NaCl…………………………………………….......10 g/l

pH 7.0 (adjusted with NaOH);ddH2O to 1000 ml; autoclaved (20 min at 121°C, liquid cycle). Appropriate antibiotics (ampicillin: 100 µg/ml; kanamycin: 30 µg/ml) were added to the medium after cooling to <40°C. To prepare plates, 15 g/l agar was added to the medium before autoclaving; approx. 20 ml medium was poured into each 10-cm Petri dishes; after hardening, plates were stored at 4°C.

TB (Terrific Broth)

Tryptone or peptone..........................12 g

Yeast extract....................................24 g

Glycerol...4 ml

ddH$_2$O to 900 ml; autoclaved (20 min at 121°C, liquid cycle); after the solution had cooled to < 40°C, 100 ml of a sterile solution of 0.17 M KH$_2$PO$_4$, 0.72 M K$_2$HPO$_4$ was added.

Antibody and specififity	Species	WB[1]	IF[1]	Source
Primary antibodies				
Plectin #46, rod-domain	rabbit serum			G. Wiche
Plectin #61, M$_1$-S$_{17}$ of P1c	rabbit serum	1:1000		G. Wiche
Integrin α$_6$, clone CD49f	rat mAb		1:100	BD Bioscience
Integrin β$_4$ H-101	rabbit serum	1:200		Santa Cruz
Camodulin, (a.a. 128-148)	mouse mAb	1:1000		Upstate
phospho PKCα/βII , Thr-638/641	rabbit serum	1:1000		Cell Signaling
Cytokeratin PR-B160-P	rabbit serum	1:1000		Covance
Cytokeratins, clone LP 34	mouse mAb	1:1000		Dako
Plectin, exon 1a	rabbit serum	1:1000		G. Wiche
Vimentin	goat serum	1 :5000		P. Traub
Secondary antibodies for WB				
HRP-anti rabbit IgG	goat	1:10000		Jackson Laboratories
HRP-anti mouse IgG	goat	1:10000		Jackson Laboratories
AP-anti rabbit IgG	goat	1:5000		Jackson Laboratories
AP-anti mouse IgG	goat	1:10000		Jackson Laboratories
HRP-anti goat IgG	donkey	1:10000		Jackson Laboratories
Secondary antibodies for IF				
Alexa 488-anti-rabbit IgG	goat		1:1000	Invitrogen
Texas Red-anti rat IgG	goat		1:50	Accurate Chemical & Scientific Corp.

1) Dilutions used for Western blotting (WB) and immunofluorescence (IF) analysis, respectively

Table 2. List of antibodies used for Western blotting and immunoflurescence labeling

In the course of this thesis a several plasmids for expression of various proteins have been used or generated. Details about them are given in DNA methods section.

DNA methods

Preparations of competent bacteria for heat-shock transformation

__TF buffer 1__: 10 mM MOPS, 10 mM RbCl, pH 7
__TF buffer 2:__ 100 mM MOPS, 10 mM RbCl, 50 mM $CaCl_2$, 15 % (w/v) glycerol, pH 6.5

All solutions were made fresh, sterilized by filtration (0.22 μm filter) and equilibrated to 4°C before use. A single colony was picked from the plate and grown overnight in 5 ml of LB at 37°C. 500 ml LB was inoculated with the overnight culture, and incubated in the shaker at 37°C until an OD_{600} of 0.4 was reached. Cells were pelleted by centrifugation (1500 *g*, 5 min., 4°C) and resuspended at 4°C in 10 mL of ice-cold TF buffer 1. Centrifugation was repeated; cells were resuspended in 10 mL of ice-cold TF buffer 2, and incubated on ice for 30 minutes. Aliquots of 50 or 100 μl were flash-frozen in liquid nitrogen and stored at -80°C.

Heat-shock transformation of E.coli

Competent cells (stored at -80°C) were thawed on ice and ~50 ng plasmid DNA was added to 100 μl of cell suspension and incubated on ice for 15 minutes. Afterwards, cell suspension was heated to 42°C for 90 seconds, followed by incubation on ice for at least 2 minutes. Cells were diluted with 1 ml of LB and incubated for 1 h, at 37°C, while shaking. Finally, cells were pelleted, resuspended in small amount of LB (50-100 μl), plated on selective medium, and incubated overnight at 37°C.

Agarose gel electrophoresis

__6x DNA sample buffer:__ 10 mM Tris/HCl (pH 7.6), 0.03 % bromophenol blue, 0.03 % xylene cyanol FF, 60 % glycerol, 60 mM EDTA

0.8-1.5 % agarose gels prepared with TAE buffer were used to separate DNA fragments at electrical field strength of 2-8 V/cm. 0.5 μg/ml ethidium-bromide was added prior to pouring the gels for visualization of DNA under UV light. DNA samples were mixed with 1/6 volume 6x DNA sample buffer before loading.

Preparation of plasmid DNA

Small scale preparation of plasmid DNA from bacteria was carried out using a rapid boiling method of Holmes and Quigley (Holmes and Quigley, 1981). Large scale preparation of plasmid DNA was performed using JETSTAR Plasmid Purification Kit according the manufacturer´s protocol (Genomed).

Determination of DNA concentration

The concentration of double stranded DNA was determined by measuring the absorbance at 260 nm (A_{260}), using the relationship that an A_{260} of 1.0 corresponds to 50 µg/ml of pure DNA. DNA purity was estimated from the A_{260}/A_{280} ratio (An A_{260}/A_{280} ratio between 1.7 and 2.0 generally represents a high-quality DNA sample).

Digestion with restriction enzymes

Usually 0.5-1.0 µg plasmid DNA was digested with 1-10 U restriction enzyme in a volume of 20 µl according to the manufacturer´s conditions.

Dephosphorylation of 5´-ends by Shrimp Alkaline Phosphatase (SAP)

1 µg of linear DNA was treated with 1 U of SAP (Fermentas) in total volume of 20 µl for 30 minutes at 37°C. The enzyme was inactivated by incubation for 15 min at 65°C.

Elution from agarose gels

After separation of DNA fragments by agarose gel electrophoresis DNA fragments were isolation of from agarose gels using the QIAEXII agarose gel extraction kit (Qiagen) according to the manufacturer´s instructions.

Ligation

Vector-DNA and insert were mixed in a molar ratio of 1:1 and 1:3. The ligation reaction was performed overnight at 16°C in a volume of 20 µl containing 1-5 U of T4-DNA ligase (Fermentas).

Site directed mutagenesis

10xReaction Buffer: 200 mM Tris/HCl (pH 8.8), 100 mM KCl, 100 mM $(NH_4)_2SO_4$, 20 mM $MgSO_4$, 1 %

Triton X-100, 1 mg/ml nuclease-free BSA

Site directed mutagenesis was performed by using of QuikChange™ Site-Directed Mutagenesis Kit (Stratagene) according to the manufacturer´s instructions. For polymerase chain reaction 30 ng of template DNA (pGR74) was mixed with primers (12 mM), dNTPs (0.2 mM), and PfuTurbo™ DNA polymerase (2.5 U; Stratagene) in 50 ml of 1x reaction buffer. The Perkin Elmer Gene Amp® PCR System 2400/9700 with program shown in Table 3 was used for amplification of DNA.

Step	Temperature	Duration
initial denaturation	95°C	5 min
denaturation	95°C	30 sec.
annealing / 29 cycles	65°C	1 min
extension	72°C	8 min
final extension	72°C	16 min
storage	4°C	∞

Table 3. PCR program used for site directed mutagenesis

5 µl of the PCR reaction products were analyzed on a 0.8 % agarose gel, prior of adding 1 µl of the *Dpn* I restriction enzyme (10 U/µl) directly to the rest of amplification reaction. Reaction was incubated for 1 h at 37°C to completely digest the parental (non-mutated) dsDNA. Afterwards, 10 µl of the *Dpn* I-treated DNA were used for transformation of 200 µl of DH5α competent cells.

Primer	Primer sequence 5´-3´
Ins/TGG/FWD (sense)	CAACAAACACCTTATCAAGTGGGCCCAGAGGCACATCAG
Ins/TGG/REV (antisense)	CTGATGTGCCTCTGGGCCCAGTTGATAAGGTGTTTGTTG

Table 4. Synthetic oligonucleotides (primers) for site directed mutagenesis.

Plasmid	Insert	Tag	Used for	Source
pBN128	vimentin NR domain	N-His	expression	B. Nikolic[1]
pDS19	plectin exons 4-8	N-His	expression	D. Spazierer[1]
pFS2	vimentin N domain	N-His	expression	F.A. Steinböck[1]
pFS3	vimentin R domain	N-His	expression	F.A. Steinböck[1]
pFS129	vimentin	no	expression	F.A. Steinböck[2]
pGEX4T-1	GST/vector	N-GST	cloning	GE Healthcare
pGP1	vimentin RC domain	N-His	expression	G. Putz[1]
pGR1	integin β4-$F_{1,2}$	N-His	expression	G.A. Rezniczek[3]
pGR2	integin β4-L	N-His	expression	G.A. Rezniczek[3]
pGR5	integin β4-$F_{1,2}$L'	N-His	expression	G.A. Rezniczek[3]
pGR6	integin β4-$F_{1,2}$L$F_{3,4}$C	N-His	expression	G.A. Rezniczek[3]
pGR36	integin β4-$F_{1,2}$L	N-His	cloning/expression	G.A. Rezniczek[3]
pGR44	integin β4-$F_{3,4}$C	N-His	expression	G.A. Rezniczek[3]
pGR66	No/vector	no	cloning	G.A. Rezniczek[3]
pGR70	plectin exons 2-8/2α3α	no	cloning	G.A. Rezniczek[3]
pGR74	plectin exons 2-8	N-His	cloning/expression	G.A. Rezniczek[3]
pGR75	plectin exons 2-8/2α	N-His	expression	G.A. Rezniczek[3]
pGR103	plectin exons 6-9	N-His	expression	G.A. Rezniczek[3]
pGR130	plectin exons 2-5	N-MBP	cloning/expression	G.A. Rezniczek[3]
pGR132	MBP/vector	N-MBP	expression	G.A. Rezniczek[3]
pGR133	plectin exons 2-8	N-MBP	expression	G.A. Rezniczek[3]
pGR139	plectin exons 1c-8	N-His	cloning	G.A. Rezniczek[3]
pGR140	plectin exons 1c-8/2α3α	N-His	cloning	G.A. Rezniczek[3]
pGR142	plectin exons 1d-8/2α	N-His	expression	G.A. Rezniczek[3]
pGR145	plectin exons 1a-8	N-His	cloning/expression	G.A. Rezniczek[3]
pGR147	plectin exons 1c-8/2α	N-His	expression	G.A. Rezniczek[3]
pGR150	plectin exons 1f-8	N-His	cloning/expression	G.A. Rezniczek[3]
pGR185	DsRed/vector	C-DsRed	cloning	G.A. Rezniczek[3]
pJP5	integin β4 $F_{3,4}$	N-His	expression	J.M. de Pereda[4]
pKAB1	plectin R5	N-His	expression	K. Abdoulrahman[1]

Table 5. Plasmids and cloning vectors. Detail preparation as well as sequences encoded by and description of used plasmids is described in [1]Ševčík *et al.*, 2004, [2]Steinböck *et al.*, 2000, [3]G.A. Rezniczek PhD thesis, [4]Rezniczek *et al.*, 1998

Name	Insert	Species	Cloning	Vector	Insert origin	Tag	Expressed size kDa/pI
pJK1	plectin exons **1a-8**	mouse	EcoRI	pGR66	pGR145	No	31.97/7.17
pJK2	plectin exons **1c2α3α-8**	mouse	EcoRI	pGR66	pGR140	No	36.6/7.18
pJK4	plectin exons **1c2α3α-8**	mouse	NdeI/EcoRI	pGR66	pGR140	No	36.05/7.18
pJK5	plectin exons **2-24**	mouse	EcoRI	pGR66	pGR329/24	No	110.97/6.19
pJK6	plectin exons **1f-24**	mouse	NdeI/BglII	pJK5	pGR150	No	113.84/6.12
pJK7	plectin exons **1a-24**	mouse	NdeI/BglII	pJK5	pGR145	No	114.69/6.36
pJK8	plectin exons **1c2α3α-24**	mouse	NdeI/BglII	pJK5	pGR140	No	119.31/6.36
pJK11	plectin exons **1f-24**	mouse	NdeI/EcoRI	pGR185	pJK6	C-DsRed	140.58/6.30
pJK12	plectin exons **1a-24**	mouse	NdeI/EcoRI	pGR185	pJK7	C-DsRed	141.44/6.54
pJK13	plectin exons **1c2α3α-24**	mouse	NdeI/EcoRI	pGR185	pJK8	C-DsRed	146.06/6.54
pJK15	plectin exons **1c-24**	mouse	NdeI/EcoRI	pGR185	pGR329/24	C-DsRed	143.9/6.42
pJK16	plectin exons **22α-5**	mouse	PstI	pGR134	pGR130	N-MPB	56.65/6.01
pJK17	plectin exons **1c-8**	mouse	EcoRI	pGR70	pGR139	No	34.44/6.52
pJK19	plectin exons **2-W-8**	mouse	-	pGR74		N-His	30.06/6.96
pJK20	integrin **1126-1457)**	human	EcoRI	pGEX4T-1	pGR36	N-GST	64.77/6.01
pJK22	plectin exons **1a-8**	mouse	EcoRI	pGEX4T-1	pJK1	N-GST	59.44/6.8

Table 6. List of cDNA constructs. For description of used plasmids and cloning vectors see **Table 5**.

cDNA constructs

All constructs, except of pJK19, were made by sub-cloning (using conventional restriction enzymes) of inserts obtained from existing constructs into existing vectors (**Table 5**). Restriction enzymes/sites used for sub-cloning together with description of constructs are specified in **Table 6**. Construct, pJK19 was prepared by site-directed mutagenesis, described in previous section, using primers specified in **Table 4.** Although direct subcloning, without any PCR amplification step, has been used for preparation of all constructs (except of pJK19), all were verified by sequencing.

Protein purification and characterization

Expression of recombinant proteins

The expression plasmid coding for the recombinant un-tagged, or His, GST and MBP-tagged protein was transformed into the E.coli strain BL21 (DE3), or BL21-CodonPlus (DE3)-RIL (Stratagene), plated on agar plates containing appropriate antibiotics (100 µg/ml of ampicillin, 100 µg/ml of carbenicillin, and/or 34 µg/ml chloramphenicol) and 1 % (w/v) glucose, and grown overnight at 37°C. Next day, several colonies were used to inoculate 100 ml of TB, or LB medium supplemented with glucose (1 %) and 100 µg/ml of carbenicillin with or without addition of 34 µg/ml chloramphenicol, and grown overnight at 37°C. Cells were harvested under sterile conditions and resuspended in 4 ml of 20 % glycerol. 200µl aliquots of cell suspension were rapidly frozen in liquid nitrogen and stored at -80°C, until further use. For protein expression 0.1-4 l of TB or LB medium supplemented with glucose (1 %), ampicilin (100 µg/ml), and/or chloramphenicol (34 µg/ml) was inoculated with expression bacterial stock (app. 50-100 µl of stock per 100 ml of media) and incubated at 37°C, and higher shaking speed (220 rpm), until OD_{600} of 0.5-0.7 was reached. Protein expression was induced either by adding IPTG to final concentration of 0.1-0.4 mM, or by adding IPTG to 0.1 mM simultaneously with lactose (1 %). After 3-4 h at 30°C, or 37°C, cells were harvested (5000 g, 10 min., 4°C), cell pellets flash-frozen in liquid nitrogen and stored at -80°C.

Purification of His-tagged proteins under non-denaturating conditions

<u>Sonication buffer:</u>   50 mM Tris/HCl, 1mM EDTA, 1% Triton X-100, pH 9.0

Column buffer:	50 mM Tris/HCl, 20 % (w/v) glycerol, pH 9.0
Elution buffer:	50 mM Tris/HCl, 20 % (w/v) glycerol, 250 mM imidazole, pH 9.0

Cells pellets stored at -80°C were reruspended in 5-100 ml (usually in 1/20 of culture volume) of 1:1 mixture of cold sonication and column buffer to which lysosyme (10μg/ml) was added. After incubation on ice for 15 minutes cells were further disrupted by sonication (Bandolin Sonopuls HD70, 3x5 min, 70 % power, and 50 cycles) keeping the protein solution on ice for at least 5 minutes between repetitions. Insoluble material was removed by centrifugation (30000 - 40000 g, 20 min, 4°C) and resulting supernatant applied to a Ni-NTA His-Bind® (Novagen) or HisTrap HP (GE Healthcare) column equilibrated with 5 column volumes (CV) of column buffer. In the case when HisTrap column has been used imidazole to final concentration 20 mM was added to both sonication and column buffer. Similarly, imidazole concentration in elution buffer was increased to 500 mM. After the sample was loaded, the unbound proteins were washed out by at least 3 CV of column buffer and the bound protein was eluted with 100 % step gradient of 3 CV of elution buffer. For crystallization purposes, His-tag was removed from protein by treatment with thrombin protease (see below). Subsequently, the protein without His-tag was dialyzed against 10 mM $(NH_4)HCO_3$, pH 9.0, concentrated using an Amicon ultrafiltration device (Milipore) and lyophilized. Homogeneity of the protein was assessed by SDS-PAGE and Coomassie Blue staining.

Purification of His-tagged proteins under denaturating conditions

Lysis buffer:	50 mM Tris/HCl, 500 mM NaCl, 0.5 % (w/v) Triton, pH 8.0
Binding buffer:	20 mM Tris/HCl, 5 mM imidazole, 500 mM NaCl, 6 M urea, pH 8.0

Cells pellets stored at -80°C were reruspended in 1/20 culture volume of cold lysis buffer. To isolate inclusion bodies, cells were sonicated (Bandolin Sonopuls HD70, 3x5 minutes, 70% power, and 50 cycles) on ice, and inclusion bodies collected by centrifugation (30000-40000 g, 20 min. 4°C). Resulting pellet was resuspended in 1/20 culture volume of binding buffer and incubated for at least 1 h at room temperature. Afterwards insoluble material has been removed by centrifugation (30000 – 40000 g, 20 min. 22°C). The supernatant was directly loaded on Ni-NTA His-Bind® (Novagen) or HisTrap FF (GE Healthcare) column equilibrated with 5 CV of binding buffer. When needed, (high viscosity) supernatant was diluted 1:1 with binding buffer and filtered through a 0.45 μm membrane before applying on the column. After loading of the

sample column was washed firstly with 5 CV of binding buffer, secondly with 5 CV of binding buffer containing 20 mM imidazole. Bound proteins were eluted with 4 CV of 250 mM imidazole in binding buffer. When HisTrap columns were used, imidazole concentration in buffers has been adjusted to 20 mM in binding buffer, to 20 and 40 mM in binding buffer used for washing, and to 500 mM in binding buffer used for elution.

Purification of maltose binding protein (MBP)-tagged proteins

Column buffer: 20 mM Tris/HCl, 200 mM NaCl, 10 mM β-mercaptoethanol, 1 mM EDTA, pH 7.4

Cell pellets (for details see "Expression of recombinant proteins"), were resuspended in 1/20 column volume of column buffer (optionally supplemented with 0.5 % (v/v) Triton) and cells suspension subjected to sonication (Bandolin Sonopuls HD70, 3x5 minutes, 70 % power, and 50 cycles) on ice. Crude extract was clarified by centrifugation (30000-40000 g, 20 min. 22°C) and applied onto amylose resin column (New England Biolabs). The column was then washed with 10 CV of column buffer and the protein was eluted with 3 CV of column buffer containing 10 mM maltose. Collected fractions were analyzed by SDS-PAGE. Fractions with purified protein were pooled together, concentrated and routinely applied on gel filtration column (HiLoad 16/600 Superdex 75 pg or HiLoad 16/600 Superdex 200 pg, GE Healthcare) equilibrated with column buffer. After isocratic elution, peak fractions (OD_{280nm}) were analyzed by SDS-PAGE. Protein was concentrated using Amicon® Ultra-4 or Ultra-15 Centrifugal Filter Units (Milipore), flash-frozen in liquid nitrogen, and stored usually at -80°C.

Orthogonal purification of un-tagged plectin fragments

Sonication buffer: 50 mM Tris/HCl, 5 % (w/v) glycerol, 0.5 % (w/v) Triton X-100, 0.5 mM EDTA, pH 9.0
Column buffer A: 50 mM Tris/HCl, 100 mM Na_2SO_4, 1 % (w/v) glycerol, 1 mM DTT, pH 9.0
Elution buffer A: 20 mM Tris/HCl, 50 % (v/v) ethyleneglycol, 1 % glycerol, 1 mM DTT, pH 9.0
Column buffer B: 20 mM Tris/HCl, 10 mM NaCl, 0.5 % (w/v) glycerol, 0.5 mM DTT, pH 8.0
Column buffer C: 20 mM Tris/HCl, 100 mM NaCl, 0.5 % (w/v) glycerol, 0.5 mM DTT, pH 8.0

Cell pellets gained from 2 liters of medium were resuspended in 50 ml of sonication buffer to which lysozyme was added (0.2-0.3 mg per ml of cell suspension). After incubation at room temperature (22°C), another 50 ml of sonication buffer were added and incubated for 20 minutes on ice before subjected to sonication (Bandolin Sonopuls HD70, 3x5 minutes, 70 % power, and

50 cycles). Cell debris and insoluble material was removed by centrifugation using Sorvall centrifuge, rotor F21S (18000-20000 rpm, for 15 min., at 22°C). Supernatant volume was measured using a cylinder and adjusted to 120 ml with sonication buffer. While stirring, 12 g of solid $(NH_4)_2SO_4$ (0.1 g/ml) was added to the protein solution, which was subsequently incubated for 1 hour at room temperature. Precipitated proteins were removed by centrifugation (SS34 tubes, F21S rotor, 20000 rpm, 15 min., at 22°C) and supernatant applied onto 50 ml Phenyl-Sepharose® 6 Fast Flow column (Sigma) equilibrated with 2 CV of column buffer A. Unbound proteins were washed out with 2 CV of column buffer A. Subsequently, bound proteins were eluted with linear gradient (2.5 CV) of 0-100 % of elution buffer A in column buffer A. Presence and purity of protein in collected fraction was analyzed by SDS-PAGE. Fraction containing most of the protein were pooled together and protein solution was dialyse against 2 liters of column buffer B, overnight at 4°C. After dialysis, protein sample was loaded on 20 ml Sepharose Q HP column (GE Healthcare) equilibrated with 5 CV of fresh column buffer B. To remove unbound protein, column has been washed additionally with 5 CV of column buffer B. Bound protein was eluted with 10 CV of linear gradient of 10-300 mM NaCl in column buffer B. Collected fraction were analyzed by SDS-PAGE, and the ones containing highest amount of pure protein were pooled together. Protein solution was concentrated to 2.4-4.8 ml using Amicon ultrafiltration device (Milipore) and applied on HiLoad 16/600 Superdex 75 pg or HiLoad 16/600 Superdex 200 pg column (GE Healthcare) equilibrated with 2 CV of column buffer C. After isocratic elution, peak fractions (OD_{280nm}) were analyzed by SDS-PAGE. Protein was concentrated using Amicon® Ultra-4 or Ultra-15 Centrifugal Filter Units (Milipore), flash-frozen in liquid nitrogen, and stored usually at -80°C.

Purification of recombinant full-length vimentin

Column buffer A: 5 mM Tris/HCl, 8 M urea, 1 mM EDTA, 10 mM β-mercaptoethanol, 0.4 mM PMSF, pH 7.5

Column buffer B: 50 mM sodium formate, 8 M urea, 10 mM β-mercaptoethanol, 0.4 mM PMSF, pH 4.0

Recombinant full-length vimentin encoded by pFS129 was isolated from lysed bacterial pellets following the inclusion body preparation procedure (Nagai and Thogersen, 1987). Final pellets were dissolved in column buffer A and after centrifugation (40000 g, 15 min., 4°C) supernatants were directly applied to a 10 ml DEAE Sepharose CL-6B column (GE Healthcare) equilibrated

with column buffer A. Bound protein was eluted with a 60 ml gradient of NaCl (0-0.3 M) in column buffer A, and aliquots of fractions (2 ml) were analyzed by SDS-PAGE. Vimentin-containing fractions were pooled, diluted 1 : 5 (v/v) with column buffer B and applied to a 10 ml CM Sepharose CL-6B column (GE Healthcare) in column buffer B. After washing, bound vimentin was eluted with a linear gradient of KCl (0-0.3 M) in column buffer B, and aliquots were stored at -80°C.

Purification of calmodulin from porcine brain

Buffer A: 50 mM Tris/HCl, 1 mM EDTA, 1 mM β-mercaptoethanol, 0.5 mM PMSF, pH 7.5
Buffer B: 50 mM Tris/HCl, 0.2 mM CaCl$_2$, 1 mM β-mercaptoethanol, pH 7.5
Buffer C: 50 mM Tris/HCl, 0.2 mM CaCl$_2$, 0.5 M NaCl, 1 mM β-mercaptoethanol, pH 7.5
Buffer D: 50 mM Tris/HCl, 1 mM EGTA, 1 mM β-mercaptoethanol, pH 7.5
Buffer E: 20 mM Tris/HCl, 1 mM EDTA, 1 mM β-mercaptoethanol, 0.2 % (w/v) glycerol, pH 7.5
Buffer F: 20 mM Tris/HCl, 0.2 M NaCl, 1 mM EGTA, 1 mM β-mercaptoethanol, 0.2 % (w/v) glycerol, pH 7.5

Frozen porcine brain (approximately from 4 pigs) was chopped in small pieces, and homogenized with Waring blender (2 x 30 s) in two volumes of buffer A (1 l for 500 *g*), at 4°C. Afterwards, brain suspension was further homogenized by Potter-Elvehjem homogenizator with a teflon pestle at 3000 rpm and brain debris was removed by centrifugation (GSA rotor, 11000 rpm, 30 min, 4°C). Resulting pellet was resuspended in two volumes of buffer A and same procedure (as described above) was repeated one more time. Supernatants from both centrifugations were pooled together and filtrated trough 4 layers of cheese cloth (Miracloth) and 4 filter papers (Shleicher&Schuell). Next, acetic acid (6 M) was added drop-wise to filtrated supernatant until pH 4.3, keeping the solution on ice, while mixing. After 1 hour at pH 4.3, precipitated proteins were pelleted by centrifugation (F14 rotor, 13000 rpm, 30 min., 4°C) and recovered by resuspending of pellet in buffer A at 22°C. Suspension pH was adjusted to 7.5 by using Tris-base (1 M). Protein solution was incubated for 1 h at 22°C, and precipitated (insoluble) proteins were removed by centrifugation (F14 rotor, 13000 rpm, 30 min, RT). CaCl$_2$ was added to the supernatant (to final concentration of 6 mM), and sample was applied on Phenyl Sepharose column (50 ml) equilibrated with 2 CV of buffer B. After binding, unbound proteins were washed out with 4 CV of buffer B, followed by 4 CV of buffer C. Proteins were eluted from the column with 2 CV of buffer D, and collected fraction were analyzed for the presence of calmodulin by

SDS-PAGE, followed by CCB staining. Calmodulin reach fractions were pooled together before diluting 8x with buffer E. Sample was loaded on 9 ml SOURCE 30Q column (GE Healthcare), equilibrated with buffer E. Column was washed with 5 CV of 200 mM NaCl in buffer E and bound calmodulin was eluted with linear gradient of 200-500 mM NaCl (10 CV) in buffer E. Fractions with highest amount of calmodulin (as analyzed by SDS-PAGE) were pooled together, concentrated using Amicon® Ultra-15 Centrifugal Filter Units (3000 Da cut-off membrane; Milipore), and applied on HiLoad 16/600 Superdex 200 pg column (GE Healthcare) equilibrated with buffer F. Collected fractions were analysed by SDS-PAGE and CCB staining. Aliquots (200 µl) of fractions containing pure calmodulin were frozen in liquid nitrogen and stored at -80°C.

SDS-PAGE

5x Sample buffer:	0.25 M Tris/HCl pH 6.8, 10 % (w/v) SDS, 50 % (v/v) glycerol, 0.5 M dithiothreitol, 0.1 % (w/v) bromphenolblue
Running buffer:	25 mM Tris/HCl, 200 mM glycine, 0.1 % (w/v) SDS
Staining solution:	0.05 % (w/v) Coomassie R-250, 40 % (v/v) methanol, 7 % (v/v) acetic acid
Destaining solution:	40 % (v/v) ethanol, 7 % (v/v) acetic acid

SDS-PAGE was performed according to Laemmli (Laemmli, 1970). The Mini-Protean Electrophoresesystem (Biorad) was used. The separating gel was poured, overlaid with water saturated butanol and left to polymerize. The butanol was removed and the stacking gel was poured on top of the separation gel. A comb was introduced to allow sample application after polymerization. The protein samples were mixed with 5x Sample buffer and heated to 95°C for 5-10 minutes. Running conditions were 20 mA per minigel in running buffer. After electrophoresis, the gel was incubated in the staining solution for at least 20 minutes on a shaker at room temperature, and thereafter destained by several changes of destaining solution.

Determination of protein concentration according to Bradford

Bradford reagent:	0.01 % (w/v) Coomassie Blue G-250, 5 % (v/v) ethanol, 8.5 % (v/v) phosphoric acid

For the standard curve, duplicate aliquots (2.5, 5, 7.5, 10, 12.5 and 15 µl) of BSA solution (1 mg/ml) were adjusted to 100 µl with 0.15 M NaCl. Two 100 µl aliquots of 0.15 M NaCl were used as blanks. The samples with unknown protein concentration were prepared similarly. Each sample was mixed with 1 ml of Bradford reagent and allowed to stand for 5 min at room

temperature. Absorbance at 595 nm was determined using 1-cm-path-length (1 ml) plastic microcuvettes. A standard curve was made by plotting absorbance at 595 nm *versus* known concentration of BSA and used to determine the protein concentration of the unknown samples.

Determination of protein concentration using UV/Vis absorption

Absorbance at specific wavelength (275 nm for calmodulin, 290 nm for G-actin) was determined using 1-cm-path-length (50 μl) quartz microcuvettes. Concentration of G-actin was determined using an absorption coefficient of 0.65 (Abs 0.1%, mg/ml) at 290 nm. Concentration of calmodulin was determine using extinction coeficient ε = 3300 M^{-1}cm^{-1} at 275 nm. Note, calmodulin does not contain tryptophan. Also, colorimetric dyes (i.e., Bradford Reagent) tend to underestimate the true protein concentration.

Cleavage with thrombin

To achieve almost 100 % cleavage of N-terminal His-tag fusion protein with thrombin, protease (usually 5 Units per 1mg) was directly added to protein in elution buffer and incubated overnight at 30°C, with continuous shaking. Efficiency of the cleavage was tested by SDS-PAGE.

Immunoblotting (Western blot analysis)

Transfer buffer:	25 mM Tris-base, 190 mM glycine, 20 % (v/v) methanol, pH around 8.3
Blocking solution:	PBS or TBS containing either 5 % (w/v) non-fat dry milk or 4 % (w/v) BSA
Washing solution:	PBS-T or TBS-T, with or without 5 % (w/v) non-fat dry milk or 4 % (w/v) BSA
AP buffer:	100 mM Tris/HCl, 100 mM NaCl, 5 mM MgCl$_2$, pH 9.5
AP substrate solution:	66 μl NBT (nitroblue terazolium chloride; 50 mg/ml in 70% DMF) and 33 μl BCIP (5-bromo-4-chloro-3-indolyl phosphate; 50 mg/ml in 100% DMF) added per 10 ml AP buffer

Proteins were separated by SDS-PAGE. Blotting was carried out in a Bio-Rad Mini Protean II wet-blotting chamber usually overnight at 20 V, and 4°C. Alternatively, blotting was performed at 90 V for 1 h at 4°C. Prior to blotting, gel, membrane, filter papers and sponges were pre-wetted in transfer buffer, stacked in the following order: case (clear side), sponge, two filter papers, membrane, gel, two filter papers, sponge, case (black side), and placed in the transfer apparatus with black (membrane) side facing black (positively-charged) electrode. After transfer the

membrane was blocked for 1 h at room temperature in blocking solution. The membrane was washed with washing solution and incubated in the appropriate primary antibody dilution (in washing solution) for 1 h at room temperature (or alternatively overnight at 4°C). Afterwards, the membrane was washed three times with washing solution for 10 minutes and then incubated with the alkaline phosphatase (AP)- or horseradish peroxidase (HRP)-conjugated secondary antibody dilution (in washing solution) for 1 h. The washing step was repeated and the bound secondary antibodies were visualized either using the ECL-detection system (Super Signal West PicoSystem, Pierce) or by incubating the membrane in AP substrate solution. The AP-reaction was stopped by washing the membrane in water.

Quantification of protein bands on immunoblots and SDS-PAGE gels

After immunoblotting using peroxidase-coupled secondary antibodies, protein bands were visualized by exposure to X-ray film. Several exposures for different time periods were performed. Similarly, several sample dilutions were analysed by SDS-PAGE and stained with CCB. The bands were then scanned and quantified using ImageQuant 5.1 software (Molecular dynamics). Normalization calculations were done in Microsoft Excel 2002. Values obtained were plotted against corresponding exposure times or sample dilutions to establish the range of signal linearity. For quantitative comparisons only band intensities falling into these linear ranges were used.

Protein-protein interaction assays

Dot blot assay

Solution P:	20 mM Tris/HCl, 0.2 % (w/v) glycerol, 100 mM NaCl, 0.5 mM DTT, pH 7.5
Solution R:	1% milk in 20 mM Tris/HCl, 100 mM NaCl, pH 7.5
Solution S:	20 mM Tris/HCl, 100 mM NaCl, 0.01 % (v/v) Tween 20, pH 7.5

P1aABD was labeled with Alexa Fluor$^{®}$680 using a Protein Labeling Kit (Molecular Probes) according to the manufacturers` instructions. Purified recombinant His-tagged fusion proteins containing integrin β4 fragments, as well as P1aABD were dialyzed overnight against solution P, and subsequently precleared by centrifugation (100000 g, 2 h, 4°C). Samples were diluted in solution P and spotted (4 µg/spot) onto a nitrocellulose membrane using a Biorad 96-wells dot blot system. Immobilized proteins were incubated with solution R (blocking) for 1 h, or stained

with CBB. Samples of Alexa Fluor[®]680 conjugated P1aABD were diluted to 3 μg/ml in solution S, and incubated in the dark with nitrocellulose strips for 1.5 h at RT. Strips were then washed three times in solution S, and scanned using an Odyssey Infrared Imager (Li-Cor, Bioscience, USA).

Actin co-sedimentation assay

Buffer G: 5 mM Tris/HCl, 0.2 mM $CaCl_2$, 0.2 mM ATP, 0.5 mM DTT, pH 8.0
Buffer I: 50 mM Tris/HCl, 0.5 M KCl, 20 mM $MgCl_2$, 20 mM ATP, pH 8.0
Buffer F: 5 mM Tris/HCl, 50 mM KCl, 2 mM $MgCl_2$, 2 mM ATP, pH 8.0

Actin was purified from rabbit skeletal muscle following the protocol described in Spudich and Watt (1971). Samples of purified rabbit skeletal actin (16 μM) in 20 μl of buffer G, were polymerized by addition of 1/10 volume of buffer I, and incubation for 1 h at RT. Pre-incubated mixtures (30 min, room temperature) of 8 μM purified plectin fragments (P1fABD, P1aABD, or P1cABD) and 0-160 μM CaM in 20 μl of buffer F (supplemented with either 4 mM $CaCl_2$, or 10 mM EGTA) were added to polymerized actin samples and incubated for another 30 minutes. Actin filaments and proteins bound were sedimented by centrifugation (217000 g, 30 min, 20°C), and equivalent volumes of the supernatant and pellet fractions were analyzed by SDS-PAGE. CBB-stained protein bands were quantitated using ImageQuant 5.1 software package (Molecular Dynamics). For determining dissociation constants, the same assay has been used, except that increasing concentrations of individual plectin fragments (0-130 μM) were mixed with constant amounts of actin (8 μM). The amount of protein bound to F-actin was fit to a single rectangular hyperbola using Prism 4 (GraphPad Software).

Vimentin co-sedimentation assay

Solution A: 5 mM Tris/acetate, pH 8.3, 0.1 mM EDTA, 10 mM β-mercaptoethanol
Solution B: 20 mM Tris/HCl, pH 8.0, 150 mM NaCl, 1 mM EDTA, and 0.1% (v/v) Tween-20

Co-sedimentation assays were carried out essentially as described by Spurny *et al.* (2007) with some modifications regarding protein preparation and solution used. To prepare vimentin filaments, recombinant vimentin was dialyzed stepwise at room temperature against solution A, with decreasing concentrations of urea (6-0 M). The dialyzed vimentin solution was centrifuged (100000 g, 30 min, 20°C), and soluble vimentin (8 μM) was polymerized in 20 μl of solution B,

for 30 min at 37°C. Recombinant PRD5 and ABD/2α were dialyzed overnight, at 4°C against solution B. Following the dialysis, both proteins (PRD5 and ABD/2α) were centrifuged at 100000 g, for 30 min. at 4°C. 8 μM soluble plectin fragments (PRD5 and ABD/2α) in 20 μl of solution B were then added to 20 μl of polymerized vimentin samples and incubated for 1 h at 37°C. Vimentin filaments and proteins bound were sedimented by centrifugation (100000 g, 30 min, 20°C), and equivalent volumes of the supernatant and pellet fractions were analyzed by SDS-PAGE, followed by CBB staining. For controls without vimentin, 8 μM of PRD5 and ABD/2α were treated in the same manner.

Affinity purification of vimentin fragments using ABD/2α-Sepharose

Solution D: 10 mM Tris/acetate, pH 8.3, 0.1 mM EDTA, 5 mM β-mercaptoethanol

Solution E: 10 mM Tris/HCl, pH 7.5, 0.5 mM MgCl$_2$, 0.2 mM dithiothreitol, 25 mM NaCl, 50 μg/ml TPCK

ABD/2α was coupled to CNBr-activated Sepharose 4B (GE Healthcare) according to the manufacturers' protocol. Vimentin purified in urea was dialyzed step by step against 6, 4, and 2 M urea in solution D. Each dialysis step was performed for 30 minutes at room temperature, followed by dialysis against solution D overnight at 4°C. Urea-free vimentin, precentrifuged at 100000 g for 30 minutes, was digested with chymotrypsin (1 : 400, w/w) for 30 minutes at 25°C. The reaction was stopped by the addition of L-chloro-3-[4-tosylamido]- 4-phenyl-2-butanone (TPCK) (final concentration of 100 μg/ml). The digest was then immediately loaded onto ABD/2α-Sepharose column equilibrated with solution E. Bound protein was eluted with a linear gradient of 25-400 mM NaCl in solution E. Fractions collected during purification were analyzed by SDS-PAGE, followed by CCB staining.

CaM-Sepharose pull-down assay

Solution A: 20 mM Tris/HCl, 100 mM NaCl, 0.005 % (v/v) Tween 20, pH 7.5

For pull-down assays, 50 μl of pre-equilibrated CaM-Sepharose 4B beads (GE Healthcare), or of Sepharose 4B alone, were mixed with 1 ml of protein samples (1.5 μM) in solution A, supplemented with either 2 mM CaCl$_2$, or increasing concentrations of CaCl$_2$ (0.4-2000 μM), or 5 mM EGTA, or 2mM CaCl$_2$ and 80 μM W7 (Fluka), followed by incubation for 2 h at room temperature. Beads were washed three times, and bound proteins were eluted by incubation with

5x sample buffer (see above) for 10 minutes at 95°C. Eluted proteins were further analyzed by SDS-PAGE, followed by CCB staining.

P1aABD-Sepharose pull-down assay

<u>Solution A:</u>   20 mM Tris/HCl, 100 mM NaCl, 0.01 % (v/v) Tween 20, pH 7.5

For pull-down assays, purified samples of P1aABD were coupled to CNBr-activated Sepharose 4B (GE Healthcare) according to the manufacturers' protocol. 40 μl of these beads was added to samples (1 ml) of β4-F1,2LF3,4C, or β4-F1,2 (both at 0.5 μM) in solution A, supplemented with either 2 mM CaCl$_2$, or 5 mM EGTA. Mixtures were incubated for 1.5 h at room temperature and proteins bound to the beads were analyzed as described above. For competitive binding assays, samples of integrin β4 fragment F1,2LF3,4C (0.5 μM) were mixed with P1aABD-Sepharose beads immediately or 0.5 h before incubation with increasing amounts of CaM (0-10 μM) in a total volume of 1 ml of solution A supplemented with either 0.5 mM CaCl$_2$, or 1 mM EGTA. For determining dissociation constants, increasing concentration of CaM (0-1.26 μM) or β4-F1,2LF3,4C (0-1.13 μM) were mixed with constant amounts of P1aABDSepharose (30 μl). After incubation for 1.5 h at room temperature, supernatant (free) fractions were removed by centrifugation at 1500 g for 1 minute at 20°C. Beads were washed three times, and proteins in the resultant pellet and supernatant fractions were analyzed by SDS-PAGE. CBB-stained protein bands were quantitated using ImageQuant 5.1 software package (Molecular Dynamics). The amount of CaM or β4-F1,2LF3,4C bound to P1aABD-Sepharose was fit to a single rectangular hyperbola using Prism 4 (GraphPad Software).

Eu^{3+}-protein interaction assay

<u>Labeling buffer:</u>   50 mM NaHCO$_3$, pH 8.5
<u>Coating buffer:</u>   25 mM Na$_2$B$_4$O$_7$, pH 9.3
<u>Overlay buffer:</u>   PBS, 1 mM EGTA, 2 mM MgCl$_2$, 1 mM dithiothreitol, 0.1 % Tween-20, pH 7.5

Prior to labeling, recombinant vimentin (pFS129) purified in urea (for details see above), was dialyzed stepwise against 6, 4, 2, and 0 M urea in labeling buffer. Precipitated protein was removed by centrifugation (100000 g, 30 min., 4°C) and soluble vimentin (1 mg/ml) was mixed with labeling reagent (Delphia Eu^{3+}; N$_1$-(p-isothiocyanatobenzyl)-diethylenetriamine-N$_1$,N$_2$,N$_3$,N$_3$-tetraacetic acid chelated with Eu^{3+}) in 1:10 (v/v) reagent to protein ratio. After

incubation for 12-24 h at room temperature, protein was separated from unbound reagent by gel filtration chromatography, using a Bio-Rad P6 resin column. Labeling efficiency was determined by measuring protein content and amount of bound Eu^{3+}. 96-well microtiter plates (Nunc Maxisorb) were coated (overnight at 4°C) with 100 μl of recombinant plectin fragments or BSA diluted with coating buffer to the final concentration of 100 nM. After coating, plate was washed two times with PBS, and blocked with 4 % BSA in PBS, for at least 1 h at room temperature. Plate was again washed two times with PBS, and overlaid with dilutions of Eu^{3+}-labeled vimentin (10-500 nM) in 100 μl of overlay buffer for 90 minutes at room temperature. Subsequently, unbound protein was removed by extensive washing (six times) with overlay buffer, and protein bound was determined by releasing the vimentin-bound Eu^{3+} with enhancement solution and measuring fluorescence with a time-resolved fluorometer (Delfia 1234, Wallac). The fluorescence values were converted to concentrations by comparison with the Eu^{3+} standard (1 nM).

Blot overlay assays

Solution C:	1.5 mM KH_2PO_4, 8 mM NaH_2PO_4, 137 mM NaCl, 2.6 mM KCl, pH 7.4
Solution D:	4.3 mM Na_2HPO_4, 1.4 mM KH_2PO_4, 137 mM NaCl, 2.7 mM KCl, 1 mM EGTA, 2 mM $MgCl_2$, 0.1 % (v/v) Tween 20, 1 mM dithiothreitol, pH 7.5
5x Sample buffer:	0.25 M Tris/HCl pH 6.8, 10 % (w/v) SDS, 50 % (v/v) glycerol, 0.5 M dithiothreitol, 0.1 % (w/v) bromphenolblue

Purified samples of proteins were subjected to SDS-PAGE using 5x sample buffer with or without dithiothreitol. Proteins were transferred to nitrocellulose membranes, blocked with 5 % (w/v) nonfat milk powder in solution C. Blots were overlaid with full-length mouse vimentin or P1cABD/2α (both at concentrations of 5 μg/mL) in solution D. After 1 h of incubation, membranes were washed thoroughly with solution C supplemented with 0.1 % (v/v) Tween 20. For detection of bound proteins we used affinity-purified goat anti-(mouse vimentin) IgG (Giese and Traub, 1986), diluted 1:5000 (v/v), or isoform-specific affinity-purified rabbit antibodies to P1c (Andrä *et al.*, 2003), diluted 1:1000 (v/v), in combination with secondary HRP-coupled antisera and the SuperSignal® kit (Pierce, Rockford, IL, USA).

Crystallization

Initial attempts to crystallize plectin fragments prepared by using of His-Tag (P1aABD and P1cABD/2α) were performed at 22°C using the hanging-drop vapor diffusion technique. Microcrystals appeared within one week under conditions summarized in **Table 7**, which were further optimized. Initial attempts to crystallize plectin fragments prepared by using of untagged versions of protein (P1aABD and P1cABD/2α3α) were performed at 22°C and 4°C using the sitting- drop vapor diffusion technique and a nanodrop-dispensing robot (Cartesian MicroSys 4000). After 2-3 weeks at 22°C the conditions indicated in **Table 7** displayed hits. The hanging-drop vapor diffusion method was used for the refinement of crystallization conditions of all fragments of plectin using 24-well Linbro plates sealed with siliconized cover slides. Drops (usually 2 μl) containing equivalent amounts of protein and precipitant solutions were mixed and equilibrated against 0.4 ml of reservoir solution at 22°C. Optimized conditions in which individual plectin fragments crystallize or form crystalline-like particles are summarized in **Table 7**. In each case micro- and/or macro-seeding into drops equilibrated for 24 h or overnight at 22°C was found to be important for obtaining final crystals or crystalline-like particles.

Protein	Construct	Protein concentration	Protein solution	Initial conditions	Optimized conditions
P1aABD	pGR145	10 mg/ml	50 mM Tris/HCl, pH 9.0	0.1 M Tris pH 8.5, 0.2 M MgCl$_2$, 3.4 M 1,6-hexanediol	0.1 M Tris pH 8.5,0.2 M MgCl$_2$, 3.4 M 1,6-hexanediol
P1cABD /2α	pGR147	10 mg/ml	50 mM Tris/HCl, pH 9.0	0.1 M MES, pH 6.5, 0.2 M magnesium acetate, 10 % (w/v) PEG 8000	0.1 M sodium cacodylate, pH 6.5, 0.2 M magnesium acetate, 10 % (w/v) PEG 8000
P1aABD	pJK1	10 mg/ml	20 mM Tris/HCl, 100 mM NaCl, 1 % (v/v) glycerol, 1 mM dithiotreitol, pH 8.0	0.1 M Hepes, pH 7.5, 0.1 M MgCl$_2$, 10 % (w/v) PEG 4000	0.1 M Tris, pH 8.5, 0.5 % (w/v) n-Hexyl-β-D-glucoside, 0.2 M MgCl$_2$, 5 % (w/v) PEG 4000
P1cABD /2α3α	pJK2	10 mg/ml	20 mM Tris/HCl, 150 mM NaCl, 1 % (v/v) glycerol, 1 mM dithiotreitol, pH 8.0	0.1M Hepes pH 7.0, 10 mM cobalt chloride, 1.5 M ammonium sulfate	0.1M MES, pH 6.3, 10 mM cobalt chloride, 1.5 M ammonium sulfate

Table 7. Conditions used for crystallization of various plectin fragments. Detail descriptions of constructs can be found in **Table 5 and 6**.

Mammalian cell culture methods

Maintenance of cell line

KGM (keratinocytes growth medium; BioWhittaker CC-3104)

Keratinocyte basal medium…………………….............500 ml

Hydrocortisone (CC-4031)………………………........0.5 ml

GA-1000 (CC-4081)……………………………….......0.5 ml

BPE (CC-4002)…………………………………….........2 ml

hEGF (CC-4015)……………………………………......0.5 ml

Insulin (CC-4021)…………………………….............0.5 ml

FCS……………………………………………….......2%

Insulin-Transfferin-Selenium (GibcoBRL)…………….......5 ml

$CaCl_2$ (50 mM)………………………………….......500 µl

FCS (Fetal Calf Serum)

To remove Ca^{2+} from FCS, 5g Chelex were mixed with 100 ml FCS and stirred at 4°C for 1h. FCS was then sterilized by filtration.

Collagen coating of dishes

Collagen I solution (Sigma) was diluted 1:10 in PBS, 5 ml of this dilution was then added per 10 cm plate and incubated for at least 2h at 37°C or overnight at 4°C. Prior usage plates were washed once with PBS.

Frozen immortalized (p53$^{-/-}$) mouse keratinocytes (Andrä *et al.*, 2003) were thawed in a 37°C water-bath and transferred to a 15 ml tube. 10 ml of adequate growth medium was added, the cells pelleted by centrifugation at 180 *g* for 3 min (Heraeus Megafuge) and resuspended in an adequate growth medium. Keratinocytes were cultured on collagen I coated dishes in KGM and incubated at 37°C in a humidified atmosphere containing 5 % CO_2. When cells reached confluence, they were washed once with PBS and then incubated with trypsin (0.05 % (w/v) trypsin, 0.2 % (w/v) EDTA, sterilized by filtration) for 10 min at 37°C. Growth medium was added to inhibit the trypsin and detached cells were transferred to a 15 ml tube. Cells were centrifuged as before, the cell pellet resuspended in medium and splitted into new culture dishes. For freezing, cells were trypsinized, resuspended in freezing medium (growth medium containing 12.5% DMSO) and aliquoted into cryotubes (Nunc). The cryotubes were kept at -80°C for 24h and then put into a liquid nitrogen tank for storage.

Differentiation of keratinocytes

To induce stratification and subsequently differentiation of cultured keratinocyte monolayers, the $CaCl_2$ level in the medium (KGM) was raised from 0.05 mM to 1.3 mM.

Preparation of cell fractions

Lysis buffer:	50 mM Tris/HCl, pH 6.8, 10 mM DTT, 3 % (w/v) SDS, and 10 % (v/v) glycerol, 5 mM EDTA, supplemented with Complete Mini protease inhibitor cocktail (Roche)
Triton buffer:	1% Triton X-100, 5 mM EDTA, and a protease inhibitor mix (1 mM PMSF, 10 μM leupeptin, 10 μM pepstatin, and 25 μg/ml aprotinin) in PBS
High-salt buffer:	10 mM Tris, 140 mM NaCl, 1.5 M KCl, 5 mM EDTA, 0.5% Triton X-100, pH 7.6, supplemented protease inhibitor mix
Urea buffer:	10 mM Tris/HCl, 8 M Urea, 1 mM EDTA, 50 mM DTT, 5 mM EDTA, pH 8.0

To prepare total cell lysates, differentiated keratinocytes were washed twice with cold (4°C) PBS and lysed directly with lysis buffer (200 μl per 1x 6 cm dish). Lysed cells were scraped off with a cell scraper into the buffer and cell debris was homogenized by pressing through a 27 gauge needle. Aliquots of cell lysates containing equal amounts of protein were supplemented with bromphenol blue and DTT to 1 % (w/v) and 100 mM, respectively, separated by SDS-PAGE and subjected to immunoblotting. For the Triton X-100 and high-salt extract fractions, cells were washed with ice-cold PBS and then scraped off with a cell scraper into PBS. Afterwards, cells were pelted (750 *g*, 10 min., 4°C), resuspended in Triton buffer, and incubated for 2 min. at 4°C on an orbital shaker. Cell debris was pelleted by centrifugation (16000 *g*, 10 min, 4°C) and supernatant collected as a soluble fraction. The pellet was homogenized in High-salt buffer. After incubation for 30 min at 4°C, the homogenate was pelleted (16000 *g*, 10 min, 4°C) and the pellet (insoluble fraction) was rehomogenized in Urea buffer. Equal amounts of soluble and insoluble fractions were analysed by SDS-PAGE and subjected to immunoblotting.

Immunoprecipitation

Lysis buffer:	TBS supplemented with 0.5 % (v/v) Triton X-100, 0.1 mM $CaCl_2$, 0.5 mg/ml DNAse I , 0.2 mg/ml RNAse A, 1 mM PMSF, 10 mM benzamidine, 10 μg/ml aprotonin, 10 μg/ml pepstatin/leupeptin, and phosphatase inhibitor cocktail 1 (1:100, Sigma-Aldrich).

Differentiated keratinocytes, (4 h at 1.3 mM $CaCl_2$) were rinsed twice with cold TBS, and then lysed in lysis buffer. Cell suspension was incubated for 10 min at room temperature, and clarified by centrifugation (15800 g, 30 min, 4°C). Lysates were pre-cleared by incubation with protein A Sepharose beads (25 µl/ml of lysate; Amersham Biosciences) for 1 h at 4°C, followed by centrifugation. Cleared supernatants were incubated with antiserum to plectin (#46) overnight at 4°C. To recover antibody-antigen complexes, protein A beads were added and suspensions rotated for 2 h at 4°C. Beads were sedimented and washed three times with TBS supplemented with 0.5 % (v/v) Triton X-100 and 0.1 mM $CaCl_2$. Finally, the beads were resuspended in SDS-PAGE sample buffer, heated for 5 minnutes at 95°C, and subjected to immunoblotting.

References

Ackerl, R., Walko, G., Fuchs, P., Fischer, I., Schmuth, M., and Wiche, G. (2007) Conditional targeting of plectin in prenatal and adult mouse stratified epithelia causes keratinocyte fragility and lesional epidermal barrier defects. *J Cell Sci.* 120, 2435-2443.

Algermissen, B., Sitzmann, J., Nürnberg, W., Laubscher, J. C., Henz, B. M., and Bauer, F. (2000) Expression of the thrombin receptor on human keratinocytes: potential biologic function as an inducer of cell proliferation. *Arch. Dermatol. Res.* 80, 287-291.

Andrä, K., Lassmann, H., Bittner, R., Shorny, S., Fässler, R., Propst, F., and Wiche, G. (1997) Targeted inactivation of plectin reveals essential function in maintaining the integrity of skin, muscle and heart cytoarchitecture. *Genes Dev.* 11, 3143-3156.

Andrä, K., Nikolic, B., Stöcher, M., Drenckhahn, D., and Wiche, G. (1998) Not just scaffolding: plectin regulates actin dynamics in cultured cells. *Genes Dev.* 12, 3442-3451.

Andrä , K., Kornacker, I., Jörgl, A., Zörer, M., Spazierer, D., Fuchs, P., Fischer, I., and Wiche, G. (2003) Plectin-isoform-specific rescue of hemidesmosomal defects in plectin (-/-) keratinocytes. *J Invest. Dermatol.* 120, 189-197.

Bernier, G., Mathieu, M., De Repentigny, Y., Vidal, S. M., and Kothary, R. (1996) Cloning and characterization of mouse ACF7, a novel member of the dystonin subfamily of actin binding proteins. *Genomics* 38, 19-29.

Bonet-Kerrache, A., Fabbrizio, E., and Mornet, D. (1994) N-terminal domain of dystrophin. *FEBS Lett.* 355, 49-53.

Borrego-Diaz, E., Kerff, F., Lee, S. H., Ferron, F., Li, Y., and Dominguez, R. (2006) Crystal structure of the actin-binding domain of alpha-actinin 1: evaluating two competing actin-binding models. *J Struct. Biol.* 155, 230-8.

Bouameur, J. E., Schneider, Y., Begré, N., Hobbs, R. P., Lingasamy, P. Fontao, P., Green, K. J., Favre, B., and Borradori, L. (2013) Phosphorylation of serine 4642 in the C-terminus of plectin by MNK2 and PKA modulates its interaction with intermediate filaments. *J Cell Sci.* 126, 4195-4207.

Bresnick, A. R., Warren, V., and Condeelis, J. (1990) Identification of a short sequence essential for actin binding by Dictyostelium ABP-120. *J Biol. Chem.* 265, 9236-40.

Burgstaller, G., Gregor, M., Winter, L., and Wiche, G. (2010) Keeping the vimentin network under control: cell-matrix adhesion-associated plectin 1f affects cell shape and polarity of fibroblasts. *Mol. Biol. Cell* 21, 3362-3375.

Castañón, M. J., Walko, G., Winter, L., and Wiche, G. (2013) Plectin-intermediate filament partnership in skin, skeletal muscle, and peripheral nerve. *Histochem. Cell Biol.* 140, 33-53.

Castresana, J., and Saraste, M. (1995) Does Vav bind to F-actin through a CH domain? *FEBS Lett.* 374, 149-51.

Chen, L. B., and Buchanan, J, M. (1975) Mitogenic activity of blood components. I. Thrombin and prothrombin. *Proc. Natl. Acad. Sci. U.S.A.* 72, 131-135.

Choi, H. J., Park-Snyder, S., Pascoe, L. T., Green, K. J., and Weis, W. I. (2002) Structures of two intermediate filament-binding fragments of desmoplakin reveal a unique repeat motif structure. *Nat. Struct. Biol.* 9, 612-20.

Choi, H. J., and Weis, W. I. (2011) Crystal structure of a rigid four-spectrin-repeat fragment of the human desmoplakin plakin domain. *J Mol. Biol.* 409, 800-12.

Clark, A. R., Sawyer, G. M., Robertson, S. P., and Sutherland-Smith, A. J. (2009) Skeletal dysplasias due to filamin A mutations result from a gain-of-function mechanism distinct from allelic neurological disorders. *Hum. Mol. Genet.* 18, 4791-4800.

Corrado, K., Mills, P. L., and Chamberlain, J. S. (1994) Deletion analysis of the dystrophin-actin binding domain. *FEBS Lett.* 344, 255-60.

Correia, I., Chu, D., Chou, Y. H., Goldman, R. D., and Matsudaira, P. (1999) Integrating the actin and vimentin cytoskeletons: Adhesion-dependent formation of fimbrin-vimentin complexes in macrophages. *J Cell Biol.* 146, 831-842.

Coughlin, S. R. (1999) How the protease thrombin talks to cells. *Proc. Natl. Acad. Sci. U.S.A.* 96, 11023-11027.

Crawley, J. T. B., Zanardelli, S., Chion, C. K. N. K., and Lane, D. A. (2007) The central role of thrombin in hemostasis. *J Thromb. Haemost.* 5 (Suppl. 1), 95-101.

DeLano, W. L. (2000) The PyMOL Molecular Graphics System on World Wide Web. http://www.pymol.org

de Pereda, J. M., Lillo, M. P., and Sonnenberg, A. (2009) Structural basis of the interaction between integrin alpha6beta4 and plectin at the hemidesmosomes. *EMBO J* 28, 1180-90.

Djinovic Carugo, K., Banuelos, S., and Saraste, M. (1997) Crystal structure of a calponin homology domain. *Nat. Struct. Biol.* 4, 175-9.

Dong, A., Xu, X., Edwards, A. M., Midwest Center for Structural Genomics, and Structural Genomics Consortium. (2007) In situ proteolysis for protein crystallization and structure determination. *Nat. Methods* 4, 1019-1021.

Dunker, A. K., Lawson, J. D., Brown, C.J., Williams, R. M., Romero, P., Oh, J. S., Oldfield, C. J., Campen, A. M., Ratliff, C. M., Hipps, K. W., Ausio, J., Nissen, M. S., Reeves, R., Kang, C., Kissinger, C. R., Bailey, R. W., Griswold, M. D., Chiu, W., Garner, E. C., and Obradovic, Z. (2001) Intrinsically disordered protein. *J Mol. Graph. Model.* 19, 26-59.

Dyson, H.J., and Wright, P. E. (2005) Intrinsically unstructured proteins and their functions. *Nat. Rev. Mol. Cell Biol.* 6, 197-208.

Eger, A., Stockinger, A., Wiche, G., and Foisner, R. (1997) Polarisation dependent association of plectin with desmoplakin and the lateral submembrane skeleton in MDCK cells. *J Cell Sci.* 110, 1307-1316.

Egelman, E. H. (2004) More insights into structural plasticity of actin binding proteins. *Structure* 12, 909-910.

Elliott, C. E., Becker, B., Oehler, S., Castañón, M. J., Hauptmann, R., and Wiche, G. (1997) Plectin transcript diversity: identification and tissue distribution of variants with distinct first coding exons and rodless isoforms. *Genomics* 42, 115-125.

Errante, L. D., Wiche, G., and Shaw, G. (1994) Distribution of plectin, an intermediate filament-associated protein, in the adult rat central nervous system. *J Neurosci. Res.* 37, 515-28.

Fabbrizio, E., Bonet-Kerrache, A., Leger, J. J., and Mornet, D. (1993) Actin-dystrophin interface. *Biochemistry* 32, 10457-63.

Foisner, R., and Wiche, G. (1987) Structure and hydrodynamic properties of plectin molecules. *J Mol. Biol.* 198, 515-31.

Foisner, R., Leichtfried, F. E., Herrmann, H., Small, J. V., Lawson, D., and Wiche, G. (1988) Cytoskeleton-associated plectin: in situ localization, in vitro reconstitution, and binding to immobilized intermediate filament proteins. *J Cell Biol.* 106, 723-33.

Foisner, R., Traub, P., and Wiche, G. (1991) Protein kinase A- and protein kinase C-regulated interaction of plectin with lamin B and vimentin. *Proc. Natl. Acad. Sci. U. S. A.* 88, 3812-6.

Foisner, R., Feldman, B., Sander, L., Seifert, G., Artlieb, U., and Wiche, G. (1994) A panel of monoclonal antibodies to rat plectin: distinction by epitope mapping and immunoreactivity with different tissues and cell lines. *Acta Histochem.* 96, 421-438.

Fontao, L., Geerts, D., Kuikman, I., Koster, J., Kramer, D., and Sonnenberg, A. (2001) The interaction of plectin with actin: evidence for cross-linking of actin filaments by dimerization of the actin-binding domain of plectin. *J Cell Sci.* 114, 2065-76.

Fraley, T. S., Tran, T. C., Corgan, A. M., Nash, C. A., Hao, J., Critchley, D. R., and Greenwood, J. A. (2003). Phosphoinositide binding inhibits alpha-actinin bundling activity. *J Biol. Chem.* 278, 24039-45.

Fraley, T. S., Pereira, C. B., Tran, T. C., Singleton, C., and Greenwood, J. A. (2005) Phosphoinositide binding regulates alpha-actinin dynamics: mechanism for modulating cytoskeletal remodeling. *J Biol. Chem.* 280, 15479-82.

Franzot, G., Sjoblom, B., Gautel, M., Djinovic Carugo, K. (2005) The crystal structure of the actin binding domain from alpha-actinin in its closed conformation: structural insight into phospholipid regulation of alpha-actinin. *J Mol. Biol.* 348, 151-65.

Frijns, E., Sachs, N., Kreft, M., Wilhelmsen, K., and Sonnenberg, A. (2010) EGF-induced MAPK signaling inhibits hemidesmosome formation through phosphorylation of the integrin {beta}4. *J Biol. Chem.* 285, 37650-62.

Fuchs, P., Zörer, M., Rezniczek, G. A., Spazierer, D., Oehler, S., Castañón, M. J., Hauptmann, R., and Wiche, G. (1999) Unusual 5'transcript complexity of plectin isoforms: novel tissue-specific exons modulate actin binding activity. *Hum. Mol. Genet.* 8, 2461-2472.

Fujii, T., Takagi, H., Arimoto, M., Ootani, H., and Ueeda, T. (2000) Bundle formation of smooth muscle desmin intermediate filaments by calponin and its binding site on the desmin molecule. *J Biochem.* 127, 457-465.

Fukami, K., Furuhashi, K., Inagaki, M., Endo, T., Hatano, S., and Takenawa, T. (1992) Requirement of phosphatidylinositol 4,5-bisphosphate for alpha-actinin function. *Nature* 359, 150-152.

Full, S. J., Deinzer, M. L., Ho, P. S., and Greenwood, J. A. (2007) Phosphoinositide binding regulates alpha-actinin CH2 domain structure: analysis by hydrogen/deuterium exchange mass spectrometry. *Protein Sci.* 16, 2597-604.

Furuhashi, K., Inagaki, M., Hatano, S., Fukami, K., and Takenawa, T. (1992) Inositol phospholipid-induced suppression of F-actin-gelating activity of smooth muscle filamin. *Biochem. Biophys. Res. Commun.* 184, 1261-5.

Galkin, V. E., Orlova, A., VanLoock, M. S., Rybakova, I. N., Ervasti, J. M., and Egelman, E. H. (2002) The utrophin actin-binding domain binds F-actin in two different modes: implications for the spectrin superfamily of proteins. *J Cell Biol.* 157, 243-51.

Galkin, V. E., Orlova, A., Salmazo, A., Djinovic-Carugo, K., and Egelman, E. H. (2010) Opening of tandem calponin homology domains regulates their affinity for F-actin. *Nat. Struct. Mol. Biol.* 17, 614-6.

Gallwitz, M., Enoksson, M., Thorpe, M., Hellman, L. (2012) The Extended Cleavage Specificity of Human Thrombin. *PLoS ONE* 7(2), e31756.

Garcia-Alvarez, B., Bobkov, A., Sonnenberg, A., and De Pereda, J.M. (2003) Structural and functional analysis of the actin binding domain of plectin suggests alternative mechanisms for binding to F-actin and integrin beta 4. *Structure* 11, 615-625.

Geerts, D., Fontao, L., Nievers, M. G., Schaapveld, R. Q., Purkis, P. E., Wheeler, G. N., Lane, E. B., Leigh I. M., and Sonnenberg, A. (1999) Binding of integrin alpha6beta4 to plectin prevents plectin association with F-actin but does not interfere with intermediate filament binding. *J Cell Biol.* 147, 417-434.

Georges-Labouesse, E., Messaddeq, N., Yehia, G., Cadalbert, L., Dierich, A., and Le Meur, M. (1996) Absence of integrin alpha 6 leads to epidermolysis bullosa and neonatal death in mice. *Nat. Genet.* 13, 370-3.

Giese, G., and Traub, P. (1986) Induction of vimentin synthesis in mouse myeloma cells MPC-11 by 12-0-tetradecanoylphorbol-13- acetate. *Eur. J Cell Biol*. 40, 266-274.

Gimona, M., and Mital, R. (1998) The single CH domain of calponin is neither sufficient nor necessary for F-actin binding. *J Cell Sci.* 111, 1813-1821.

Gimona, M., and Winder, S. J. (1998) Single calponin homology domains are not actin-binding domains. *Curr. Biol.* 8, R674-5.

Gimona, M., Djinovic-Carugo, K., Kranewitter, W. J., and Winder, S. J. (2002) Functional plasticity of CH domains. *FEBS Lett.* 513, 98-106.

Gipson, I. K., Spurr-Michaud, S., Tisdale, A., Elwell, J., and Stepp, M. A. (1993) Redistribution of the hemidesmosome components α6β4 integrin and bullous pemphigoid antigens during epithelial healing. *Exp. Cell Res*. 207, 86-98.

Glenney, J. R., Kaulfus, P., Matsudaira, P., and Weber, K. (1981) F-actin binding and bundling properties of fimbrin, a major cytoskeletal protein of microvillus core filaments. *J Biol. Chem.* 256, 9283-9288.

Goldsmith, S. C., Pokala, N., Shen, W., Fedorov, A. A., Matsudaira, P., and Almo, S. C. (1997) The structure of an actin-crosslinking domain from human fimbrin. *Nat. Struct. Biol.* 4, 708-12.

Greenwood, J. A., Theibert, A. B., Prestwich, G. D., and Murphy-Ullrich, J. E. (2000) Restructuring of focal adhesion plaques by PI 3-kinase. Regulation by PtdIns (3,4,5)-p(3) binding to alpha-actinin. *J Cell Biol.* 150, 627-42.

Gregor, M., Zeold, A., Oehler, S., Marobela, K. A., Fuchs, P., Weigel, G., Hardie, D. G., and Wiche, G. (2006) Plectin scaffolds recruit energy-controlling AMP-activated protein kinase (AMPK) in differentiated myofibres. *J Cell Sci.* 119, 1864-75.

Hampton, C. M., Taylor, D. W., and Taylor, K. A. (2007) Novel structures for alpha-actinin:F-actin interactions and their implications for actin-membrane attachment and tension sensing in the cytoskeleton. *J Mol. Biol.* 368, 92-104.

Hanein, D., Volkmann, N., Goldsmith, S., Michon, A. M., Lehman, W., Craig, R., DeRosier, D., Almo, S., and Matsudaira, P. (1998) An atomic model of fimbrin binding to F-actin and its implications for filament crosslinking and regulation. *Nat. Struct. Biol.* 5, 787-92.

Hemmings, L., Kuhlman, P. A., and Critchley, D. R. (1992) Analysis of the actin-binding domain of alpha-actinin by mutagenesis and demonstration that dystrophin contains a functionally homologous domain. *J Cell Biol.* 116, 1369-80.

Herrmann, H., and Wiche, G. (1987) Plectin and IFAP-300K are homologous proteins binding to microtubule-associated proteins 1 and 2 and to the 240-kilodalton subunit of spectrin. *J Biol. Chem.* 262, 1320-5.

Herrmann, H., Strelkov, S. V., Burkhard, P., and Aebi, U. (2009) Intermediate filaments: primary determinants of cell architecture and plasticity. *J Clin. Invest.* 119, 1772-83.

Hijikata, T., Nakamura, A., Isokawa, K., Imamura, M., Yuasa, K., Ishikawa, R., Kohama, K., Takeda, S., and Yorifuji, H. (2008) Plectin 1 links intermediate filaments to costameric sarcolemma through beta-synemin, alpha-dystrobrevin and actin. *J Cell Sci.* 121, 2062-74.

Holmes, D. S., and Quigley, M. (1981) A rapid boiling method for the preparation of bacterial plasmids. *Anal. Biochem.* 114, 193-7.

Ishikawa, K., Sumiyoshi, H., Matsuo, N., Takeo, N., Goto, M., Okamoto, O., Tatsukawa, S., Kitamura, H., Fujikura, Y., Yoshioka, H., and Fujiwara, S. (2010) Epiplakin accelerates the lateral organization of keratin filaments during wound healing. *J Dermatol. Sci.* 60, 95-104.

Janda, L., Damborsky, J., Rezniczek, G. A., and Wiche, G. (2001) Plectin repeats and modules: strategic cysteines and their presumed impact on cytolinker functions. *Bioessays* **23,** 1064-9.

Jarrett, H. W., and Foster, J. L. (1995) Alternate binding of actin and calmodulin to multiple sites on dystrophin. *J Biol. Chem.* 270, 5578-5586.

Jefferson, J. J., Leung, C. L., and Liem, R. K. (2004) Plakins: goliaths that link cell junctions and the cytoskeleton. *Nat. Rev. Mol. Cell Biol.* 5, 542-53.

Jefferson, J. J., Ciatto, C., Shapiro, L., and Liem, R. K. (2007) Structural analysis of the plakin domain of bullous pemphigoid antigen1 (BPAG1) suggests that plakins are members of the spectrin superfamily. *J Mol. Biol.* 366, 244-57.

Karakesisoglou, I., Yang, Y., and Fuchs, E. (2000) An epidermal plakin that integrates actin and microtubule networks at cellular junctions. *J Cell Biol.* 149, 195-208.

Keep, N. H., Norwood, F. L., Moores, C. A., Winder, S. J., and Kendrick-Jones, J. (1999a) The 2.0 A structure of the second calponin homology domain from the actin-binding region of the dystrophin homologue utrophin. *J Mol. Biol.* 285, 1257-64.

Keep, N. H., Winder, S. J., Moores, C. A., Walke, S., Norwood, F. L., and Kendrick-Jones, J. (1999b) Crystal structure of the actin-binding region of utrophin reveals a head-to-tail dimer. *Structure* 7, 1539-46.

Kelly, D. F., and Taylor, K. A. (2005) Identification of the beta1-integrin binding site on alpha-actinin by cryoelectron microscopy. *J Struct. Biol.* 149, 290-302.

Ketema, M., Wilhelmsen, K., Kuikman, I., Janssen, H., Hodzic, D., and Sonnenberg, A. (2007) Requirements for the localization of nesprin-3 at the nuclear envelope and its interaction with plectin. *J Cell Sci.* 120, 3384-94.

Kitajima, Y., Owaribe, K., Nishizawa, Y., Jokura, Y., and Yaoita, H. (1992) Phorbol ester- and calcium-induced reorganization of 180-kDa bullous pemphigoid antigen on the ventral surface of cultured human keratinocytes as studied by immunofluorescence and immunoelectron microscopy. *Exp. Cell Res.* 203, 17-24.

Konieczny, P., Fuchs, P., Reipert, S., Kunz, W. S., Zeöld, A., Fischer, I., Paulin, D., Schröder, R., and Wiche, G. (2008) Myofiber integrity depends on desmin network targeting to Z-disks and costameres via distinct plectin isoforms. *J Cell Biol.* 181, 667-681.

Koss-Harnes, D., Hoyheim, B., Anton-Lamprecht, I., Gjesti, A., Jorgensen, R. S., Jahnsen, F. L., Olaisen, B., Wiche, G., and Gedde-Dahl, T. Jr. (2002) A site-specific plectin mutation causes dominant epidermolysis bullosa simplex Ogna: two identical de novo mutations. *J Invest. Dermatol.* 118, 87-93.

Kostan, J., Gregor, M., Walko, G., and Wiche, G. (2009) Plectin isoform dependent regulation of keratin-integrin alpha6beta4 anchorage via Ca^{2+}/calmodulin. *J Biol. Chem.* 284, 18525-18536.

Koster, J., Kuikman, I., Kreft, M., and Sonnenberg, A. (2001) Two different mutations in the cytoplasmic domain of the integrin beta 4 subunit in nonlethal forms of epidermolysis bullosa prevent interaction of beta 4 with plectin. *J Invest. Dermatol.* 117, 1405-11.

Koster, J., Geerts, D., Favre, B., Borradori, L., and Sonnenberg, A. (2003) Analysis of the interactions between BP180, BP230, plectin and the integrin alpha6beta4 important for hemidesmosome assembly. *J Cell Sci.* 116, 387-99.

Koster, J., van Wilpe, S., Kuikman, I., Litjens, S. H., and Sonnenberg, A. (2004) Role of binding of plectin to the integrin beta4 subunit in the assembly of hemidesmosomes. *Mol. Biol. Cell* 15, 1211-1223.

Kriwacki, R. W., Hengst, L., Tennant, L., Reed, S. I., and Wright, P. E. (1996) Structural studies of p21Waf1/Cip1/Sdi1 in the free and Cdk2-bound state: conformational disorder mediates binding diversity. *Proc. Natl. Acad. Sci. U. S. A.* 93, 11504-11509.

Kuhlman, P. A., Hemmings, L., and Critchley, D. R. (1992) The identification and characterisation of an actin-binding site in alpha-actinin by mutagenesis. *FEBS Lett.* 304, 201-6.

Laemmli, U. K. (1970) Cleavage of Structural Proteins during the Assembly of the Head of Bacteriophage T4. *Nature* 227, 680-685.

Lebart, M. C., Mejean, C., Boyer, M., Roustan, C., and Benyamin, Y. (1990) Localization of a new alpha-actinin binding site in the COOH-terminal part of actin sequence. *Biochem. Biophys. Res. Commun.* 173, 120-6.

Lee, S. H., Weins, A., Hayes, D. B., Pollak, M. R., and Dominguez, R. (2008) Crystal structure of the actin-binding domain of alpha-actinin-4 Lys255Glu mutant implicated in focal segmental glomerulosclerosis. *J Mol. Biol.* 376, 317-24.

Leung, C. L., Sun, D., Zheng, M., Knowles, D. R., and Liem, R. K. (1999) Microtubule actin cross-linking factor (MACF): a hybrid of dystonin and dystrophin that can interact with the actin and microtubule cytoskeletons. *J Cell Biol.* 147, 1275-1286.

Leung, C. L., Zheng, M., Prater, S. M., and Liem, R. K. (2001) The BPAG1 locus: Alternative splicing produces multiple isoforms with distinct cytoskeletal linker domains, including predominant isoforms in neurons and muscles. *J Cell Biol.* 154, 691-7.

Leung, C. L., Green, K. J., and Liem, R. K. (2002) Plakins: a family of versatile cytolinker proteins. *Trends Cell Biol.* 12, 37-45.

Levine, B. A., Moir, A. J., Patchell, V. B., and Perry, S. V. (1990) The interaction of actin with dystrophin. *FEBS Lett.* 263, 159-62.

Levine, B. A., Moir, A. J., Patchell, V. B., and Perry, S. V. (1992) Binding sites involved in the interaction of actin with the N-terminal region of dystrophin. *FEBS Lett.* 298, 44-8.

Lin, A. Y., Prochniewicz, E., James, Z. M., Svensson, B., Thomas, D. D. (2011) Large-scale opening of utrophin's tandem calponin homology (CH) domains upon actin binding by an induced-fit mechanism. *Proc. Natl. Acad. Sci. U. S. A.* 108, 12729-33.

Lipscomb, E. A., and Mercurio, A. M. (2005) Mobilization and activation of a signaling competent alpha6 beta4 integrin underlies its contribution to carcinoma progression. *Cancer Metastasis Rev.* 24, 413-23.

Litjens, S. H., Koster, J., Kuikman, I., van Wilpe, S., de Pereda, J. M., and Sonnenberg, A. (2003) Specificity of binding of the plectin actin-binding domain to β4 integrin. *Mol. Biol. Cell* 14, 4039-4050.

Litjens, S. H., de Pereda, J. M., and Sonnenberg, A. (2006) Current insights into the formation and breakdown of hemidesmosomes. *Trends Cell Biol.* 16, 376-383.

Liu, C. G., Maercker, C., Castañón, M. J., Hauptmann, R., and Wiche, G. (1996) Human plectin: organization of the gene, sequence analysis, and chromosome localization (8q24). *Proc. Natl. Acad. Sci. U.S.A.* 93, 4278-4283.

Liu, J., Taylor, D. W., and Taylor, K. A. (2004) A 3-D reconstruction of smooth muscle alpha-actinin by CryoEm reveals two different conformations at the actin-binding region. *J Mol. Biol.* 338, 115-25.

Lorenzi, M., and Gimona, M. (2008) Synthetic actin-binding domains reveal compositional constraints for function. *Int. J Biochem. Cell Biol.* 40, 1806-16.

Lunter, P. C., and Wiche, G. (2002) Direct binding of plectin to Fer kinase and negative regulation of its catalytic activity. *Biochem. Biophys. Res. Commun.* 296, 904-10.

Mabuchi, K., Li, B., Ip, W., and Tao, T. (1997) Association of calponin with desmin intermediate filaments. Bundle formation of smooth muscle desmin intermediate filaments by calponin and its binding site on the desmin molecule. *J Biol. Chem.* 272, 22662-22666.

Margadant, C., Frijns, E., Wilhelmsen, K., and Sonnenberg, A. (2008) Regulation of hemidesmosome disassembly by growth factor receptors. *Curr. Opin. Cell Biol.* 20, 589-96.

Mariotti, A., Kedeshian, P. A., Dans, M., Curatola, A. M., Gagnoux-Palacios, L., and Giancotti, F. G. (2001) EGF-R signaling through Fyn kinase disrupts the function of integrin alpha6beta4 at hemidesmosomes: role in epithelial cell migration and carcinoma invasion. *J Cell Biol.* 155, 447-458.

McGough, A., Way, M., and DeRosier, D. (1994) Determination of the alpha-actinin-binding site on actin filaments by cryoelectron microscopy and image analysis. *J Cell Biol.* 126, 433-43.

McLean, W. H., Pulkkinen, L., Smith, F. J., Rugg, E. L., Lane, E. B., Bullrich, F., Burgeson, R. E., Amano, S., Hudson, D. L., Owaribe, K., McGrath, J. A., McMillan, J. R., Eady, R. A., Leigh, I. M., Christiano, A. M., and Uitto, J. (1996) Loss of plectin causes epidermolysis bullosa with muscular dystrophy: cDNA cloning and genomic organization. *Genes Dev.* 10, 1724-1735.

Mejean, C., Lebart, M. C., Roustan, C., and Benyamin, Y. (1995) Inhibition of actin-dystrophin interaction by inositide phosphate. *Biochem. Biophys. Res. Commun.* 210, 152-8.

Mercurio, A. M., Rabinovitz, I., and Shaw, L. M. (2001) The alpha 6 beta 4 integrin and epithelial cell migration. *Curr. Opin. Cell Biol.* 13, 541-5.

Moores, C. A., Keep, N. H., and Kendrick-Jones, J. (2000) Structure of the utrophin actin-binding domain bound to F-actin reveals binding by an induced fit mechanism. *J Mol. Biol.* 297, 465-80.

Morris, G. E., Nguyen, T. M., Nguyen, T. N., Pereboev, A., Kendrick-Jones, J., and Winder, S. J. (1999) Disruption of the utrophin-actin interaction by monoclonal antibodies and prediction of an actin-binding surface of utrophin. *Biochem. J* 337, 119-23.

Nagai, K., and Thogersen, H. C. (1987) Synthesis and sequencespecific proteolysis of hybrid proteins produced in Escherichia coli. *Methods Enzymol.* 153, 461-481.

Nakamura, F., Hartwig, J. H., Stossel, T. P., and Szymanski, P. T. (2005) Ca^{2+} and calmodulin regulate the binding of filamin A to actin filaments. *J Biol. Chem.* 280, 32426-32433.

Nakano, A., Pulkkinen, L., Murrell, D., Rico, J., Lucky, A. W., Garzon, M., Stevens, C. A., Robertson, S., Pfendner, E., and Uitto, J. (2001) Epidermolysis bullosa with congenital pyloric atresia: novel mutations in the beta 4 integrin gene (ITGB4) and genotype/phenotype correlations. *Pediatr. Res.* 49, 618-26.

Niessen, C. M., Hulsman, E. H., Oomen, L. C., Kuikman, I., and Sonnenberg, A. (1997) A minimal region on the integrin beta4 subunit that is critical to its localization in hemidesmosomes regulates the distribution of HD1/plectin in COS-7 cells. *J Cell Sci.* 110, 1705-16.

Nikolic, B., MacNulty, E., Mir, B., and Wiche, G. (1996) Basic amino acid residue cluster within nuclear targeting sequence motif is essential for cytoplasmic plectin-vimentin network junctions. *J Cell Biol.* 134, 1455-1467.

Norwood, F. L., Sutherland-Smith, A. J., Keep, N. H., and Kendrick-Jones, J. (2000) The structure of the N-terminal actin-binding domain of human dystrophin and how mutations in this domain may cause Duchenne or Becker muscular dystrophy. *Structure* 8, 481-91.

Ortega, E., Buey, R. M., Sonnenberg, A., and de Pereda J. M. (2011) The structure of the plakin domain of plectin reveals a non-canonical SH3 domain interacting with its fourth spectrin repeat. *J Biol. Chem.* 286, 12429-38.

Osmanagic-Myers, S., and Wiche, G. (2004) Plectin-RACK1 (receptor for activated C kinase 1) scaffolding: a novel mechanism to regulate protein kinase C activity. *J Biol. Chem.* 279, 18701-18710.

Osmanagic-Myers, S., Gregor, M., Walko, G., Burgstaller, G., Reipert, S., and Wiche, G. (2006) Plectin-controlled keratin cytoarchitecture affects MAP kinases involved in cellular stress response and migration. *J Cell Biol.* 174, 557-568.

Peterson, J. J., Rayburn, H. B., Lager, D. J., Raife, T. J., Kealey, G. P., Rosenberg, R. D., and Lentz, S. R. (1999) Expression of thrombomodulin and consequences of thrombomodulin deficiency during healing of cutaneous wounds. *Am. J Pathol.* 155, 1569-1575.

Pfendner, E., Rouan, F., and Uitto, J. (2005) Progress in epidermolysis bullosa: the phenotypic spectrum of plectin mutations. *Exp. Dermatol.* 14, 241-249.

Postel, R., Ketema, M., Kuikman, I., de Pereda, J. M., and Sonnenberg, A. (2011) Nesprin-3 augments peripheral nuclear localization of intermediate filaments in zebrafish. *J Cell Sci.* 124, 755-64.

Pytela, R., and Wiche, G. (1980) High molecular weight polypeptides (270,000-340,000) from cultured cells are related to hog brain microtubule-associated proteins but copurify with intermediate filaments. *Proc. Natl. Acad. Sci. U. S. A.* 77, 4808-12.

Rabinovitz, I., Toker, A., and Mercurio, A. M. (1999) Protein kinase C-dependent mobilization of the alpha6beta4 integrin from hemidesmosomes and its association with actin-rich cell protrusions drive the chemotactic migration of carcinoma cells. *J Cell Biol.* 146, 1147-1160.

Rabinovitz, I., Tsomo, L., and Mercurio, A. M. (2004) Protein Kinase C-α phosphorylation of specific serines in the connecting segment of the β4 integrin regulates the dynamics of type II hemidesmosomes. *Mol. Cell. Biol.* 24, 4351-4360.

Raith, M., Valencia, R. G., Fischer, I., Orthofer, M., Penninger, J. M., Spuler, S., Rezniczek, G. A., and Wiche, G. (2013) Linking cytoarchitecture to metabolism: sarcolemma-associated plectin affects glucose uptake by destabilizing microtubule networks in mdx myofibers. *Skeletal Muscle* 3, 1-14.

Reipert, S., Steinbock, F., Fischer, I., Bittner, R. E., Zeold, A., and Wiche, G. (1999) Association of mitochondria with plectin and desmin intermediate filaments in striated muscle. *Exp. Cell Res.* 252, 479-91.

Rezniczek, G. A., de Pereda, J. M., Reipert, S., and Wiche, G. (1998) Linking integrin alpha6beta4-based cell adhesion to the intermediate filament cytoskeleton: direct interaction between the beta4 subunit and plectin at multiple molecular sites. *J Cell Biol.* 141, 209-225.

Rezniczek, G. A., Abrahamsberg, C., Fuchs, P., Spazierer, D., and Wiche, G. (2003) Plectin 5'-transcript diversity: short alternative sequences determine stability of gene products, initiation of translation and subcellular localization of isoforms. *Hum. Mol. Genet.* 12, 3181-3194.

Rezniczek, G. A., Konieczny, P., Nikolic, B., Reipert, S., Schneller, D., Abrahamsberg, C., Davies, K. E., Winder, S. J., and Wiche, G. (2007) Plectin 1f scaffolding at the sarcolemma of dystrophic (mdx) muscle fibers through multiple interactions with beta-dystroglycan. *J Cell Biol.* 176, 965-977.

Rezniczek, G. A., Walko, G., and Wiche, G. (2010) Plectin gene defects lead to various forms of epidermolysis bullosa simplex. *Dermatol. Clin.* 28, 33-41.

Ruhrberg, C., Hajibagheri, M. A., Simon, M., Dooley, T. P., and Watt, F. M. (1996) Envoplakin, a novel precursor of the cornified envelope that has homology to desmoplakin. *J Cell Biol.* 134, 715-29.

Ruhrberg, C., and Watt, F. M. (1997) The plakin family: versatile organizers of cytoskeletal architecture. *Curr. Opin. Genet. Dev.* 7, 392-7.

Rybakova, I. N., Patel, J. R., Davies, K. E., Yurchenco, P. D., and Ervasti, J. M. (2002) Utrophin binds laterally along actin filaments and can couple costameric actin with sarcolemma when overexpressed in dystrophin-deficient muscle. *Mol. Biol. Cell* 13, 1512-1521.

Rybakova, I. N., Humston, J. L., Sonnemann, K. J., and Ervasti, J. M. (2006) Dystrophin and utrophin bind actin through distinct modes of contact. *J Biol. Chem.* 281, 9996-10001.

Santoro, M. M., Gaudino, G., and Marchisio, P. C. (2003) The MSP receptor regulates alpha6beta4 and alpha3beta1 integrins via 14-3-3 proteins in keratinocyte migration. *Dev. Cell* 5, 257-271.

Sawyer, G. M., Clark, A. R., Robertson, S. P., and Sutherland-Smith, A. J. (2009) Disease-associated substitutions in the filamin B actin binding domain confer enhanced actin binding affinity in the absence of major structural disturbance: Insights from the crystal structures of filamin B actin binding domains. *J Mol. Biol.* 390, 1030-1047.

Seifert, G. J., Lawson, D., and Wiche, G. (1992) Immunolocalization of the intermediate filament-associated protein plectin at focal contacts and actin stress fibers. *Eur. J Cell Biol.* 59, 138-147.

Ševčík, J., Urbániková, L., Košťan, J., Janda, L., and Wiche, G. (2004) Actin-binding domain of mouse plectin: Crystal structure and binding to vimentin. *Eur. J Biochem.* 271, 1873-1884.

Sjöblom, B., Ylanne, J., and Djinovic-Carugo, K. (2008a) Novel structural insights into F-actin-binding and novel functions of calponin homology domains. *Curr. Opin. Struct. Biol.* 18, 702-8.

Sjöblom, B., Salmazo, A., and Djinovic-Carugo, K. (2008b) Alpha-actinin structure and regulation. *Cell Mol. Life Sci.* 65, 2688-701.

Sonnenberg, A., Rojas, A. M., and de Pereda, J. M. (2007) The structure of a tandem pair of spectrin repeats of plectin reveals a modular organization of the plakin domain. *J Mol. Biol.* 368, 1379-91.

Spazierer, D., Raberger, J., Gross, K., Fuchs, P., and Wiche, G. (2008) Stress-induced recruitment of epiplakin to keratin networks increases their resistance to hyperphosphorylation-induced disruption. *J Cell Sci.* 121, 825-33.

References 104

Spudich, J. A., and Watt, S. (1971) The regulation of rabbit skeletal muscle contraction. I. Biochemical studies of the interaction of the tropomyosin-troponin complex with actin and the proteolytic fragments of myosin. *J Biol. Chem.* 246, 4866-4871.

Spurny, R., Abdoulrahman, K., Janda, L., Rünzler, D., Köhler, G., Castañón, M. J., and Wiche, G. (2007) Oxidation and nitrosylation of cysteines proximal to the intermediate filament (IF)-binding site of plectin: effects on structure and vimentin binding and involvement in IF collapse. *J Biol. Chem.* 282, 8175-87.

Stegh, A. H., Herrmann, H., Lampel, S., Weisenberger, D., Andrä, K., Seper, M., Wiche, G., Krammer, P.H., and Peter, M.E. (2000) Identification of the cytolinker plectin as a major early in vivo substrate for caspase 8 during CD95- and tumor necrosis factor receptor-mediated apoptosis. *Mol. Cell Biol.* 20, 5665-5679.

Steinböck, F. A., and Wiche, G. (1999) Plectin: a cytolinker by design. *Biol. Chem.* 380, 151-8.

Steinböck, F. A., Nikolic, B., Coulombe, P. A., Fuchs, E., Traub, P., and Wiche, G. (2000) Dose-dependent linkage, assembly inhibition and disassembly of vimentin and cytokeratin 5/14 filaments through plectin's intermediate filament-binding domain. *J Cell Sci.* 113, 483-91.

Steiner-Champliaud, M. F., Schneider, Y., Favre, B., Paulhe, F., Praetzel-Wunder, S., Faulkner, G., Konieczny, P., Raith, M., Wiche, G., Adebola, A., Liem, R. K., Langbein, L., Sonnenberg, A., Fontao, L., and Borradori, L. (2010) BPAG1 isoform-b: complex distribution pattern in striated and heart muscle and association with plectin and alpha-actinin. *Exp. Cell Res.* 316, 297-313.

Stone, M. R., O'Neill, A., Catino, D., and Bloch, R. J. (2005) Specific interaction of the actin-binding domain of dystrophin with intermediate filaments containing keratin 19. *Mol. Biol. Cell* 16, 4280-4293.

Stradal, T., Kranewitter, W., Winder, S. J., and Gimona, M. (1998) CH domains revisited. *FEBS Lett.* 431, 134-7.

Strelkov, S. V., Herrmann, H., and Aebi, U. (2003) Molecular architecture of intermediate filaments. *Bioessays* 25, 243-251.

Svitkina, T. M., Verkhovsky, A. B., and Borisy, G. G. (1996) Plectin sidearms mediate interaction of intermediate filaments with microtubules and other components of the cytoskeleton. *J Cell Biol.* 135, 991-1007.

Tennenbaum, T., Li, L., Belanger, A. J., De Luca, L. M., and Yuspa, S. H. (1996) Selective changes in laminin adhesion and alpha 6 beta 4 integrin regulation are associated with the initial steps in keratinocyte maturation. *Cell Growth Differ.* 7, 615-628.

Urbániková, L., Janda, L., Popov, A., Wiche, G., and Ševčík, J. (2002) Purification, crystallization and preliminary X-ray analysis of the plectin actin-binding domain. *Acta Crystallogr. D* 58, 1368-1370.

Valencia, R. G., Walko, G., Janda, L., Novacek, J., Mihailovska, E., Reipert, S., Andrä-Marobela, K., and Wiche, G. (2013) Intermediate filament-associated cytolinker plectin 1c destabilizes microtubules in keratinocytes. *Mol. Biol. Cell* 24,768-84.

Van der Neut, R., Krimpenfort, P., Calafat, J., Niessen, C. M., and Sonnenberg, A. (1996) Epithelial detachment due to absence of hemidesmosomes in integrin beta 4 null mice. *Nat. Genet.* 13, 366-9.

Virata, M. L., Wagner, R. M., Parry, D. A., and Green, K. J. (1992) Molecular structure of the human desmoplakin I and II amino terminus. *Proc. Natl. Acad. Sci. U.S.A.* 89, 544-548.

Walko, G., Vukasinovic, N., Gross, K., Fischer, I., Sibitz, S., Fuchs, P., Reipert, S., Jungwirth, U., Berger, W., Salzer, U., Carugo, O., Castañón, M.J., and Wiche, G. (2011) Targeted proteolysis of plectin

isoform 1a accounts for hemidesmosome dysfunction in mice mimicking the dominant skin blistering disease EBS-Ogna. *PLoS Genet.* 7(12), e1002396.

Wang, P., and Gusev, N. B. (1996) Interaction of smooth muscle calponin and desmin. *FEBS Lett.* 392, 255-258.

Washington, R. W., and Knecht, D. A. (2008) Actin binding domains direct actin-binding proteins to different cytoskeletal locations. *BMC Cell Biol.* 9, 10.

Way, M., Pope, B., and Weeds, A. G. (1992a) Evidence for functional homology in the F-actin binding domains of gelsolin and alpha-actinin: implications for the requirements of severing and capping. *J Cell Biol.* 119, 835-42.

Way, M., Pope, B., Cross, R. A., Kendrick-Jones, J., and Weeds, A.G. (1992b) Expression of the N-terminal domain of dystrophin in *E. coli* and demonstration of binding to F-actin. *FEBS Lett.* 301, 243-245.

Weitzer, G., and Wiche, G. (1987) Plectin from bovine lenses. Chemical properties, structural analysis and initial identification of interaction partners. *Eur. J Biochem.* 169, 41-52.

Wiche, G., and Baker, M. A. (1982) Cytoplasmic network arrays demonstrated by immunolocalization using antibodies to a high molecular weight protein present in cytoskeletal preparations from cultured cells. *Exp. Cell Res.* 138, 15-29.

Wiche, G., Krepler, R., Artlieb, U., Pytela, R., and Denk, H. (1983) Occurrence and immunolocalization of plectin in tissues. *J Cell Biol.* 97, 887-901.

Wiche, G., Krepler, R., Artlieb, U., Pytela, R., and Aberer, W. (1984) Identification of plectin in different human cell types and immunolocalization at epithelial basal cell surface membranes. *Exp. Cell Res.* 155, 43-49.

Wiche, G. (1989) Plectin: general overview and appraisal of its potential role as a subunit protein of the cytomatrix. *Crit. Rev. Biochem. Mol. Biol.* 24, 41-67.

Wiche, G., Becker, B., Luber, K., Weitzer, G., Castañón, M. J., Hauptmann, R., Stratowa, C., and Stewart, M. (1991) Cloning and sequencing of rat plectin indicates a 466-kD polypeptide chain with a three-domain structure based on a central alpha-helical coiled coil. *J Cell Biol.* 114, 83-99.

Wilhelmsen, K., Litjens, S. H., Kuikman. I., Tshimbalanga, N., Janssen, H., van den Bout, I., Raymond, K., and Sonnenberg, A. (2005) Nesprin-3, a novel outer nuclear membrane protein, associates with the cytoskeletal linker protein plectin. *J Cell Biol.* 171, 799-810.

Wilhelmsen, K., Litjens, S. H., Kuikman, I., Margadant, C., van Rheenen, J., and Sonnenberg, A. (2007) Serine phoshorylation of the integrin β4 subunit is necessary for EGF receptor-induced hemidesmosome disruption. *Mol. Biol. Cell* 18, 3512-3522.

Winder, S. J., Hemmings, L., Bolton, S. J., Maciver, S. K., Tinsley, J. M., Davies, K. E., Critchley, D. R., and Kendrick-Jones, J. (1995) Calmodulin regulation of utrophin actin binding. *Biochem. Soc. Trans.* 23, 397S.

Winder, S. J., and Kendrick-Jones, J. (1995) Calcium/calmodulin-dependent regulation of the NH2-terminal F-actin binding domain of utrophin. *FEBS Lett.* 357, 125-128.

Winter, L., Abrahamsberg, C., and Wiche, G. (2008) Plectin isoform 1b mediates mitochondrion-intermediate filament network linkage and controls organelle shape. *J Cell Biol.* 181, 903-911.

Winter, L., and Wiche, G. (2013) The many faces of plectin and plectinopathies: pathology and mechanisms. *Acta Neuropathol.* 125, 77-93.

Wright, P. E., and Dyson, H. J. (2009) Linking folding and binding. *Curr. Opin. Struct. Biol.* 19, 31-38.

Yaoita, E., Wiche, G., Yamamoto, T., Kawasaki, K., and Kihara, I. (1996) Perinuclear distribution of plectin characterizes visceral epithelial cells of rat glomeruli. *Am. J Pathol.* 149, 319-27.

Zhang, T., Haws, P., and Wu, Q. (2004) Multiple variable first exons: a mechanism for cell- and tissue-specific gene regulation. *Genome Res.* 14, 79-89.

Summary

Plectin is a large and highly versatile cytolinker protein containing several functionally conserved domains, which allow it to interact with a plethora of molecules, but mainly with cytoskeletal network proteins, namely actin, tubulin and various intermediate filament proteins having great impact on their spatial-temporal arrangements and dynamics. In addition, plectin mediates anchorage of intermediate filaments to the plasma or nuclear membrane, and acts as a scaffold for many signaling molecules involved in cytoskeleton regulation. The importance of plectin for normal function of the cytoskeleton in various tissues is underlined by the fact that mutations in the plectin gene lead to different forms of the skin disease epidermolysis bullosa simplex, while mice deficient in plectin are dying at early stages of neonatal development. Thus to fulfill its unique function, plectin seems, by design, to associate with many different proteins in a relatively complex manner; hence the binding of plectin to its interaction partners needs to be regulated and to be tuned up in time and space. Alternative splicing of plectin transcripts leads to the expression of several plectin isoforms differing from each other by N-terminal head domains, directly preceding plectin's actin binding domain (ABD) which is common to all isoforms. Plectin's isoform-specific sequences were found to be responsible for the subcellular localization of plectin and to dictate the function of individual plectin isoforms. Although the function(s) of plectin's N-terminal head domains are starting to be uncovered, the detail mechanism(s) how these head influence the function of the giant protein "body" is not well understood and needs to be, yet, elucidated. In fact, several different mechanisms, how the first isoform specific sequences could modulate the function of plectin, have been suggested. Among these, modulating the activity of the adjacent ABD by plectin first exon encoded sequences either by forming extended binging sites with plectin ABD, or changing its structure, or attracting and/or binding to regulatory and/or signaling molecules, were hypothesized to be the most probable.

The main objective of this thesis was to investigate structural properties of plectin isoform P1a- and P1c-specific sequences and relate them to their function. Here, two main approaches were considered: (1), determination of the structure of these isoform specific sequences when fused to plectin`s ABD (2), determination of the structure of these isoform specific sequences in the complex with some novel binding partner(s), which would interact with plectin's ADB or isoform specific sequences in isoform specific manner.

In pursuance of these goals I was able to established methods for purifying plectin fragments without the help of fusion tags, enabling the isolation of homogenous protein samples without contaminating proteins. This allowed me to obtain enough material for biochemical and structural analyses. Using a crystallographic approach I could confirm that both, the P1a and the P1c isoform-specific sequences are highly flexible and most likely disordered in an un-bound state. The removal of isoform-specific sequences from plectin`s ABD using the protease thrombin supported this notion and suggested a possible physiological relevance of this proteolytic event.

In addition using several biochemical assays I was able to identified vimentin as a new binding partner of plectin`s ABD and to map its interaction site to the N-terminal part of the ABD. In addition, I could identify the N-terminal segment of vimentin´s rod domain as the molecule`s interface with plectin. Furthermore, I showed that plectin interacts with the soluble (tetrameric) form of vimentin most likely in an isoform-independent manner.

Searching for isoform-specific binding partners of plectin, I identified calmodulin as a novel binding partner of plectin, and showed that it binds to the CH1 domain of plectin 1a in a Ca^{2+}- and isoform-dependent manner. Association of calmodulin with plectin 1a was observed also in vivo, upon Ca^{2+}-triggered differentiation of keratinocytes, which led to the redistribution of plectin 1a, as well. Binding of Ca^{2+}/calmodulin to plectin, was found to prevent binding of plectin 1a, but not of plectin 1f or plectin 1c, to F-actin, although the binding affinities of these isoforms to F-actin were found to be in the same micromolar range. Finally, binding of calmodulin to plectin 1a, an isoform exclusively located in hemidesmosomes, was shown to prevent association of plectin with integrin β4. Based on these observations a model for hemidesmosome disassembly, which is required for keratinocytes migration during wound healing and keratinocytes differentiation, was developed. This model proposes that the disassembly of hemidesmosomes is mediated by both, Ca^{2+}/calmodulin binding to plectin and phosphorylation of integrin β4.

Curriculum Vitae

Július Košťan

Max F. Perutz Laboratories
Department of Structural and Computational
Biology
University of Vienna
Campus Vienna Biocenter 5   Phone: +43-1-4277 52263
A-1030 Vienna   Fax: +43-1-4277 9522
Austria   E-mail: julius.kostan@univie.ac.at

PERSONAL DATA

Date of birth: May 26th, 1978
Place of birth: Martin, Slovakia
Nationality: Slovak
Family status: Married, two children
Address: Josef Mayer Gasse 5/12/6, 2340 Mödling, Austria

EDUCATION

2001 – presence   **PhD study**,
PhD defence, expected term: November 2014
Max F. Perutz Laboratories, Department of Molecular Cell Biology,
University of Vienna, Vienna, Austria, the group of Prof. Gerhard Wiche,
PhD
Specialization: Molecular Biology
Thesis: Heads decide: Structural and functional characterization of selected
plectin isoform-specific sequences

1996 – 2001   **Master study**,
Master of Sciences, 2001
Faculty of Natural Sciences, Comenius University, Bratislava, Slovakia
Specialization: biology/molecular biology
State exam: biotechnology, molecular biology, genetics
Master's thesis: Study of alternative splicing of the type I IP$_3$ receptor from rat
brain tissue.
Diploma work: carried out in the group of Olga Križanová, PhD, at the Institute
of Molecular Physiology and Genetics of Slovak Academy of Sciences,
Bratislava, Slovakia

RESEARCH EXPERIENCE

2013 – presence   **Staff scientist,**
Laura Bassi Center for Optimized Structural Studies (COSS)
Max F. Perutz Laboratories, Department of Structural and Computational
Biology, University of Vienna, Vienna, Austria, the group of Prof. Kristina
Djinovic Carugo, PhD

2007 – 2013   **Staff scientist,**
Max F. Perutz Laboratories, Department of Structural and Computational
Biology, University of Vienna, Vienna, Austria, the group of Prof. Kristina
Djinovic Carugo, PhD

2001 – 2004   **Visitor researcher,**
Institute of Molecular Biology, Department of Structural Biology, Slovak
Academy of Sciences, Bratislava, Slovakia, the group of Jozef Ševčík, PhD
Project: Crystallization of plectin actin binding domain.

TEACHING EXPERIENCE

2011 – 2013   **Practicing lecture supervisor**,
Max F. Perutz Laboratories, Vienna, Austria
Training courses: Basic courses in Biochemistry and Molecular Biology

PUBLICATIONS

Kostan, J., Lencesova, L., Kiss, A., Ondrias, K., Kvetnansky, R., and Krizanova, O. (2002) Distribution of neuronal and non-neuronal spliced variants of type 1 IP$_3$-receptor in rat hypothalamus and brain stem. *Neurochem. Int.*41, 65-70.

Sevcik, J., Urbanikova, L., **Kostan, J.**, Janda, L., and Wiche, G. (2004) Actin-binding domain of mouse plectin: crystal structure and binding to vimentin. *Eur. J. Biochem.* 271, 1873-84.

Stroissnigg, H., Trancikova, A., Descovich, L., Fuhrmann, J., Kutschera, W., **Kostan, J.**, Meixner, A., Nothias, F., and Propst, F. (2007) S-nitrosylation of microtubule-associated protein 1B mediates nitric-oxide-induced axon retraction. *Nat. Cell Biol.* 9, 1035-45.

Kostan, J., Gregor, M., Walko, G., and Wiche, G. (2009) Plectin isoform-dependent regulation

of keratin-integrin α6β4 anchorage via Ca^{2+}/calmodulin. *J. Biol. Chem.* 284, 18525-36.

Kostan, J., Sjöblom, B., Maixner, F., Mlynek, G., Furtmüller, P.G., Obinger, C., Wagner, M., Daims, H., and Djinović-Carugo, K. (2010) Structural and functional characterization of the chlorite dismutase from the nitrite-oxidizing bacterium "Candidatus Nitrospira defluvii": identification of a catalytically important amino acid residue. *J. Struct. Biol.* 172, 331-42.

Mlynek, G., Sjöblom, B., **Kostan, J.**, Füreder, S., Maixner, F., Gysel, K., Furtmüller, P.G., Obinger, C., Wagner, M., Daims, H., and Djinović-Carugo, K. (2011) Unexpected diversity of chlorite dismutases: a catalytically efficient dimeric enzyme from Nitrobacter winogradskyi. *J. Bacteriol.* 193, 2408-17.

Hofbauer, S., Gysel, K., Mlynek, G., **Kostan, J.**, Hagmüller, A., Daims, H., Furtmüller, P.G, Djinović-Carugo, K., and Obinger, C. (2012) Impact of subunit and oligomeric structure on the thermal and conformational stability of chlorite dismutases. *Biochim Biophys Acta.* 1824, 1031-8.

Hofbauer, S., Bellei, M., Sündermann, A., Pirker, K.F., Hagmüller, A., Mlynek, G., **Kostan, J.**, Daims, H., Furtmüller, P.G., Djinović-Carugo, K., Oostenbrink, C., Battistuzzi, G., and Obinger, C. (2012) Redox thermodynamics of high-spin and low-spin forms of chlorite dismutases with diverse subunit and oligomeric structures. *Biochemistry* 51, 9501-12.

Morriswood, B., Havlicek, K., Demmel, L., Yavuz, S., Sealey-Cardona, M., Vidilaseris, K., Anrather, D., **Kostan, J.**, Djinovic-Carugo, K., Roux, K.J., and Warren, G. (2013) Novel bilobe components in Trypanosoma brucei identified using proximity-dependent biotinylation. *Eukaryot. Cell* 12, 356-67.

Hofbauer, S., Gysel, K., Bellei, M., Hagmüller, A., Schaffner, I., Mlynek, G., **Kostan, J.**, Pirker, K.F., Daims, H., Furtmüller, P.G., Battistuzzi, G., Djinović-Carugo, K., and Obinger, C. (2014) Manipulating conserved heme cavity residues of chlorite dismutase: effect on structure, redox chemistry, and reactivity. *Biochemistry* 53, 77-89.

Mlynek, G., Lehner, A., Neuhold, J., Leeb, S., **Kostan, J.**, Charnagalov, A., Stolt-Bergner, P., Djinović-Carugo, K., and Pinotsis, N. (2014) The Center for Optimized Structural Studies (COSS) platform for automation in cloning, expression, and purification of single proteins and protein-protein complexes. *Amino Acids* 46, 1565-82.

Bauer, J., Ondrovičová, G., Najmanová, L., Pevala, V., Kameník, Z., **Kostan, J.**, Janata, J., and Kutejová, E. (2014) Structure and possible mechanism of the CcbJ methyltransferase from Streptomyces caelestis. *Acta Crystallogr D Biol Crystallogr.* 70, 943-57.

Kostan, J., Salzer, U., Orlova, A., Törö, I., Hodnik, V., Senju, Y., Zou, J., Schreiner, C., Steiner, J., Meriläinen, J., Nikki, M., Virtanen, I., Carugo, O., Rappsilber, J., Lappalainen, P., Lehto, V.P., Anderluh, G., Egelman, E.H., and Djinović-Carugo, K. (2014) Direct interaction of actin filaments with F-BAR protein pacsin2. *EMBO Rep*. 15, 1154-1162.